Imaging techniques for LOW-DOSE and COLOR tomography: new challenges for PET and Cone-Beam CT with hybrid pixels

Yannick Boursier (ex-APIDIS member)

imXgam group

Centre de Physique des Particules de Marseille

in collaboration with

S. Anthoine, C. Mélot, Signal Processing Group, LATP, Marseille, France

J.-F. Aujol, Analysis Group, IMB, Bordeaux, France

Signal Processing Seminars, ICTEAM/ELEN, ISP Group

May, 18th, 2011

Outline

- I - Recalls in tomography
- II - What's new at CPPM ?
- III - CBCT and PET problem formulations and solvers
- IV - Results
- V - Future challenges
- Conclusion

I - Recalls in tomography

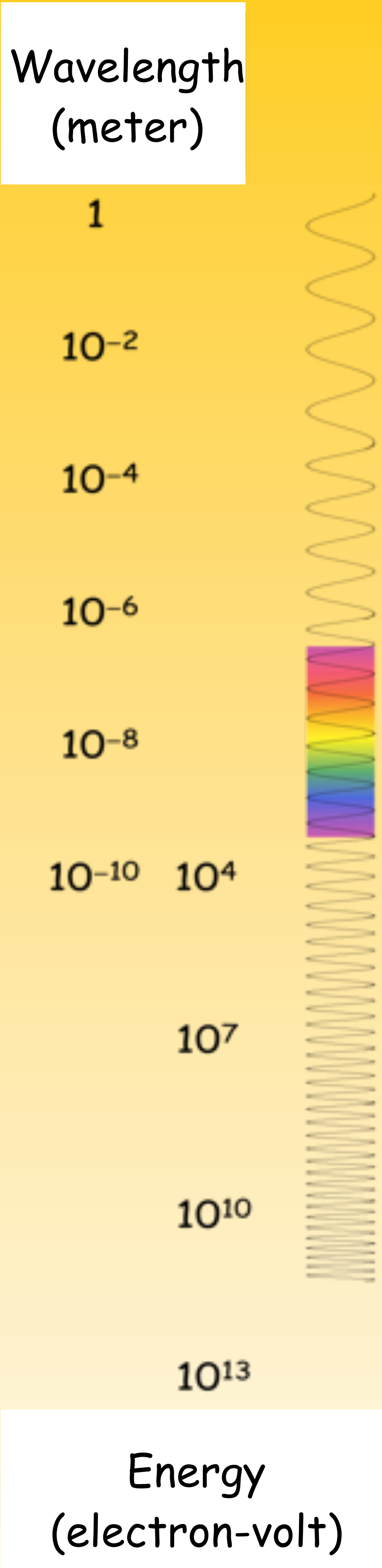

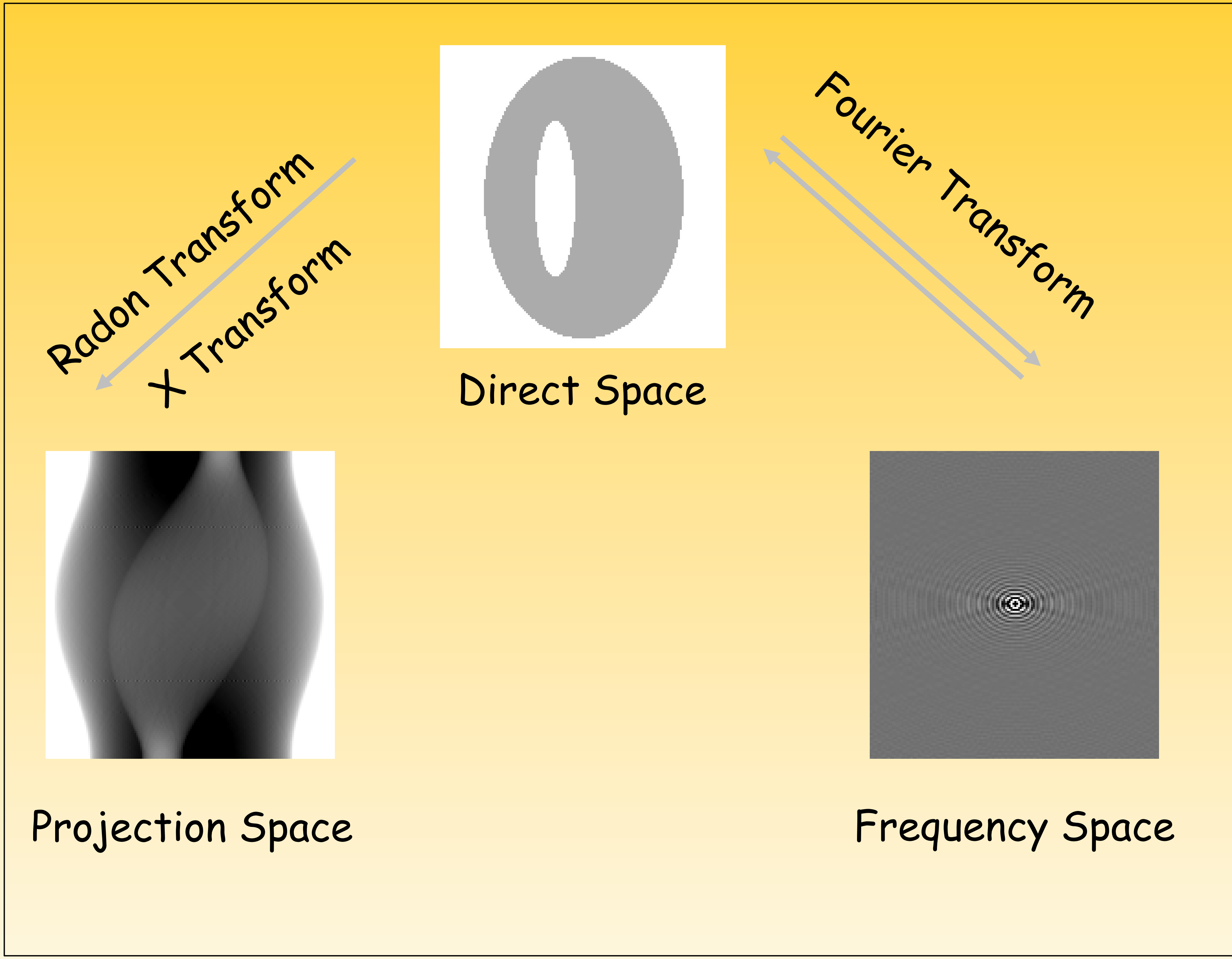

I - Recalls on Computerized Tomography

The Beer-Lambert law describes the absorption of different materials along the line of sight.

$$I = I_0 \exp\left[-\int_{t_1}^{t_2} \mu_{E,m}(t)dt\right]$$

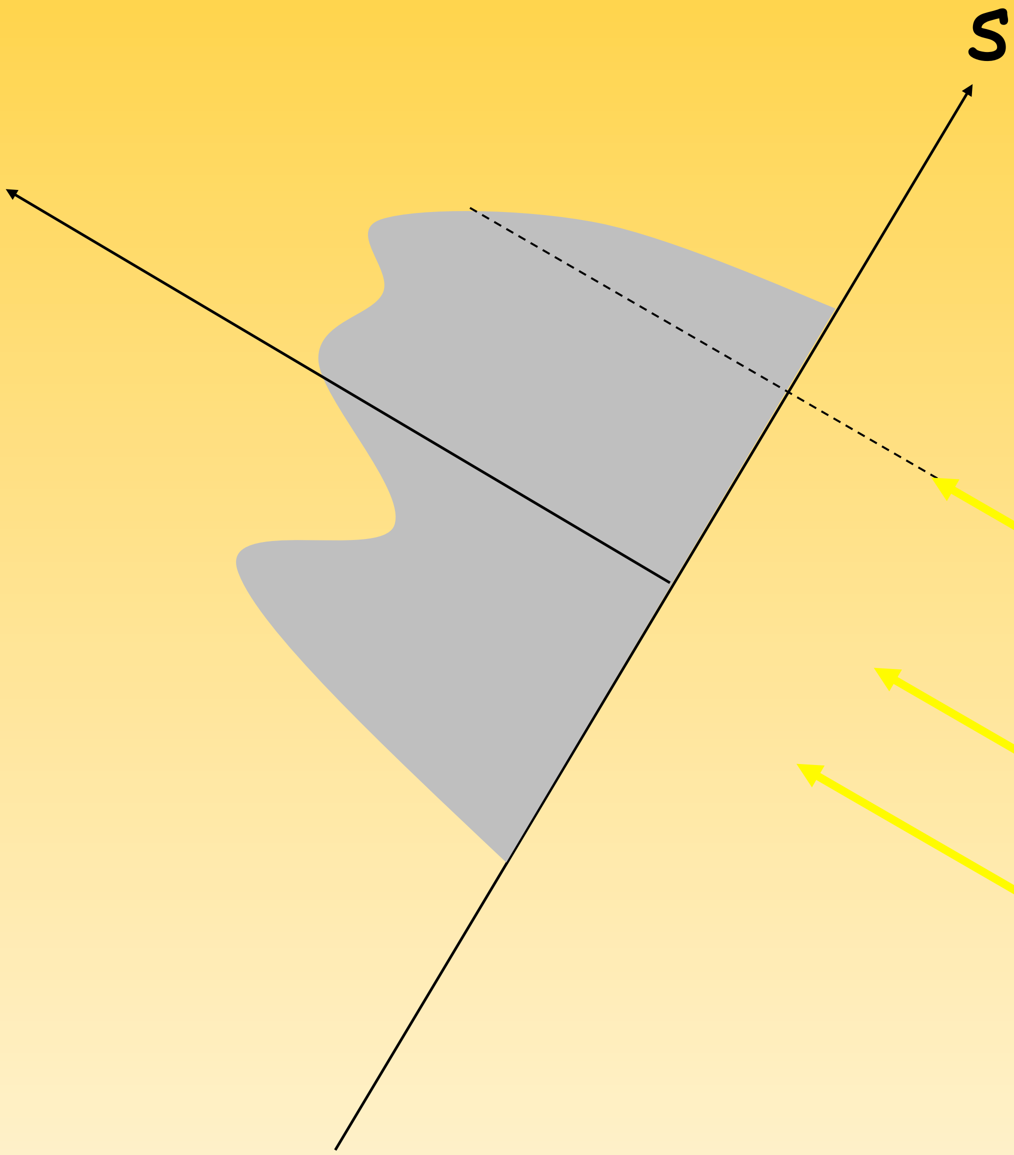

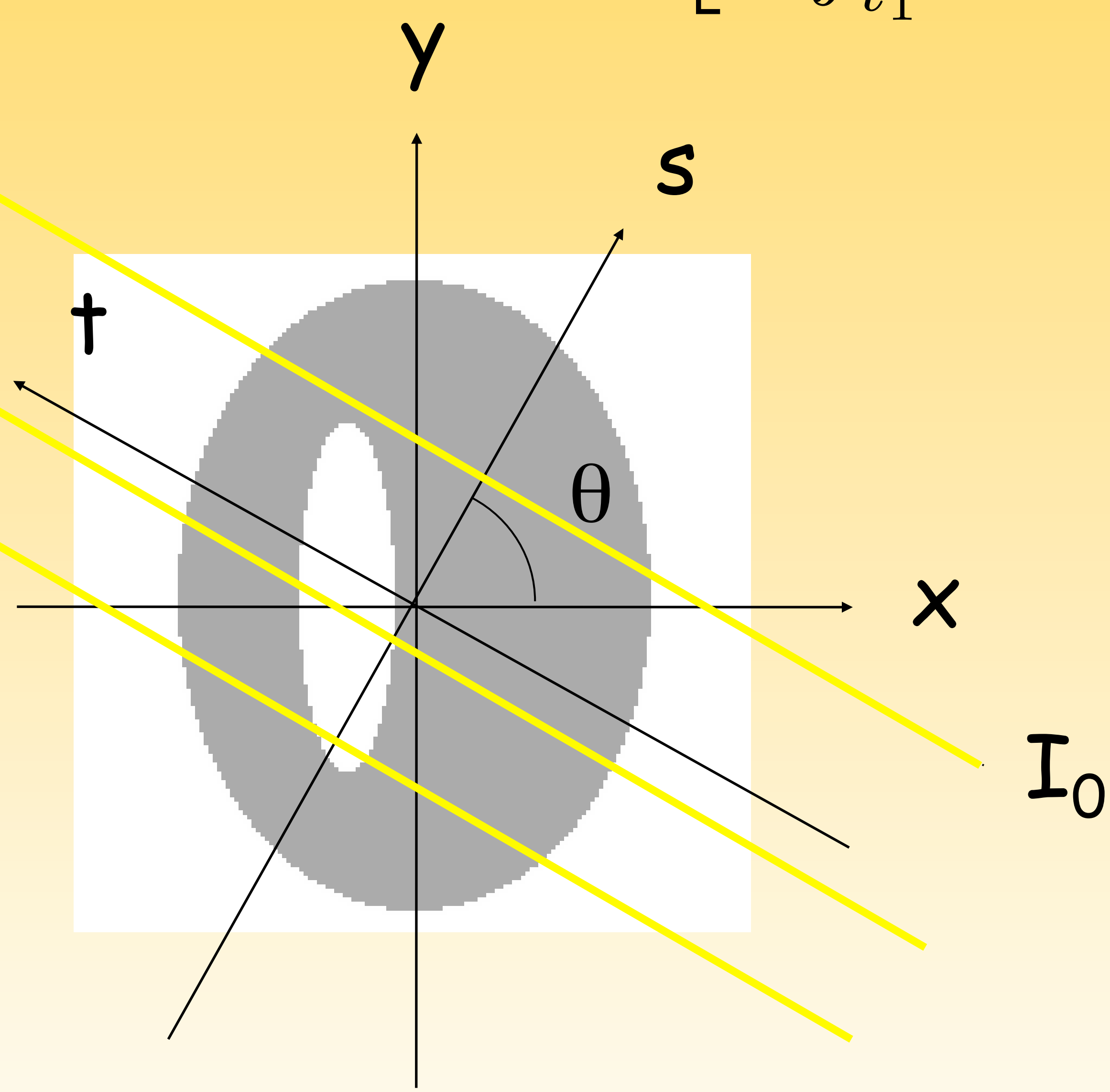

Absorption or attenuation coefficient

$$\mu = \mu_{E,m}$$

I - Recalls on Computerized Tomography

The Beer-Lambert law describes the absorption of different materials along the line of sight.

$$I = I_0 \exp\left[-\int_{t_1}^{t_2} \mu_{E,m}(t)dt\right]$$

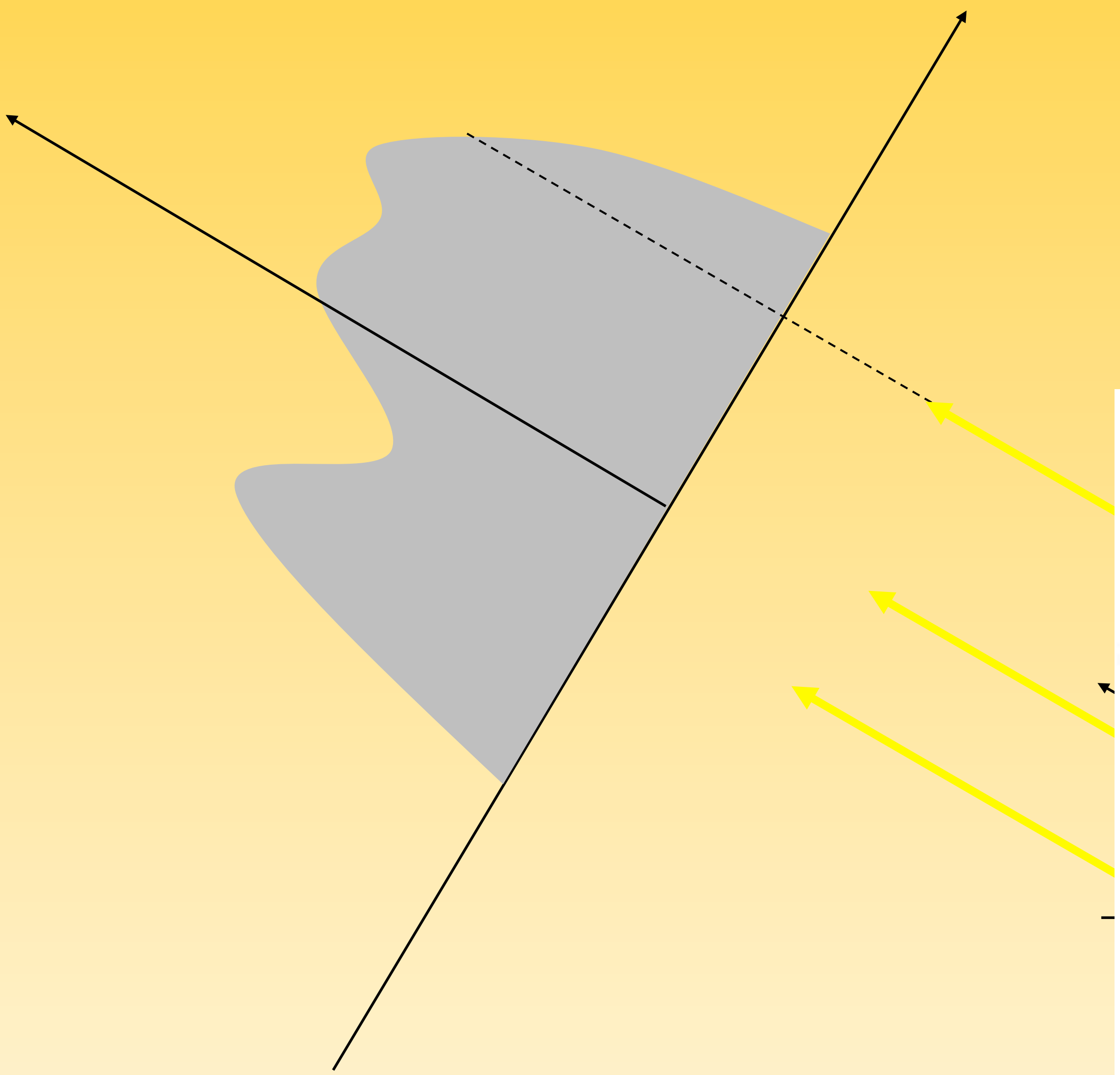

γ

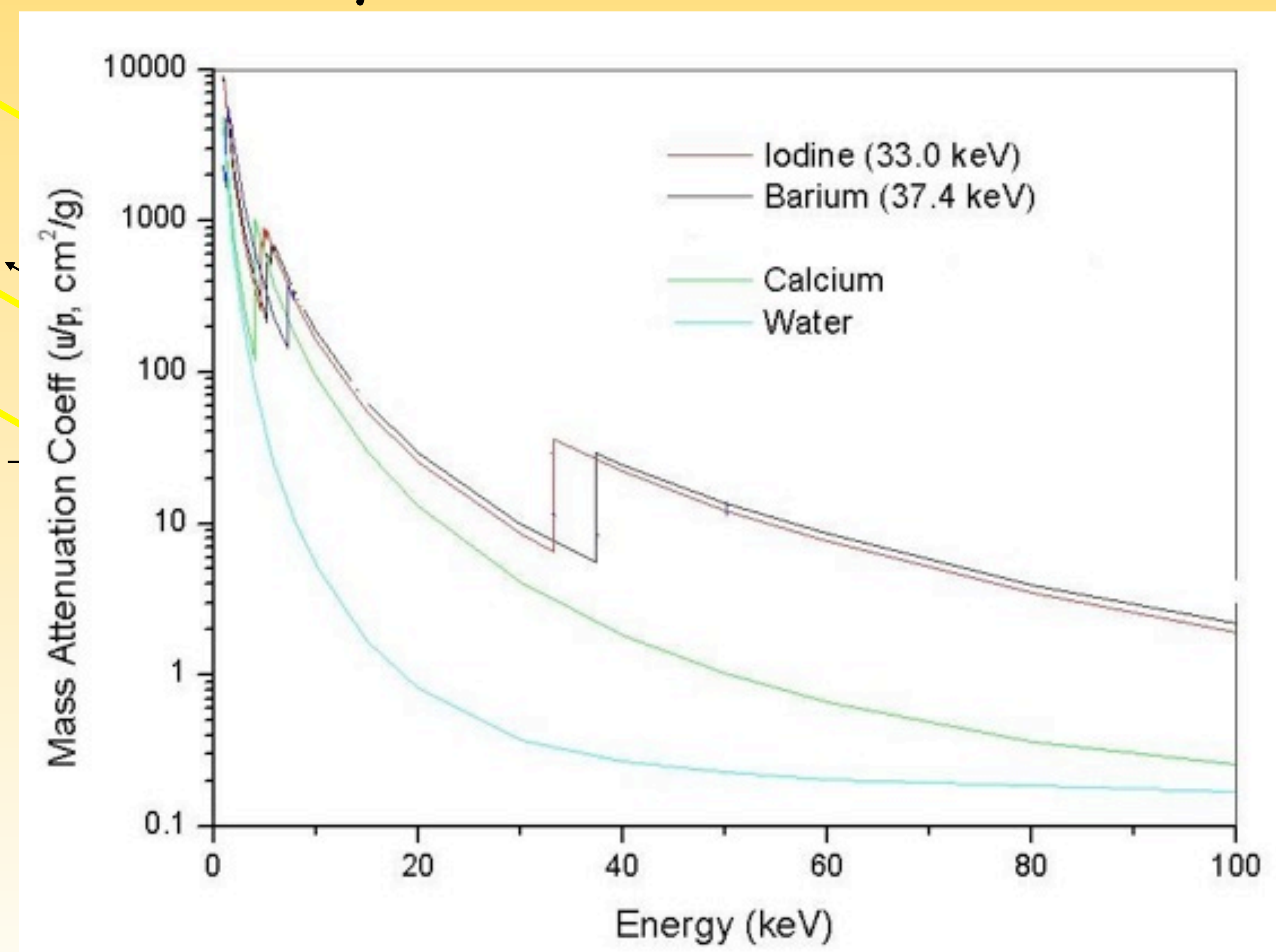

Absorption or attenuation coefficient

$$\mu = \mu_{E,m}$$

I - Recalls on Computerized Tomography

The Beer-Lambert law describes the absorption of different materials along the line of sight.

$$I = I_0 \exp\left[-\int_{t_1}^{t_2} \mu_{E,m}(t)dt\right]$$

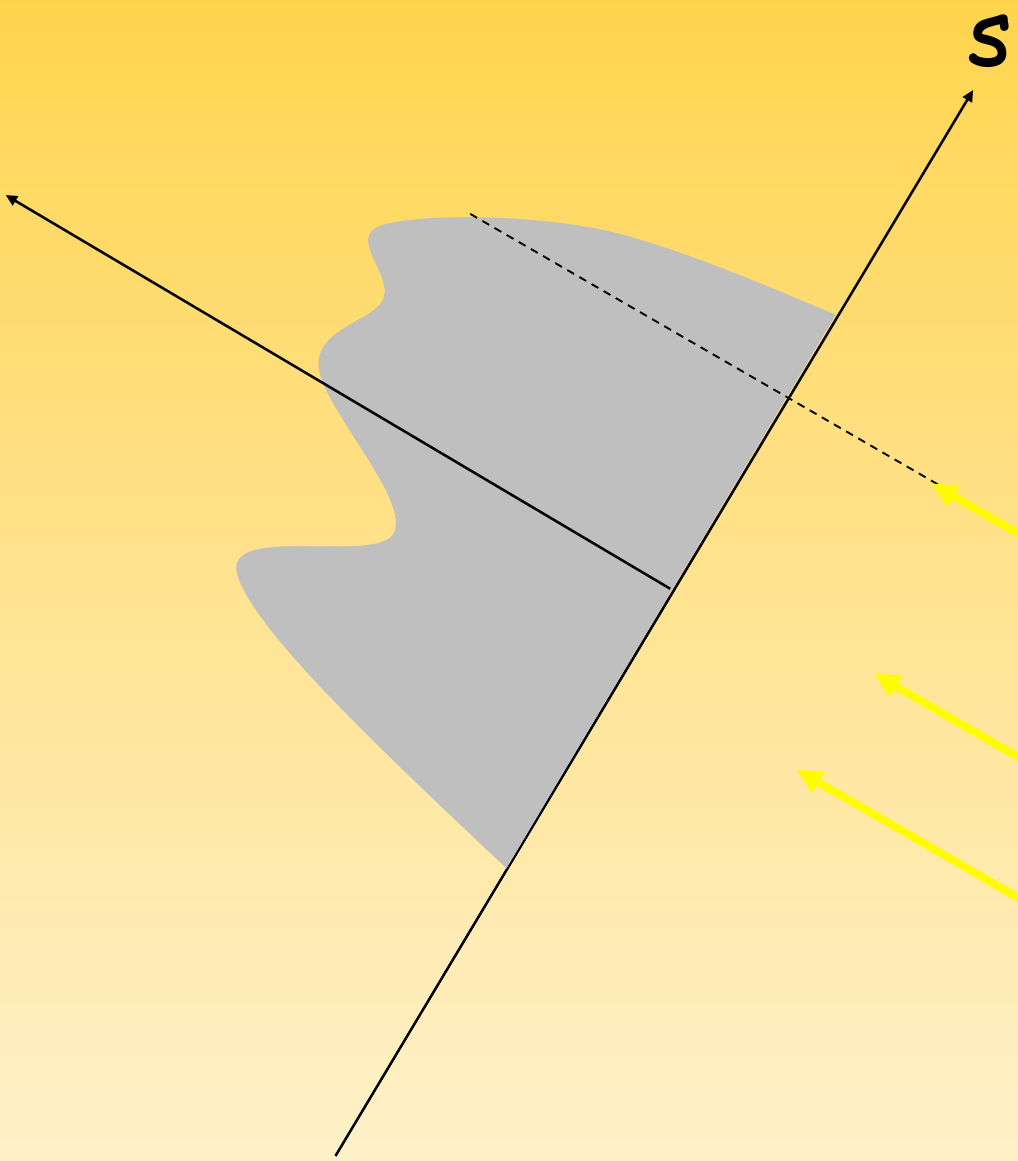

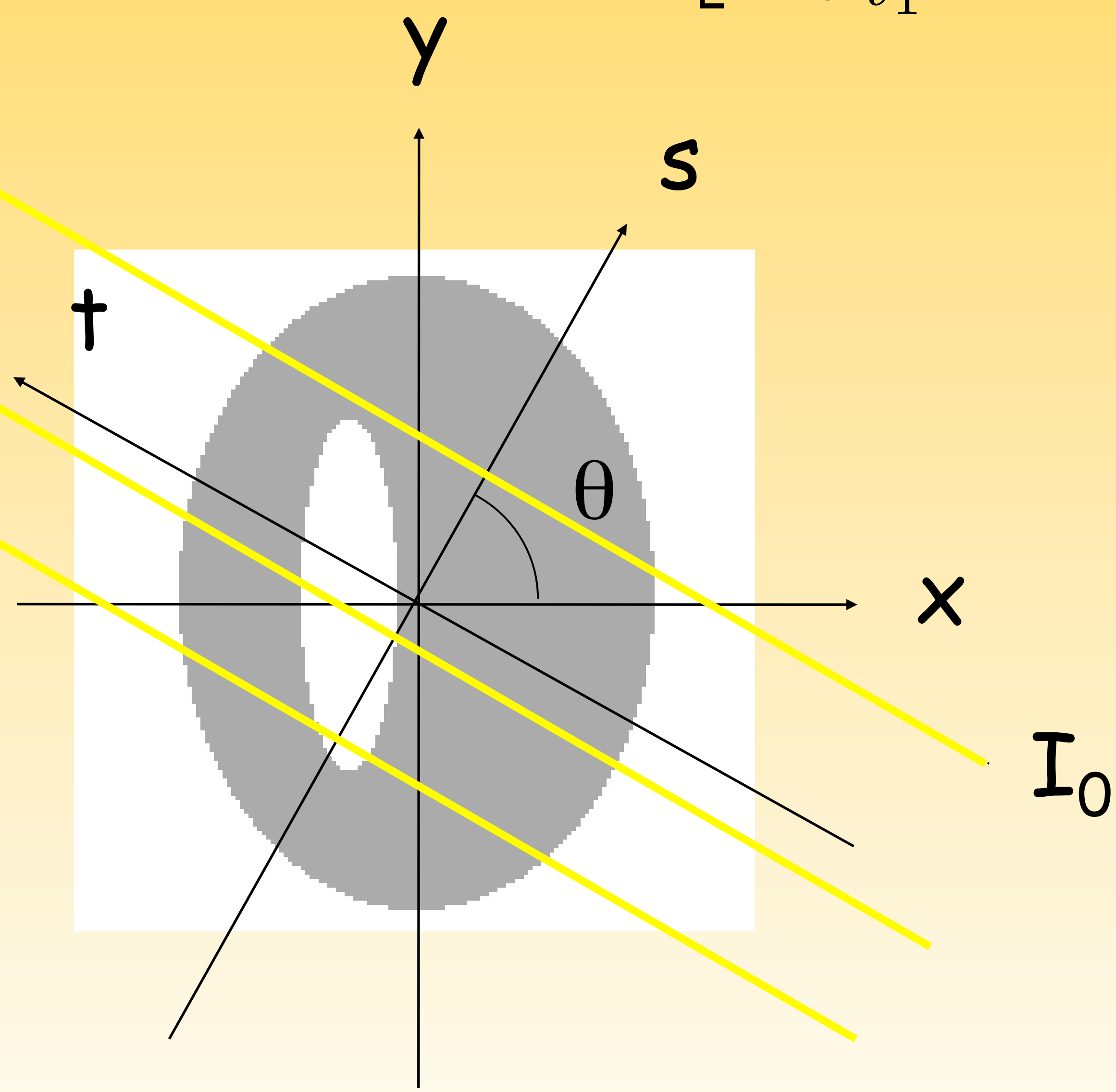

Absorption or attenuation coefficient

$$\mu = \mu_{E,m}$$

I - Recalls on Computerized Tomography

- Basis of tomography : data in 1D + angle, object in 2D.

Image to reconstruct

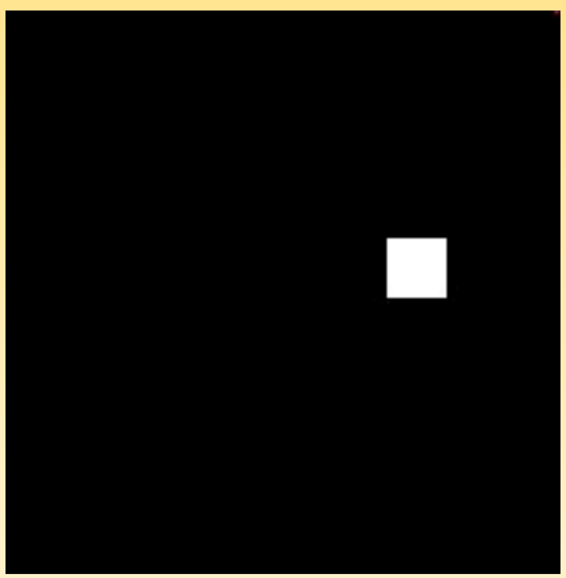

I - Recalls on Computerized Tomography

- Basis of tomography : data in 1D + angle, object in 2D.

Image to reconstruct

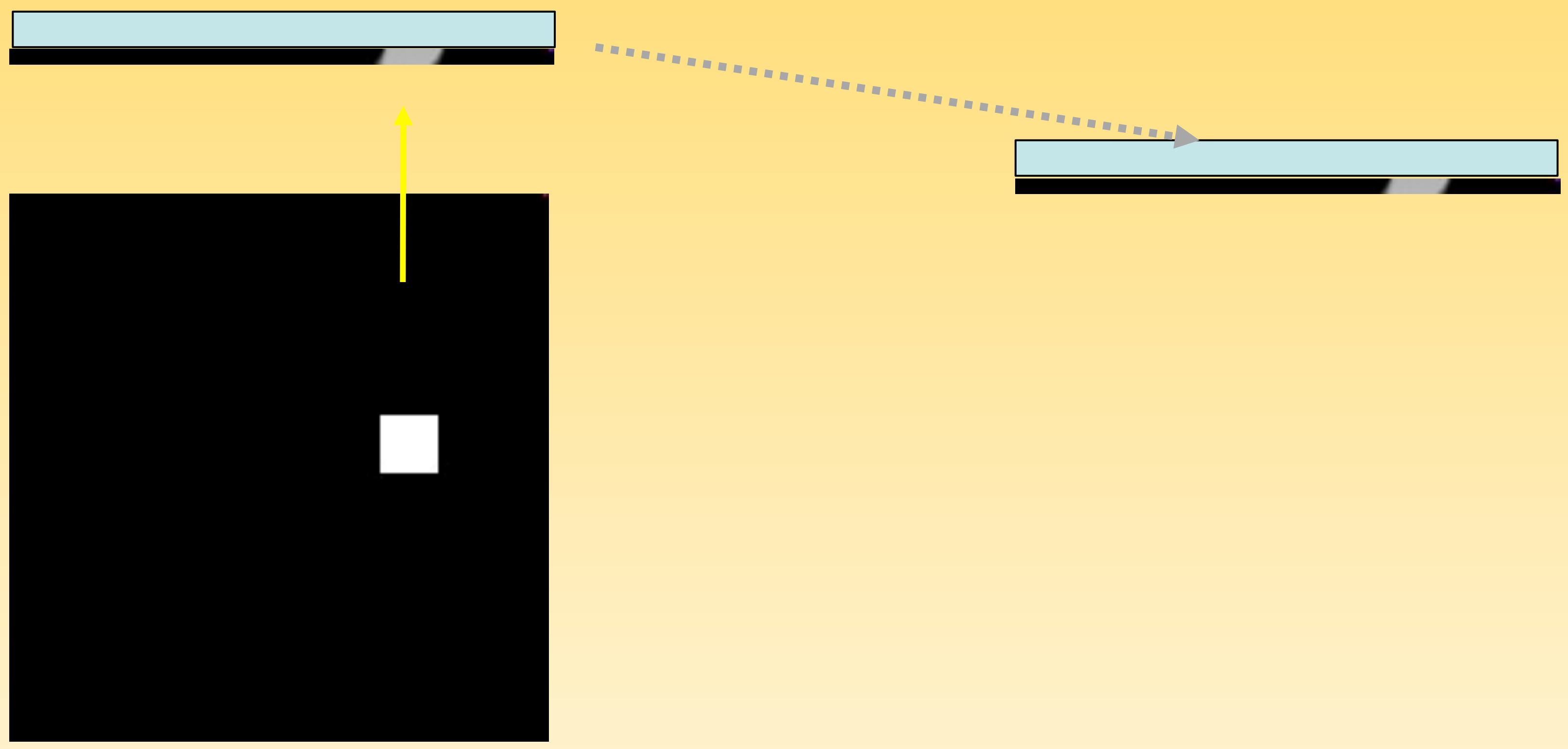

I - Recalls on Computerized Tomography

- Basis of tomography : data in 1D + angle, object in 2D.

Image to reconstruct

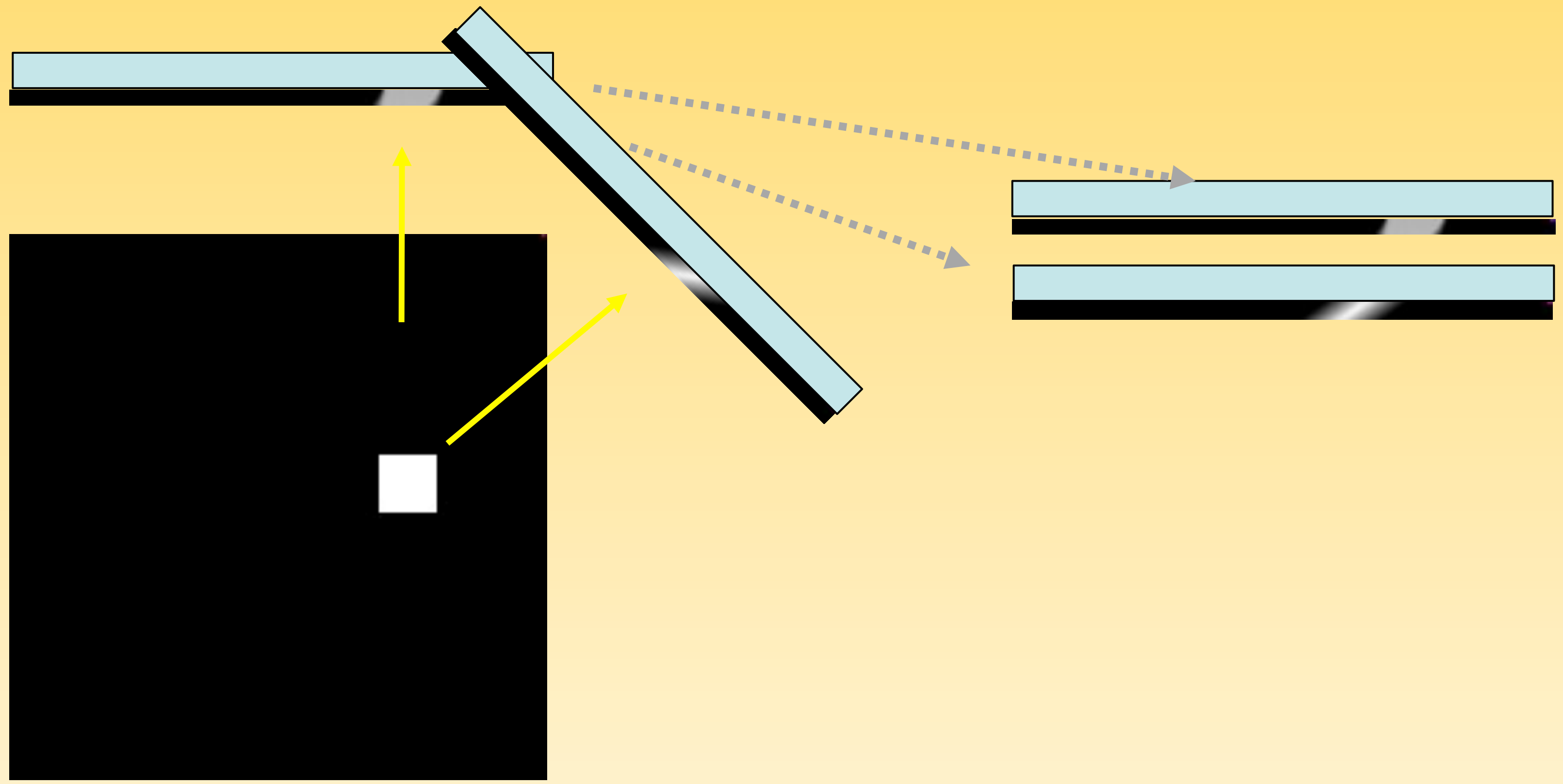

I - Recalls on Computerized Tomography

- Basis of tomography : data in 1D + angle, object in 2D.

Image to reconstruct

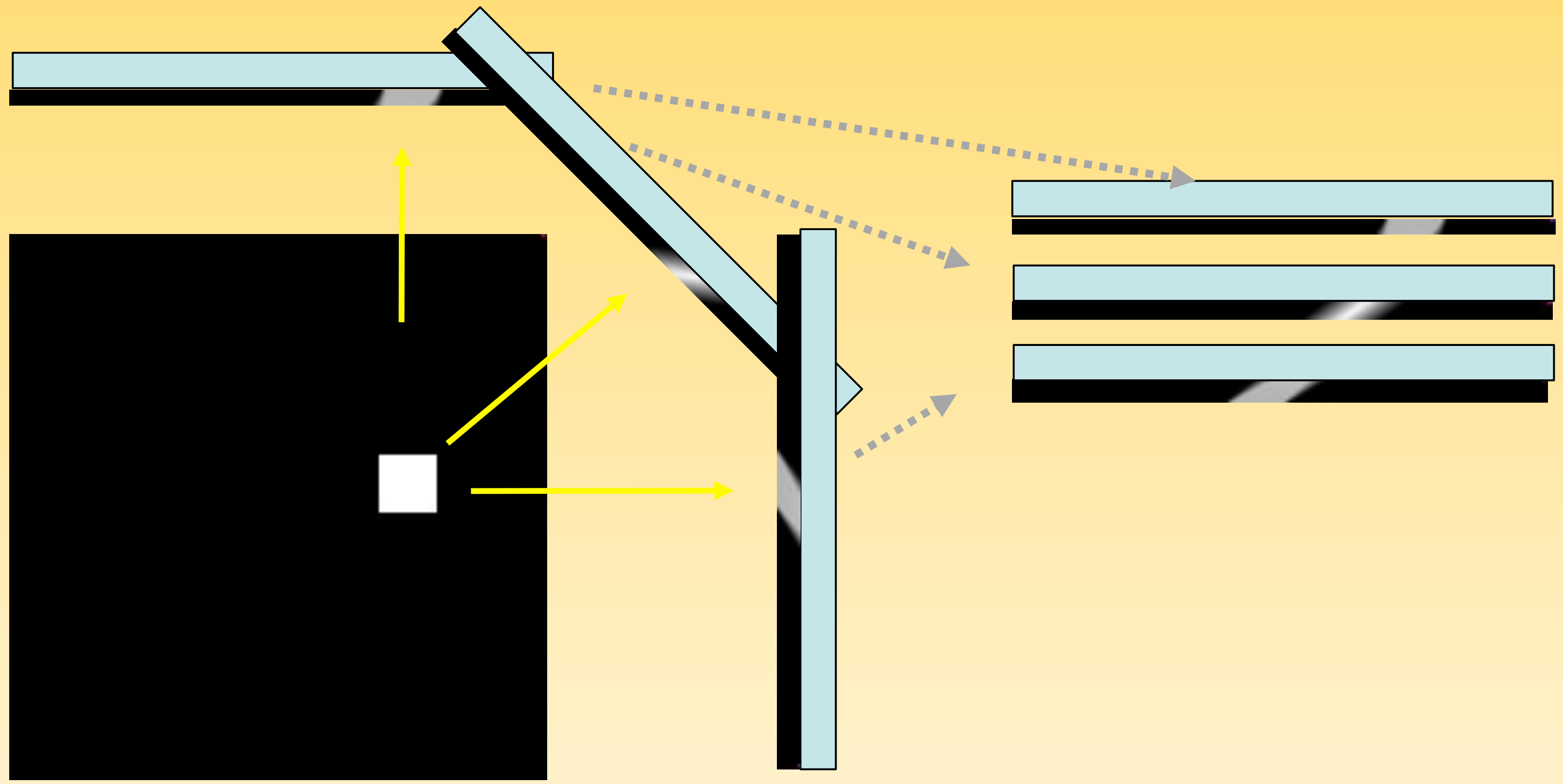

I - Recalls on Computerized Tomography

- Basis of tomography : data in 1D + angle, object in 2D.

Image to reconstruct

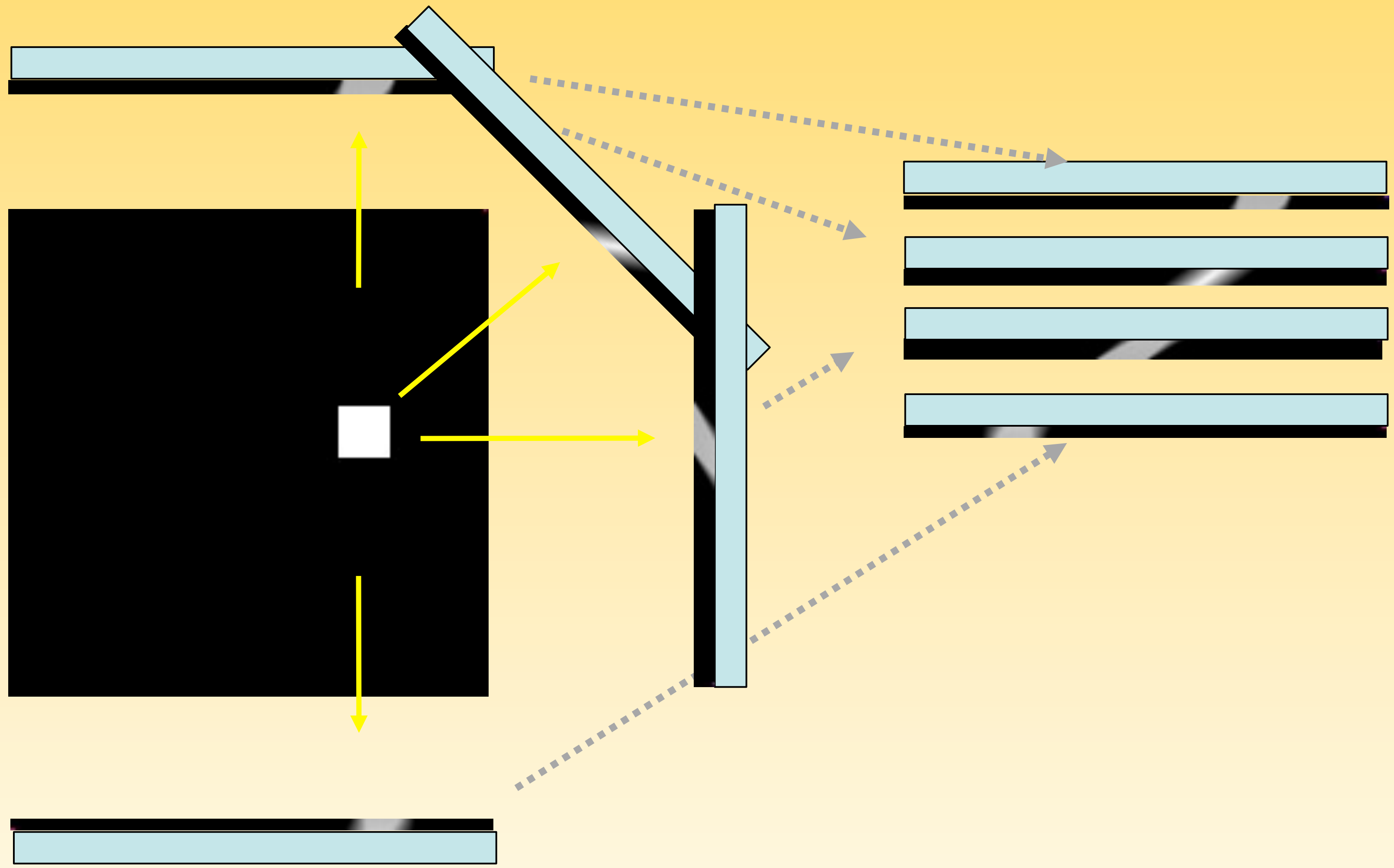

I - Recalls on Computerized Tomography

- Basis of tomography : data in 1D + angle, object in 2D.

Image to reconstruct

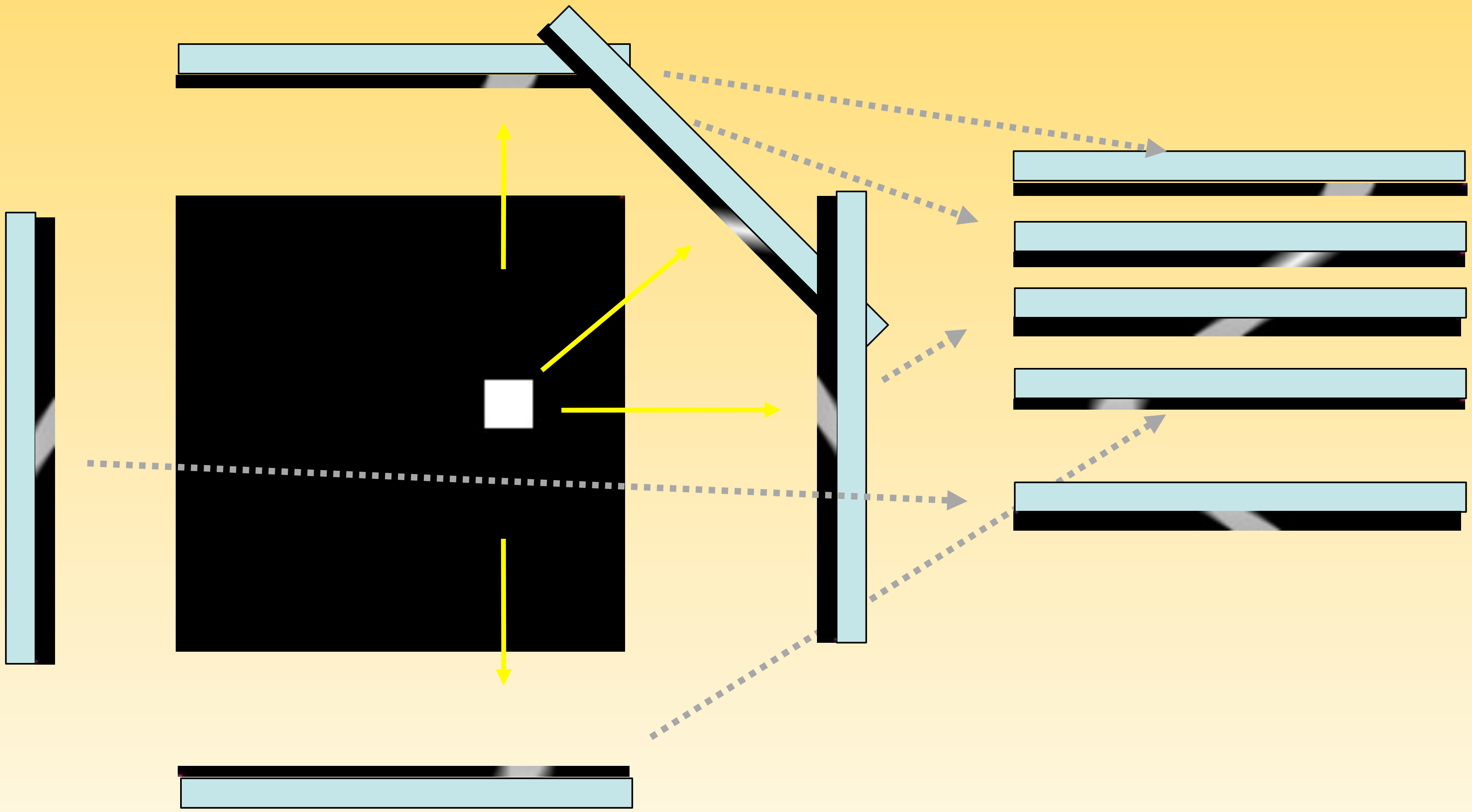

I - Recalls on Computerized Tomography

- Basis of tomography : data in 1D + angle, object in 2D.

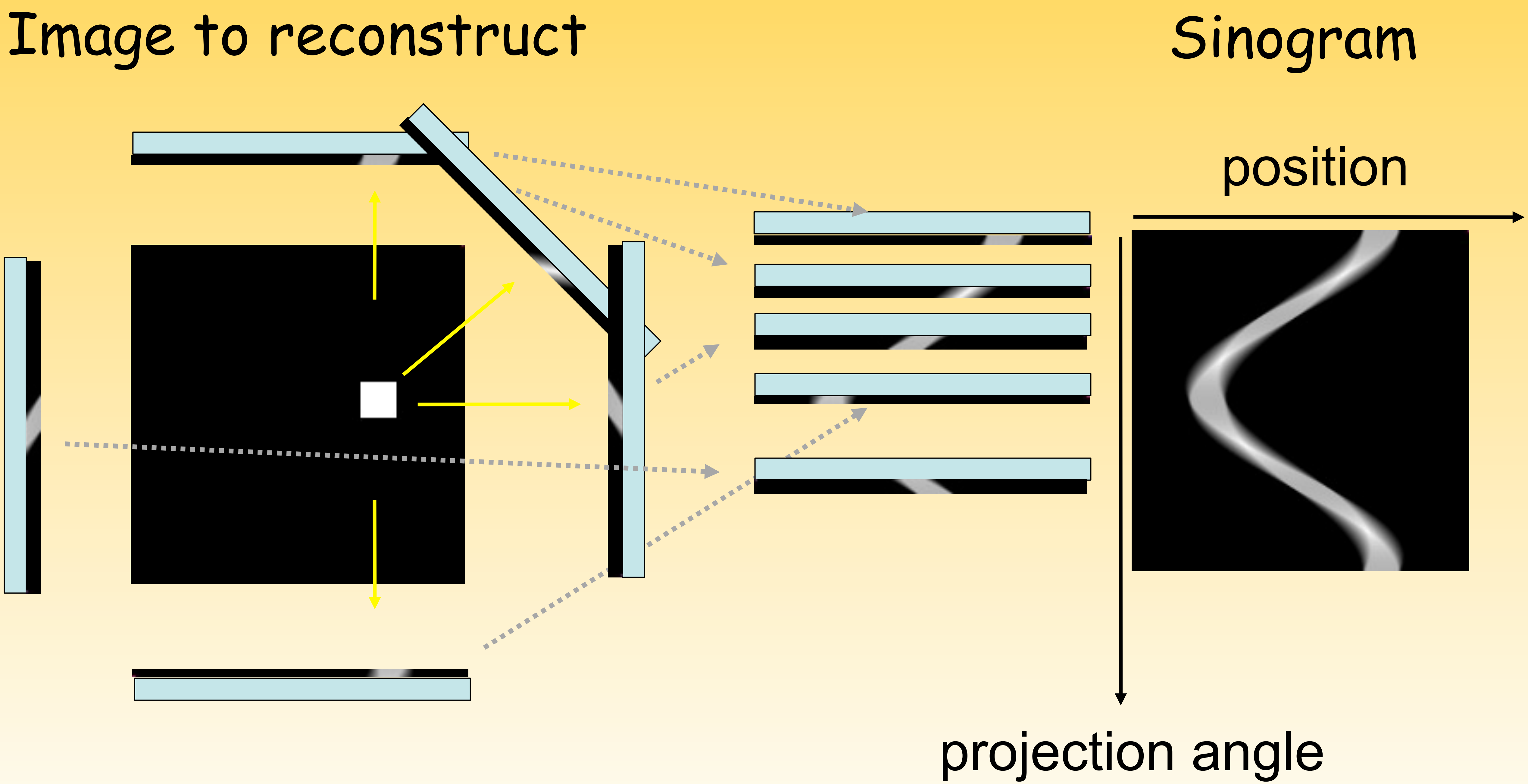

I - Recalls on Cone-Beam Computerized Tomography (CBCT)

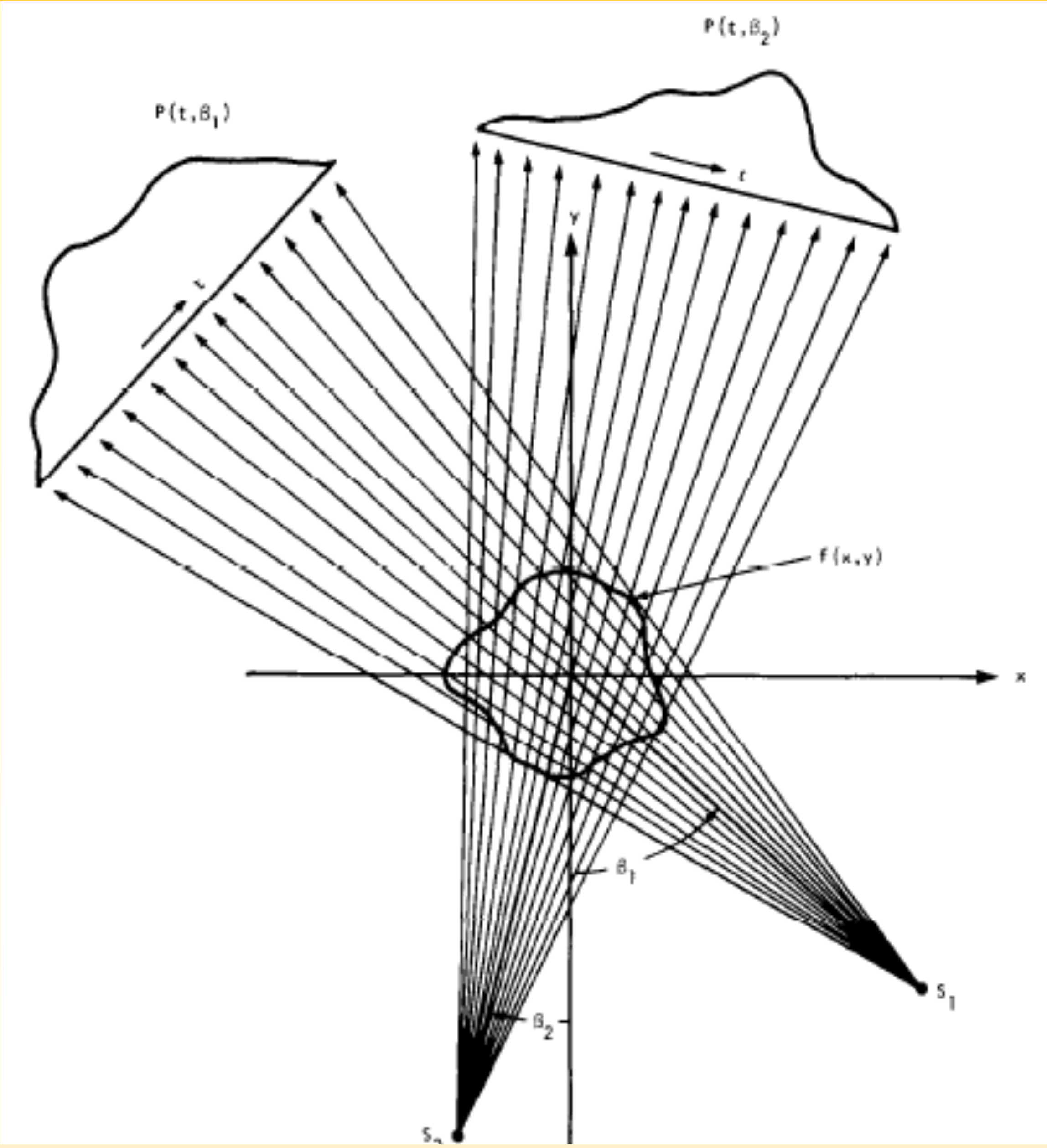

From Kak-Slaney :

<u>Principles of Computerized Tomographic Imaging</u>

I - Recalls on Cone-Beam Computerized Tomography (CBCT)

I - Recalls on Cone-Beam Computerized Tomography (CBCT)

I - Recalls on Cone-Beam Computerized Tomography (CBCT)

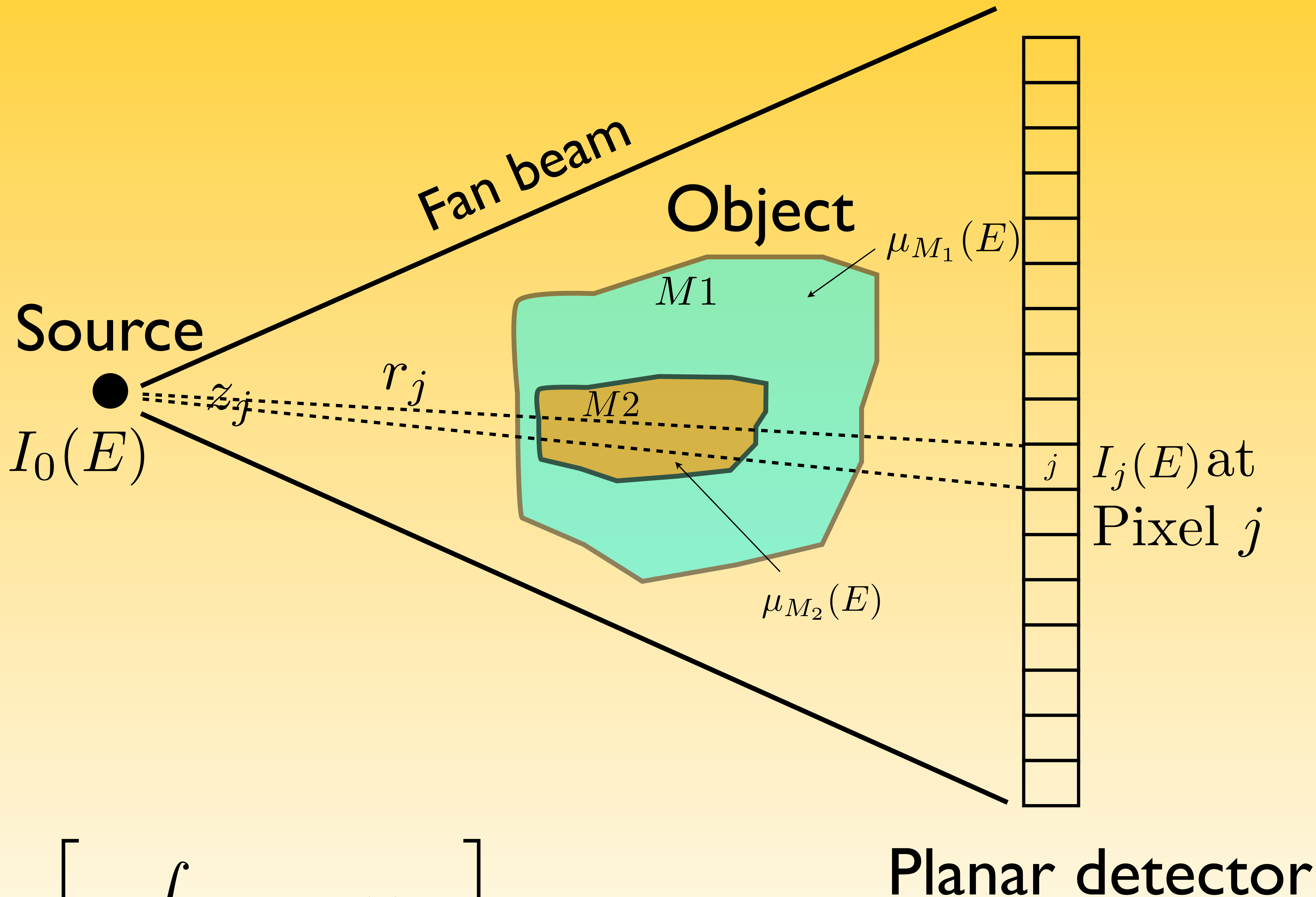

$$I_j = z_j \exp\left[-\int_{r_j} \mu_{E,m}(l)dl\right]$$

I - Recalls on Cone-Beam Computerized Tomography

- Basis of tomography : data in 2D + angle, object in 3D.

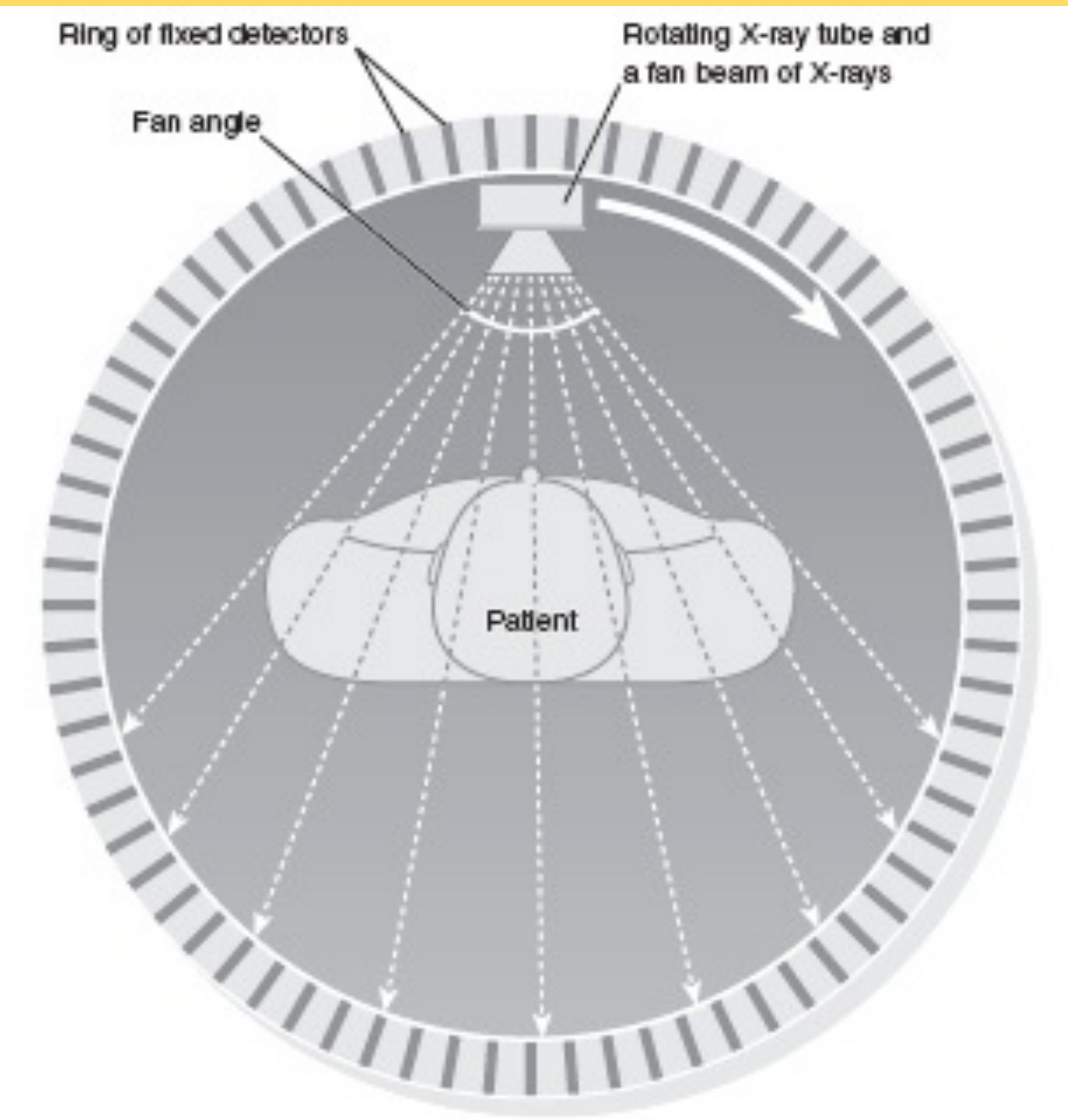

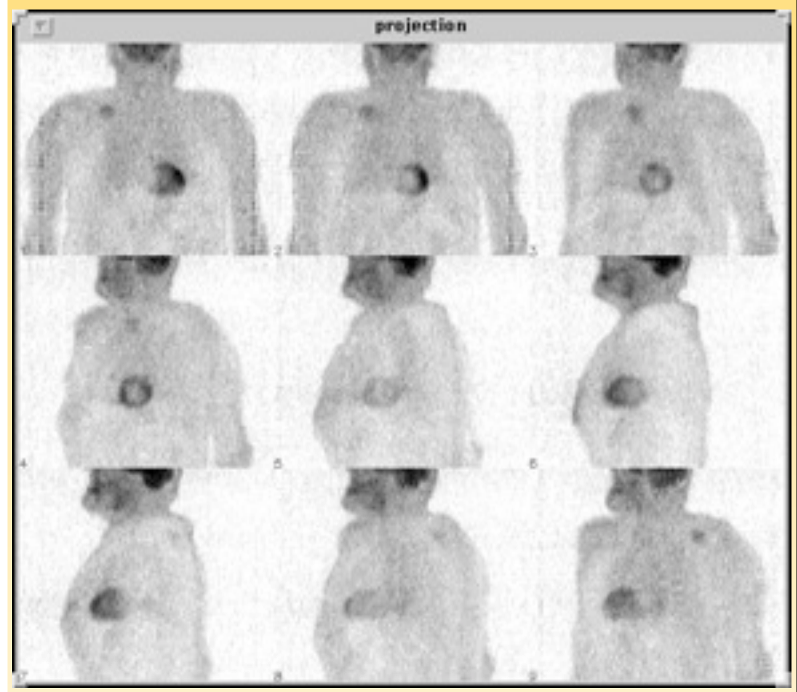

Sinogram

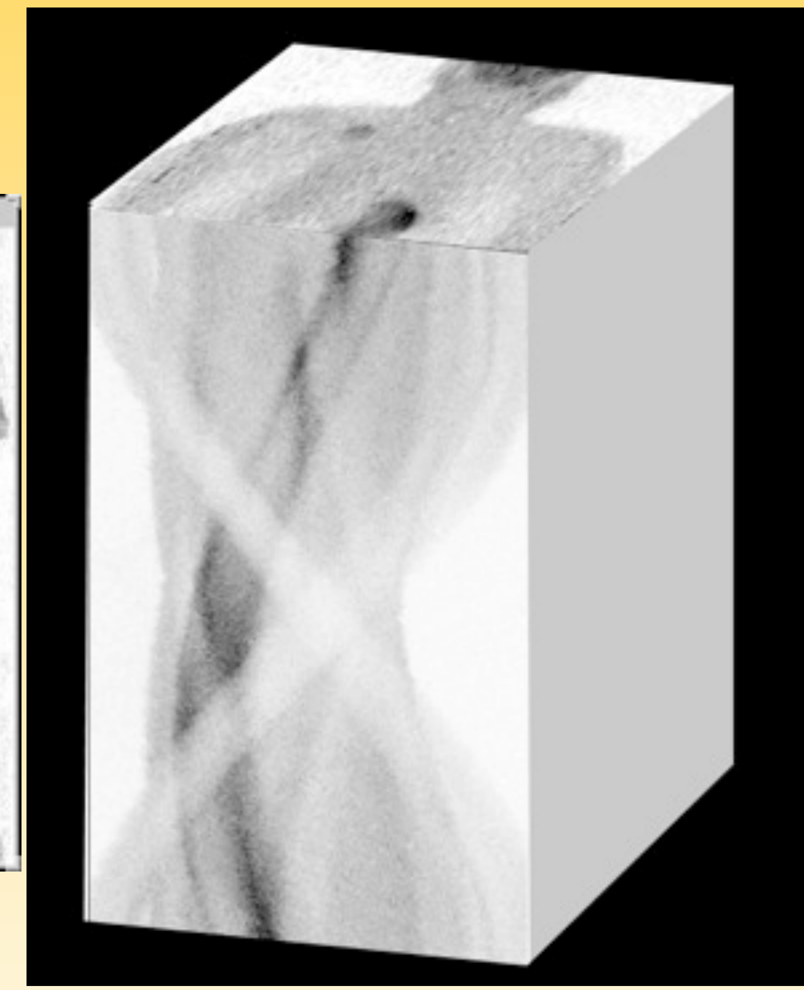

I - Recalls on Cone-Beam Computerized Tomography

- Basis of tomography : data in 2D + angle, object in 3D.

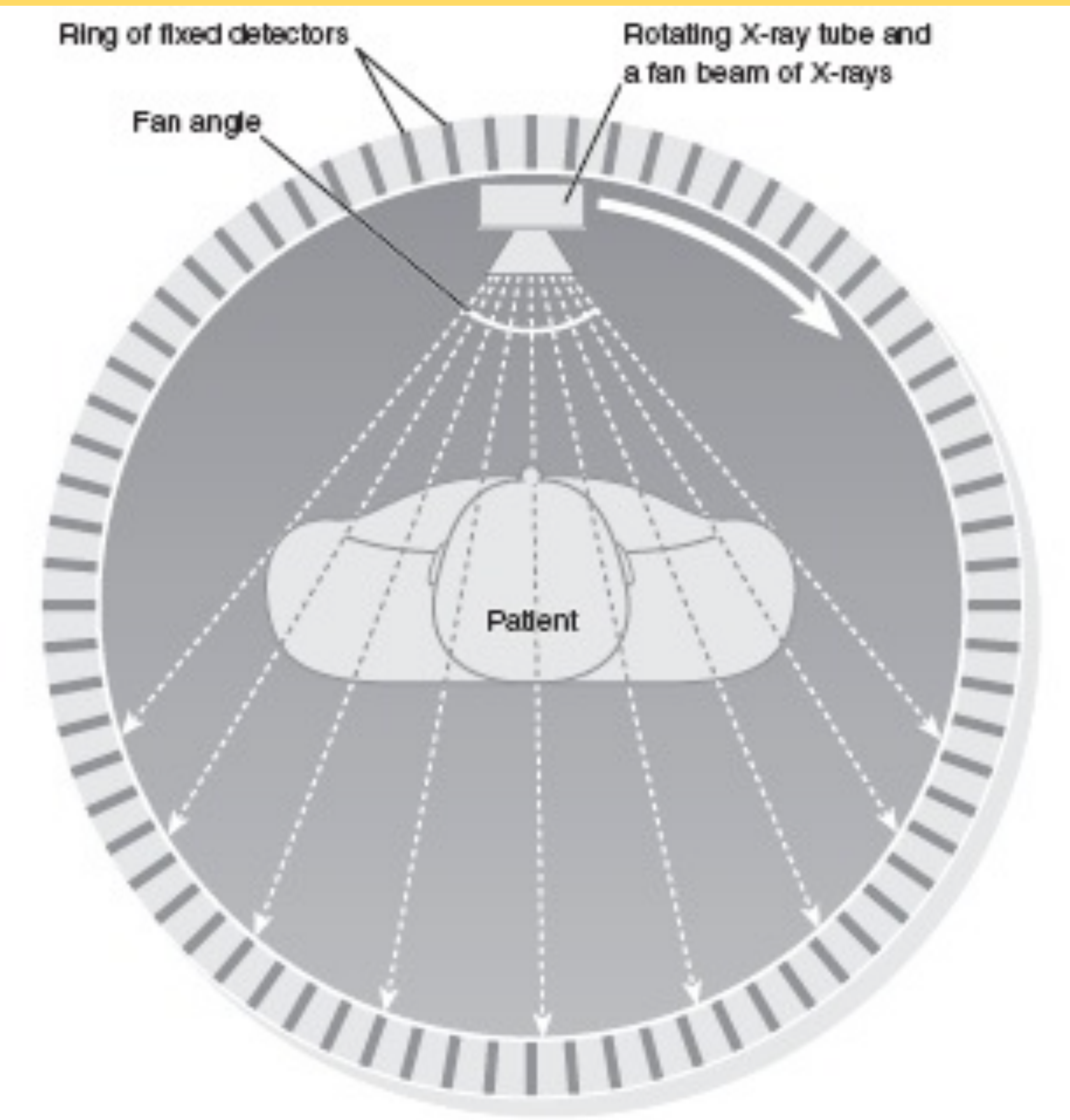

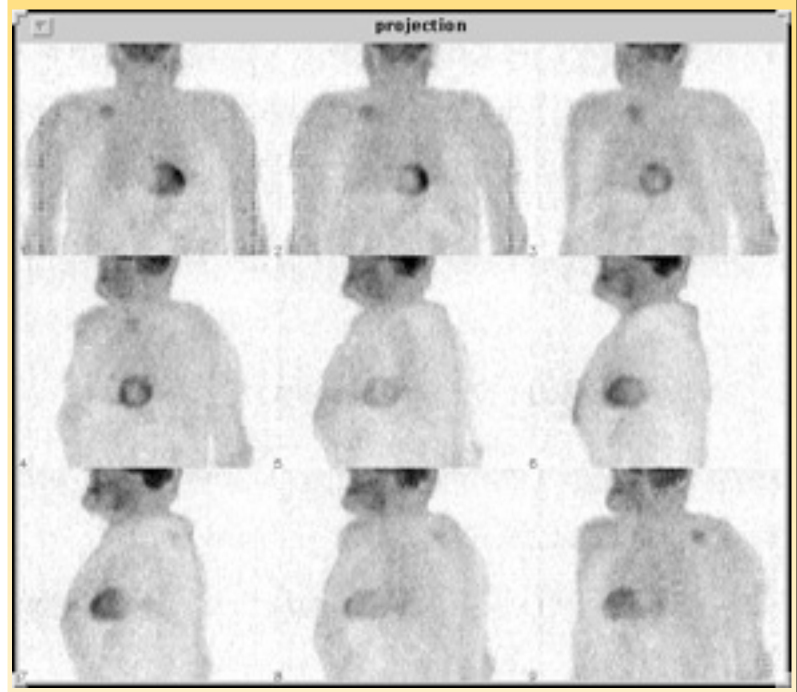

Sinogram

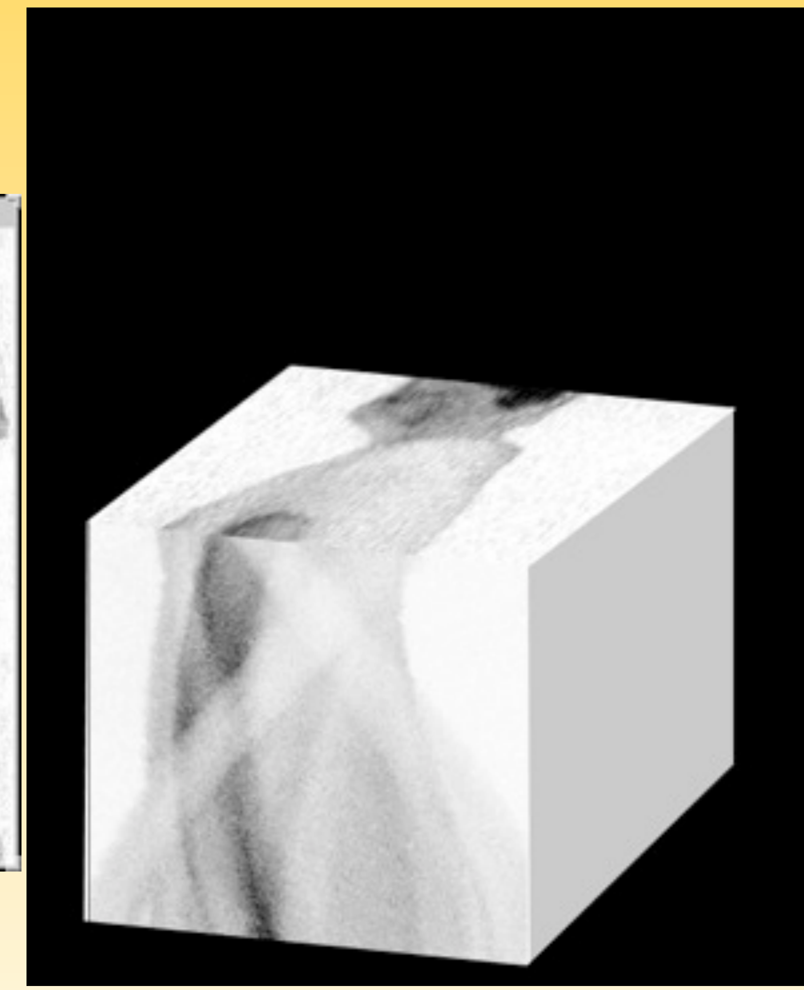

I - Recalls in emission tomography

- PET = Positron Emission Tomography

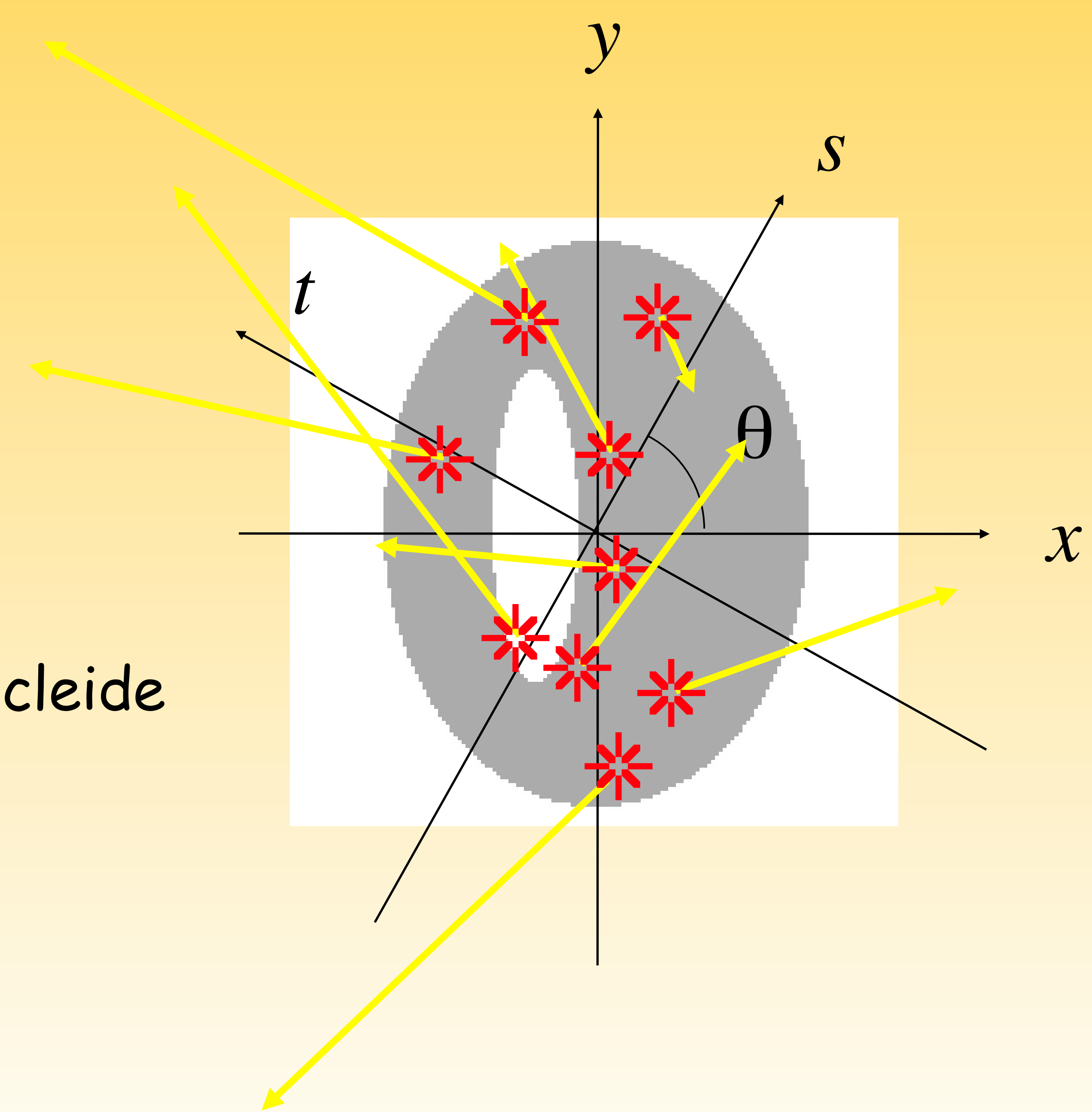

Injection of positron-emitting radionucleide

Annihilation of positron/electron

511 keV gamma rays emission

I - Recalls in tomography

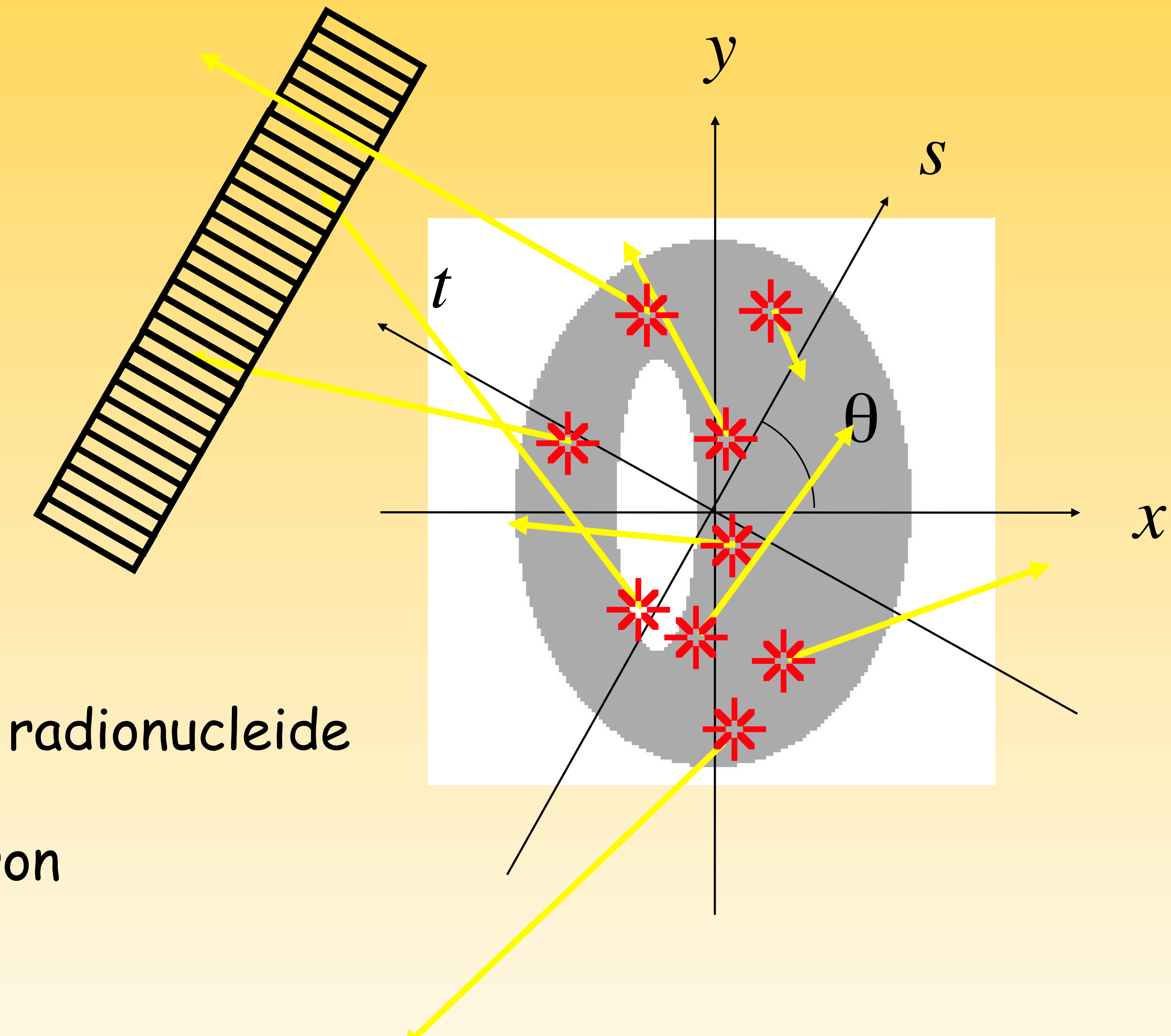

Injection of positron-emitting radionucleide

Annihilation of positron/electron

511 keV gamma rays emission

I - Recalls in tomography

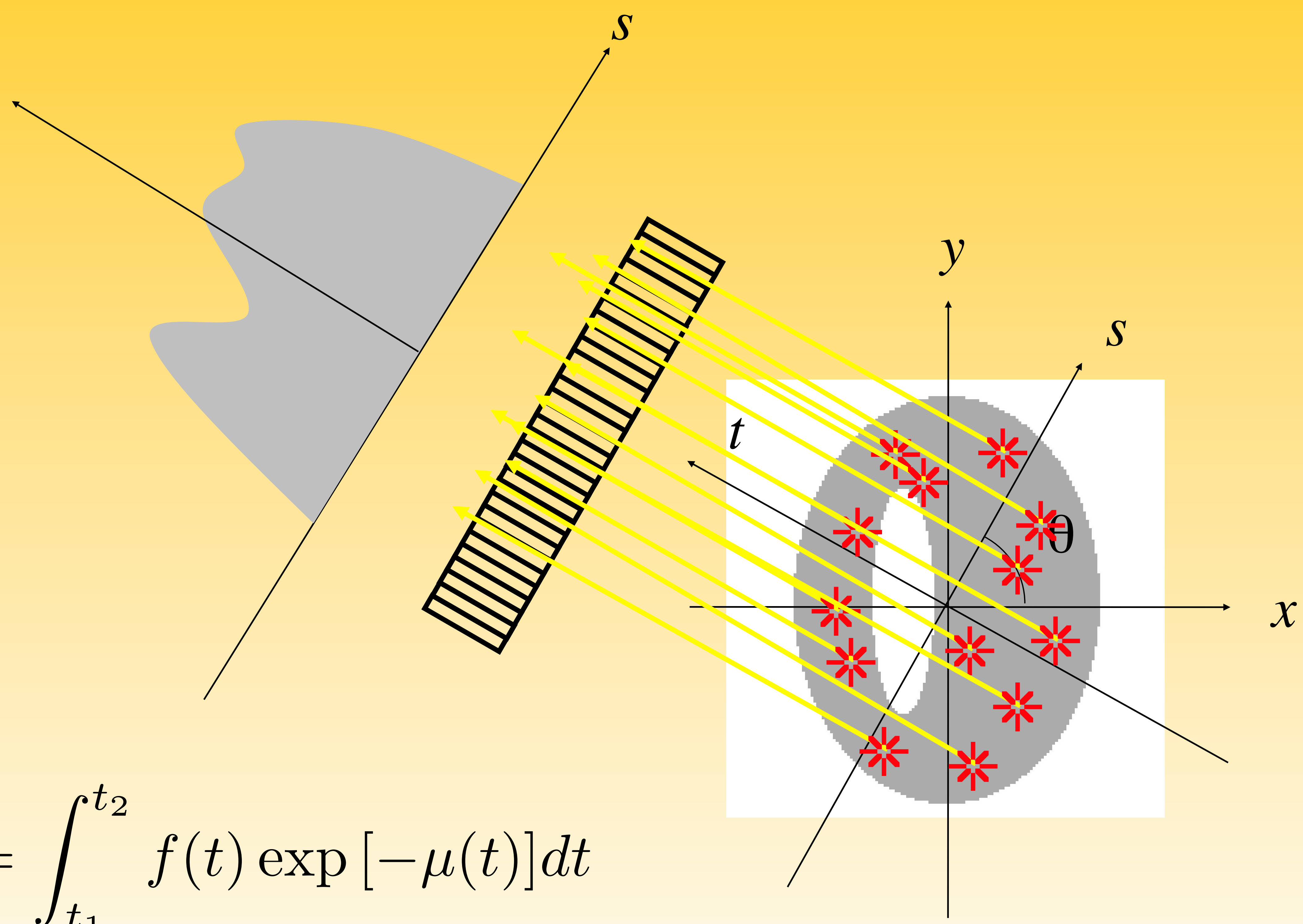

$$I = \int_{t_1}^{t_2} f(t) \exp\left[-\mu(t)\right] dt$$

Normal distribution of FDG

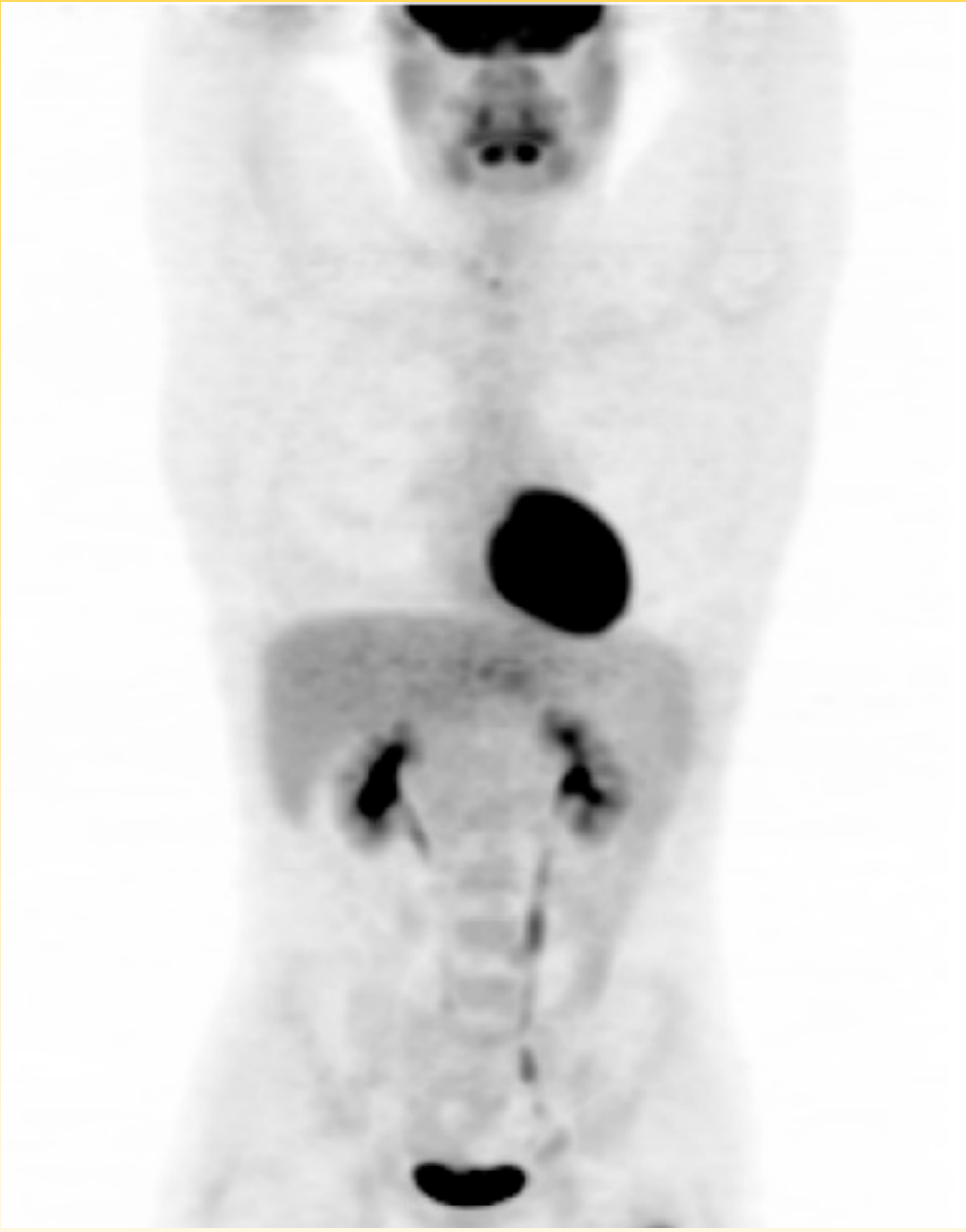

Abnormal distribution of FDG

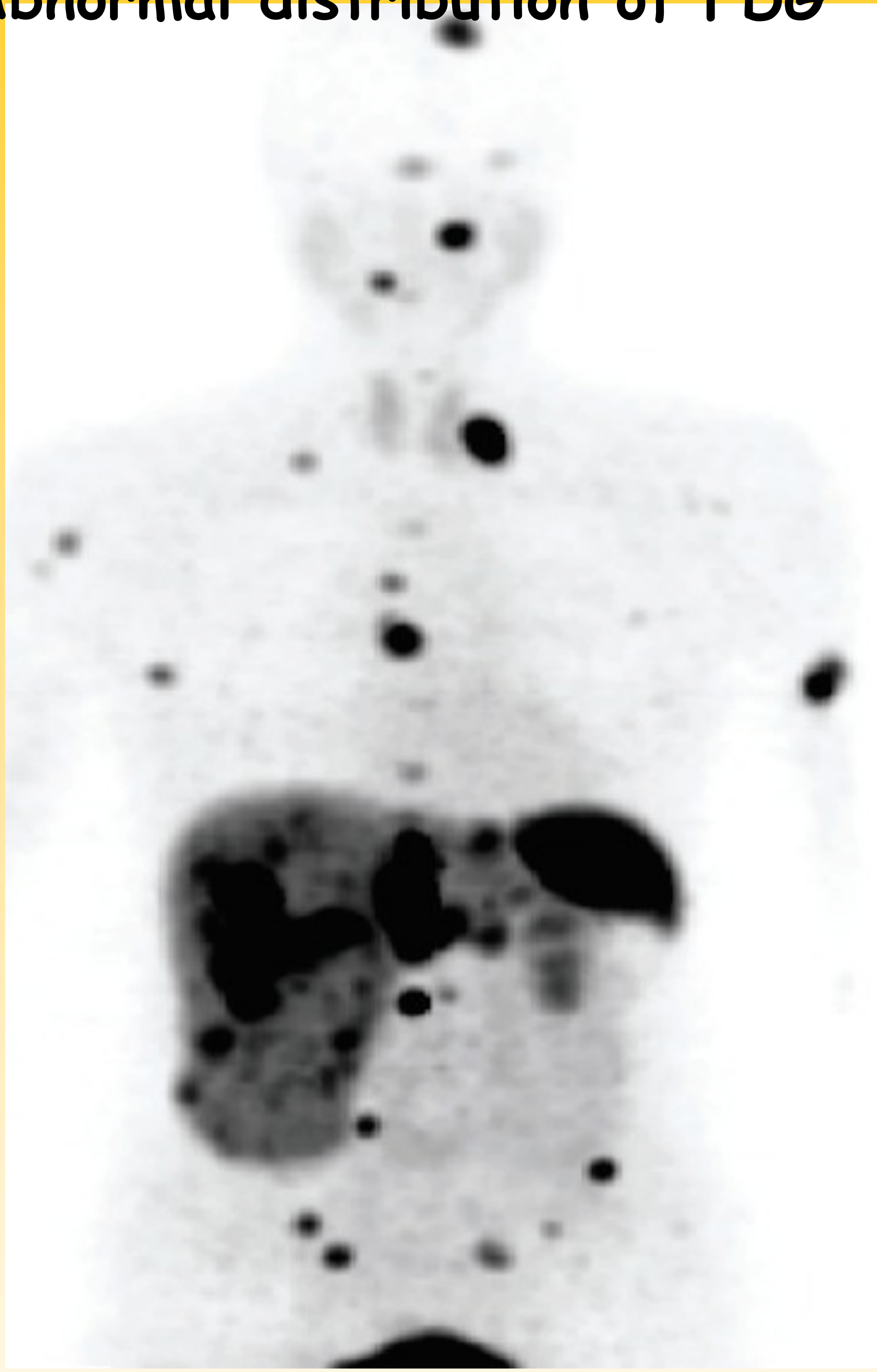

II - What's new at CPPM ? ... Biomedical imaging !

CPPM : a lab from IN2P3 for particle physics.

Physics experiences : Antares, Atlas, LHCb, D0, ... and imXgam !

Some imXgam projects :

XPIX :

Hybrid pixels for X-ray : XPAD cameras.

PIXSCAN :

Micro CT-Scanner based on hybrid pixels.

ClearPET/XPAD :

Simultaneous PET/CT imaging based on hybrid pixels.

Hybrid pixel detectors for High Energy Physics

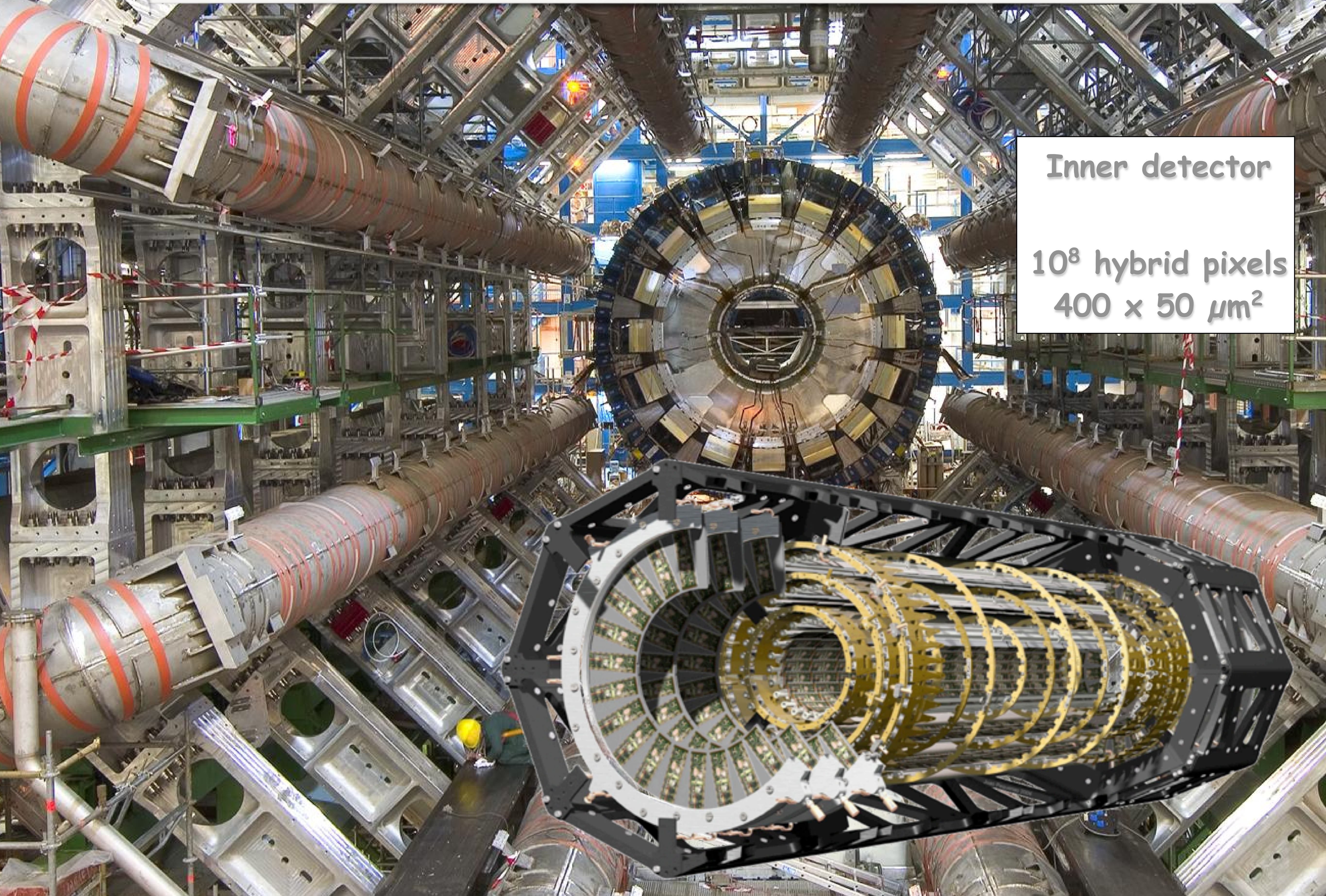

Inner detector

10^8 hybrid pixels
$400 \times 50\ \mu m^2$

Hybrid pixels

Hybrid pixel

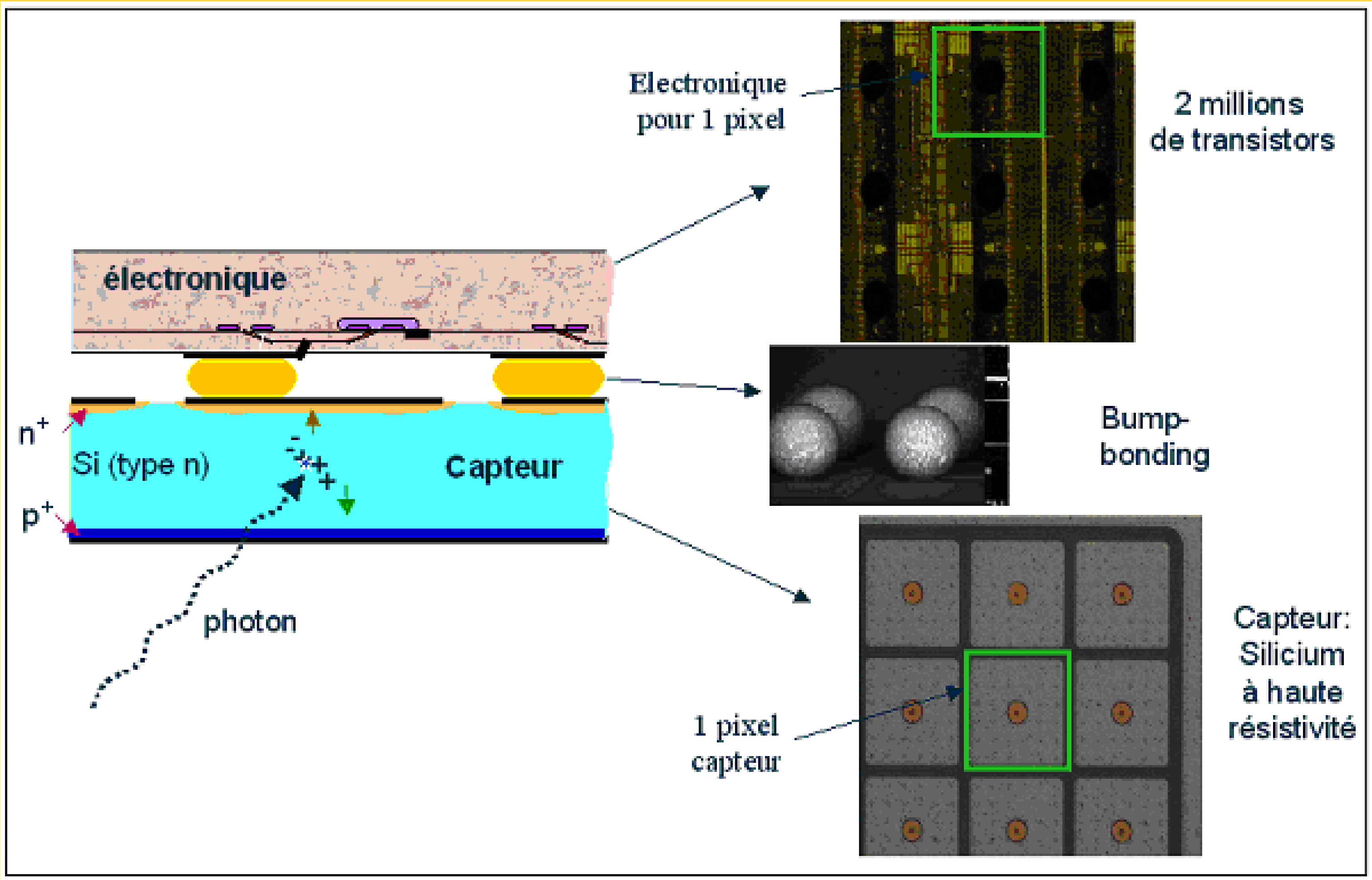

CCD

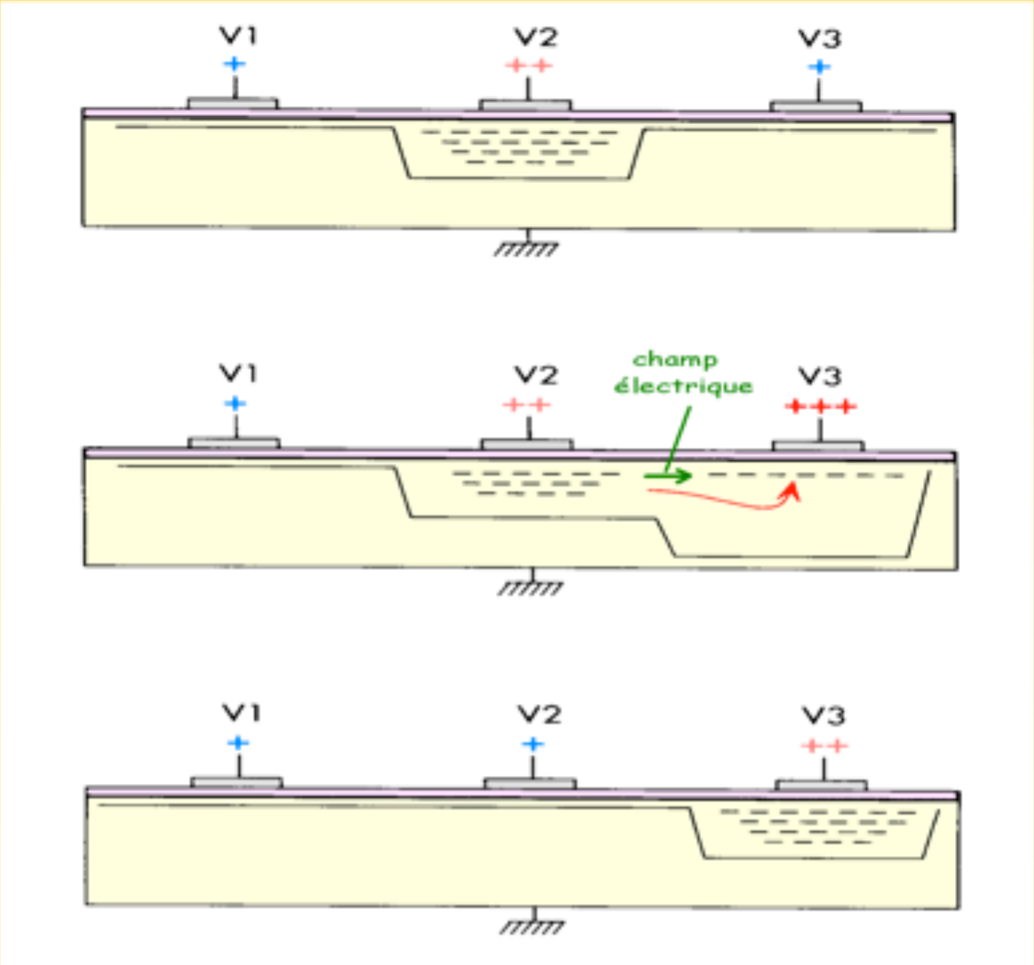

- very fast data acquisition
- choice of du substrat (Si, CdTE, AsGa)

- No Dark noise
- Energy selection
- Very large dynamic range

Fundamental difference with other detectors (CCDs-like) :

Photon counting mode !

No charge integration !

Photon counting versus charge integration

Photon counting mode

- Very low couting rate (0,01 ph/pixel/s) → **Low statistics**
- Large dynamic range (10^{-2} - 10^{6} ph/pixel/s , 80dB) → **Enhanced detectability at low contrast**

Energy threshold of detection

- Energy selection of X-rays → Discriminating diffused photons → **Enhanced contrast**

Choice of sensor

- High density sensors → Better detection efficiency → **Enhanced detectability + Low statistics**

XPAD3 camera : more than 500,000 pixels of 130 µm

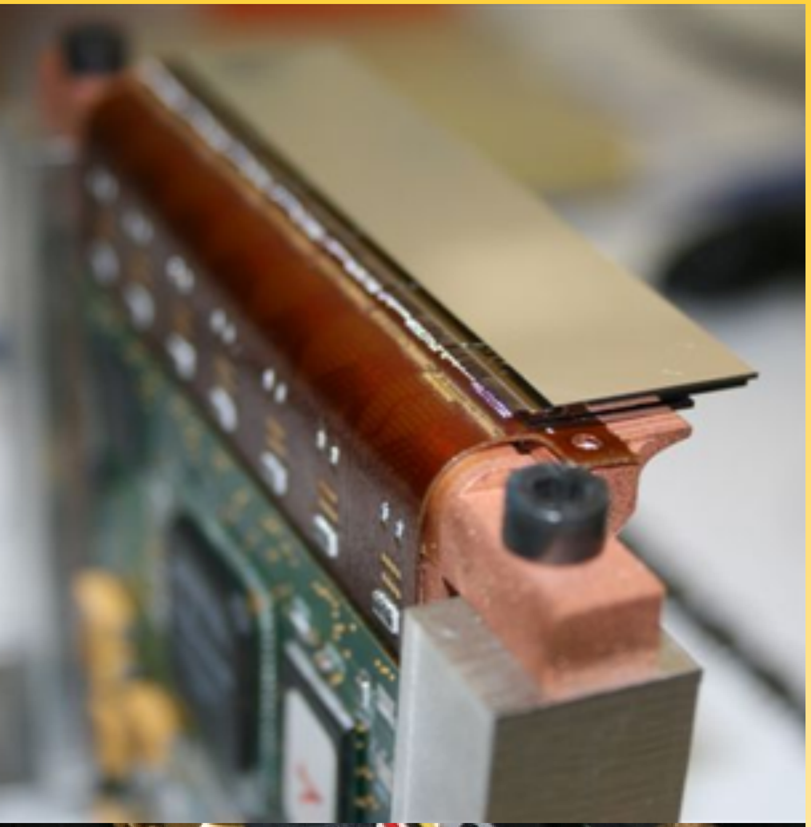

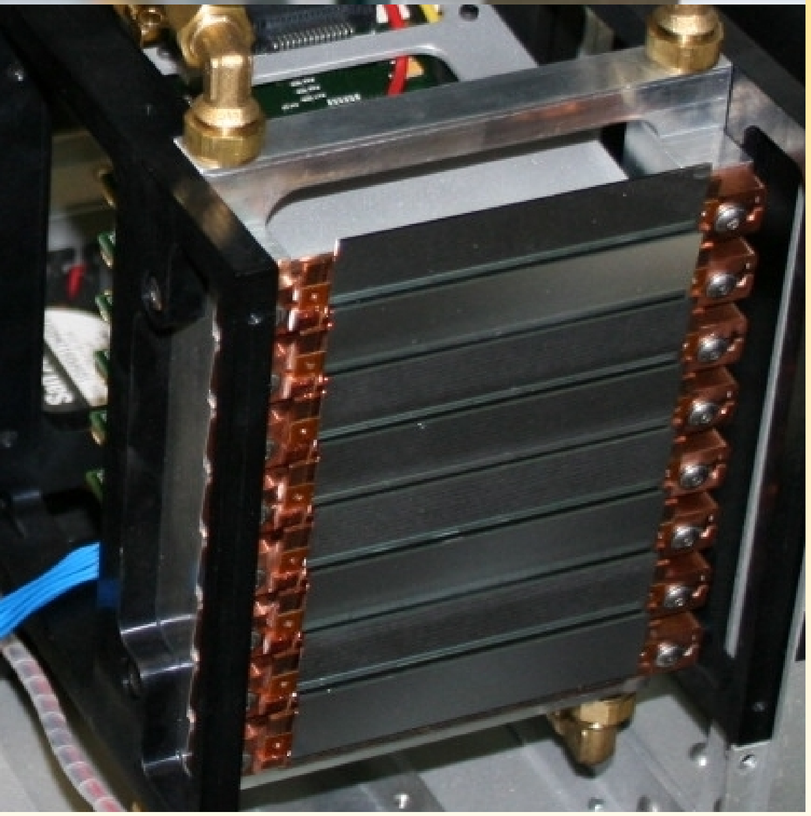

New hybrid pixel camera for X-rays XPAD3/Si

- Photon couting
- Silicon sensor : 500 µm thickness.
- 125 x 75 mm^2 : detector size
- 130 x 130 μm^2 : pixel size
- 560 x 960 pixels
- Fast readout and data transfer : up to 300 frames/s (optical fibre and PCIExpress)

Chips 1x1cm assembled in barrettes,
barrettes assembled in tiles.

Whole-body mouse with spatial resolution of 60 µm

Démonstrateur micro-CT PIXSCAN II

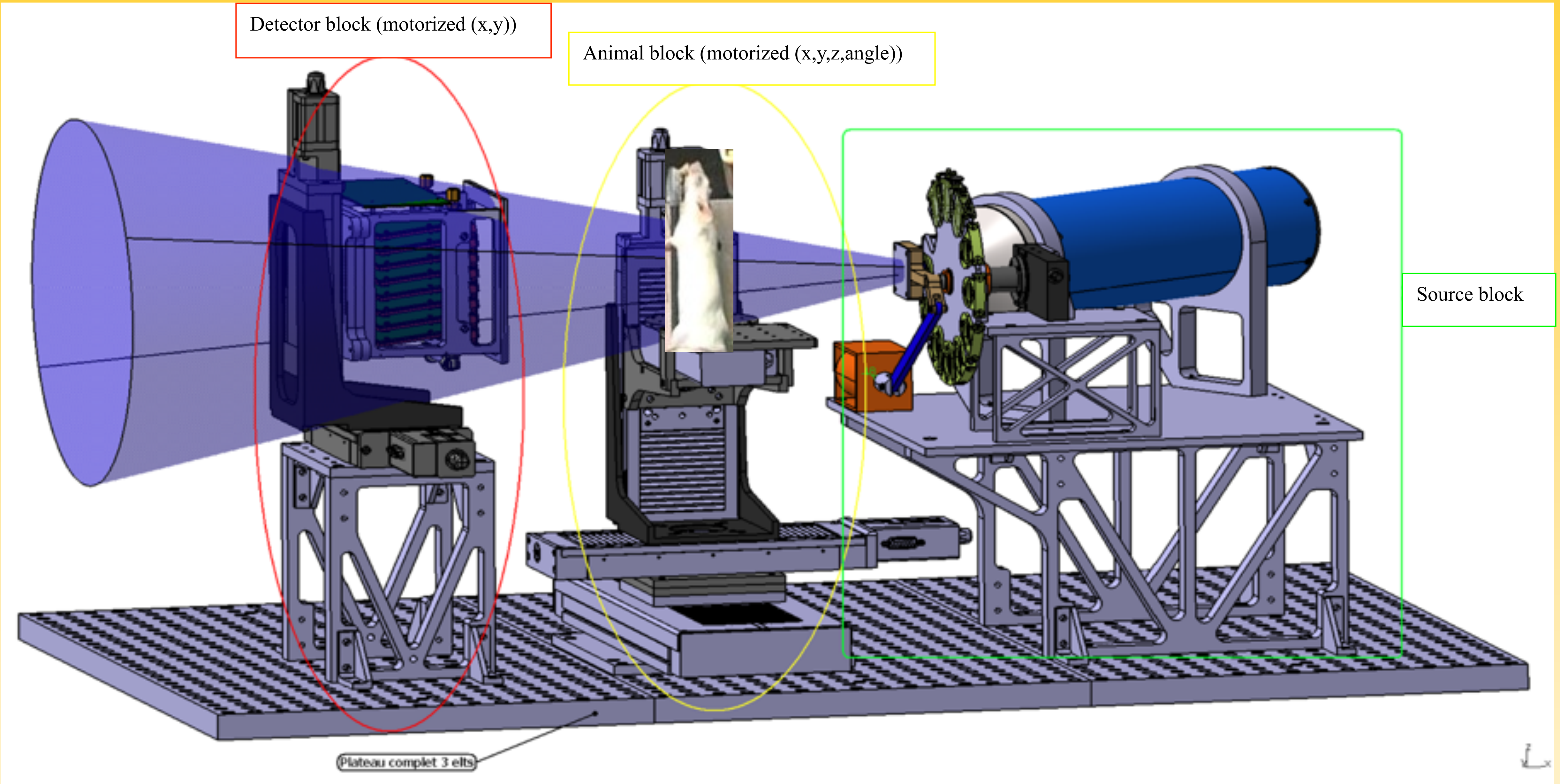

Complete system : 3 blocks

OXFORD Intruments X-ray tube

Target Voltage 10 to 90kv, Target Current up to 2 mA

W target, 13 to 40 µm focal spot size, 80 W, 33 degrees Cone Angle

micro-CT PIXSCAN II demonstrator

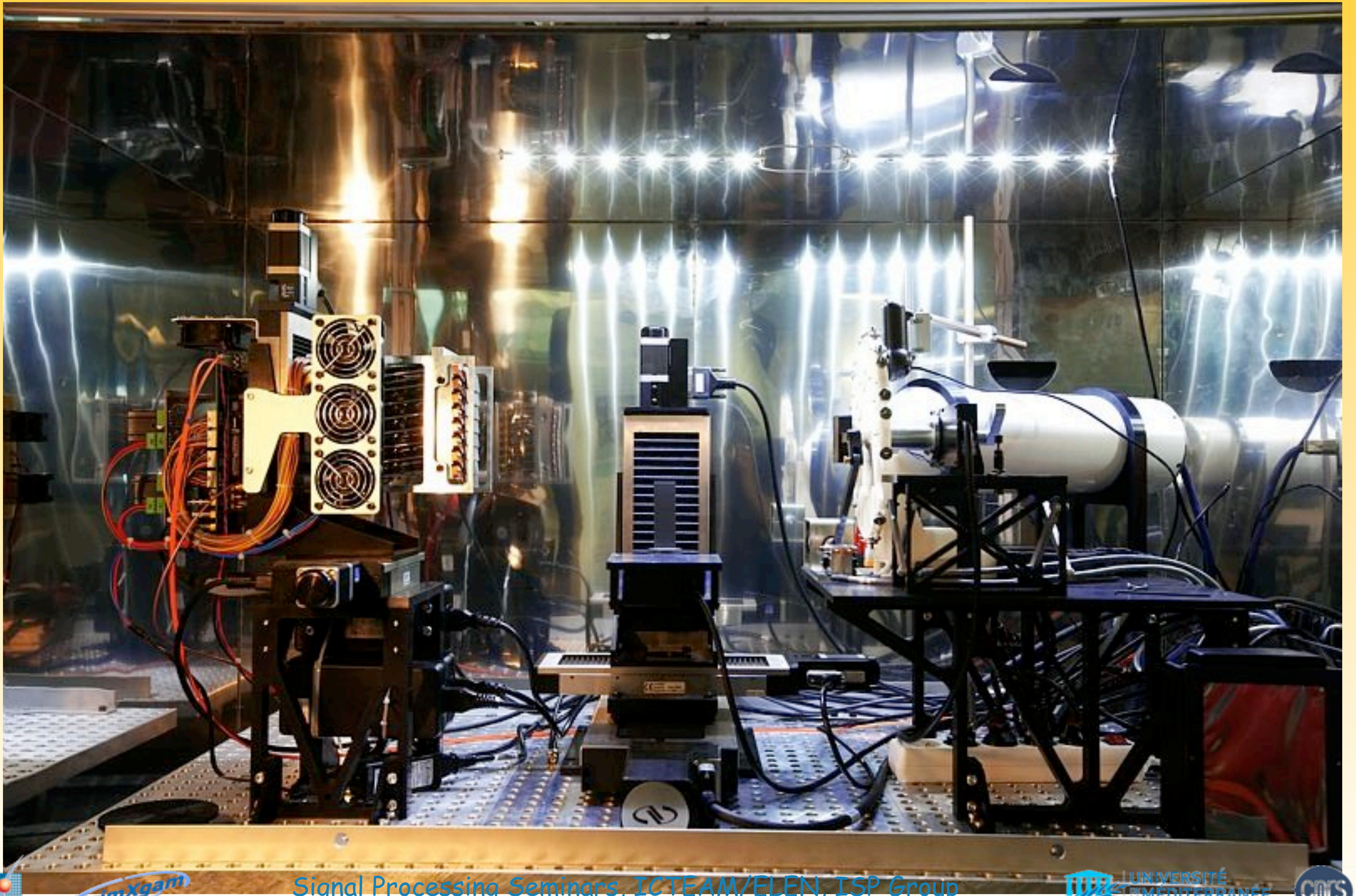

First light XPAD3/PIXSCAN II

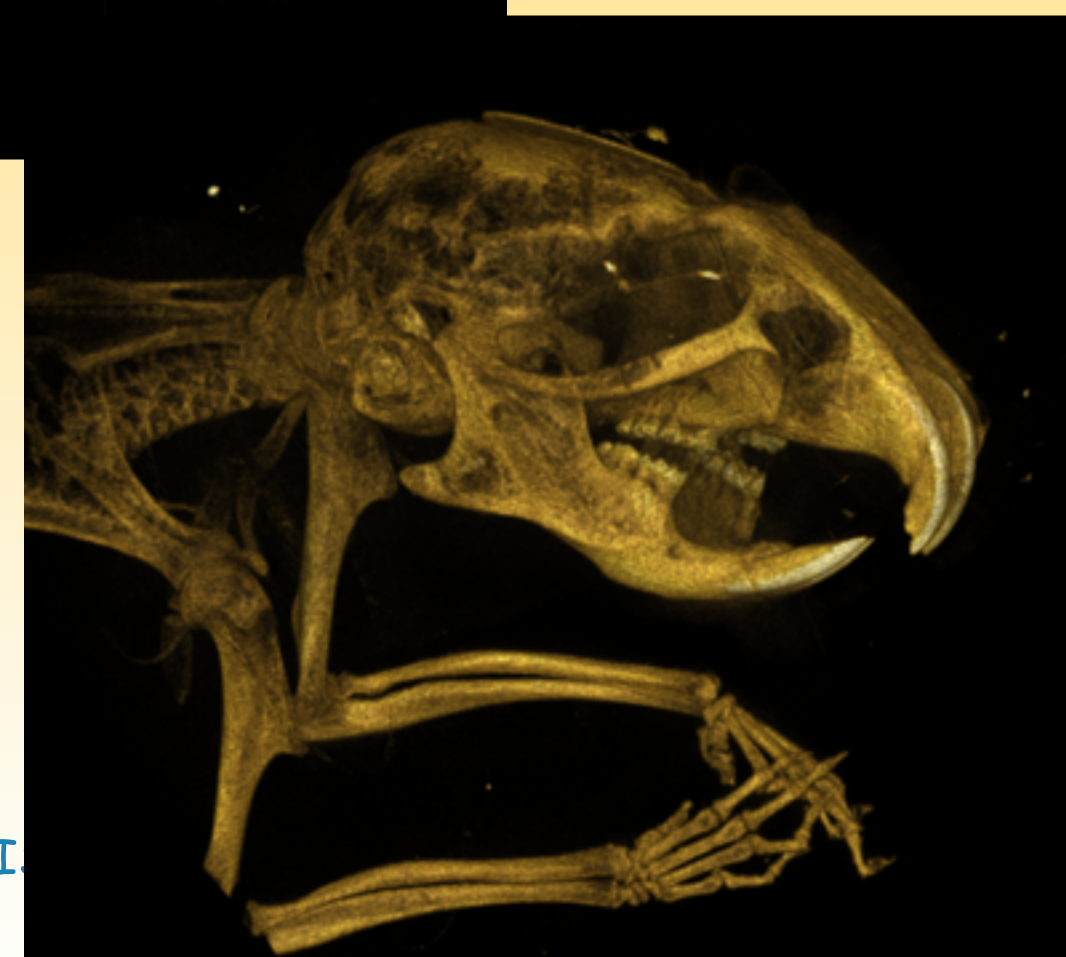

Reconstruction performed on a GPU AMD/ATI, Algorithm FDK.

But need of 720 projections and >1mGy/s at 160 mm

ClearPET + XPAD = ClearPET/XPAD

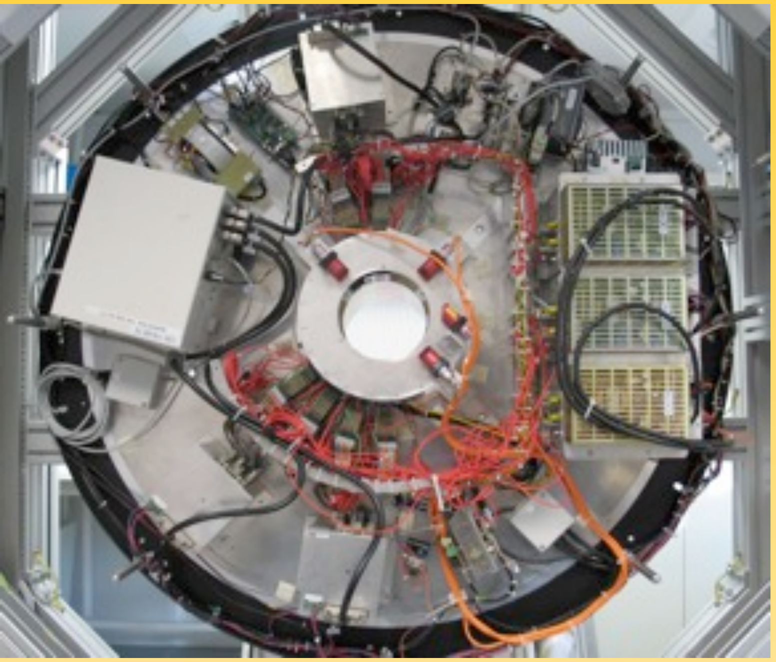

\+

=

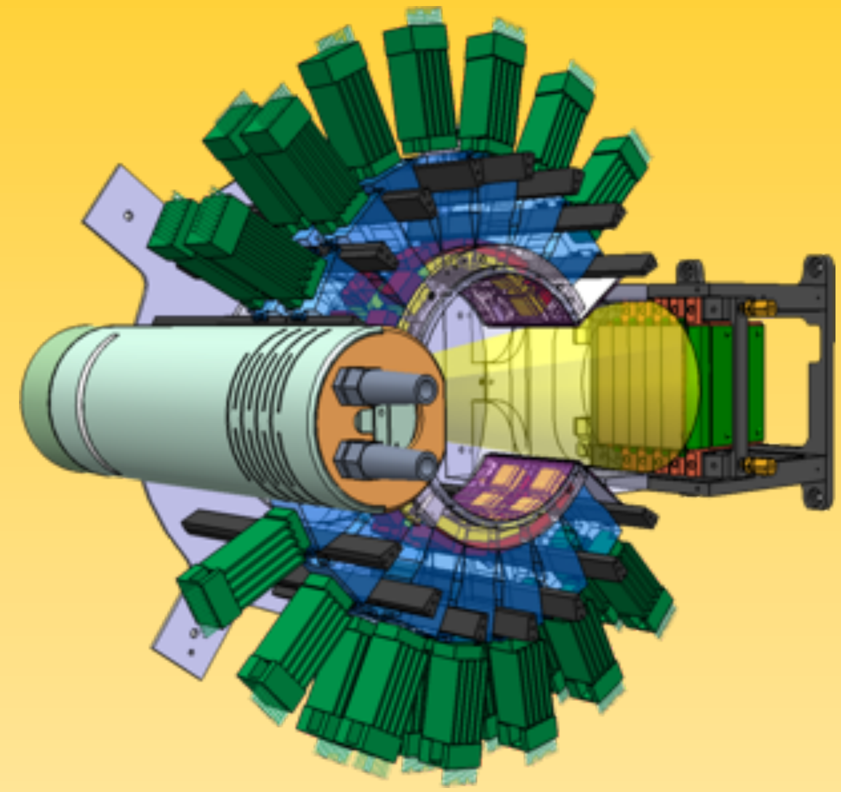

ClearPET (EPFL)

- Open geometry
- Phoswich LSO/LuYAP detectors
- 2 x 64 cristals of 2 x 2 x 8 mm^3
- PMT multi-anodes at 64 channels

XPAD (CPPM)

- XPAD3 camera
- 500 µm Si pixelized
- Pixels of 130 x 130 µm^2
- 0,5 Mpixels
- Energy selection 5-35 keV
- W X-ray source

CleartPET/XPAD

- Hybrid tomography
- Simultaneous TEP/TDM
- TEP : 55 mm axial
111 mm transverse
- TDM : 59 mm axial
38 mm transverse

Anatomy + Function

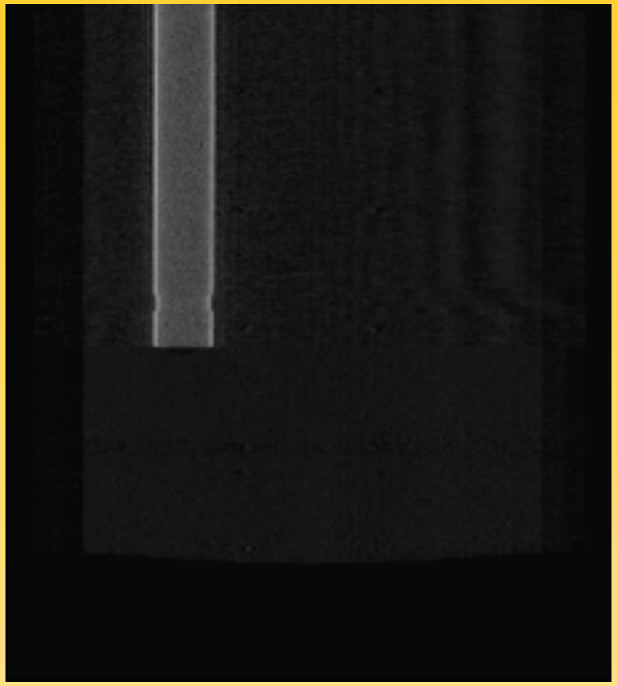

Merging process

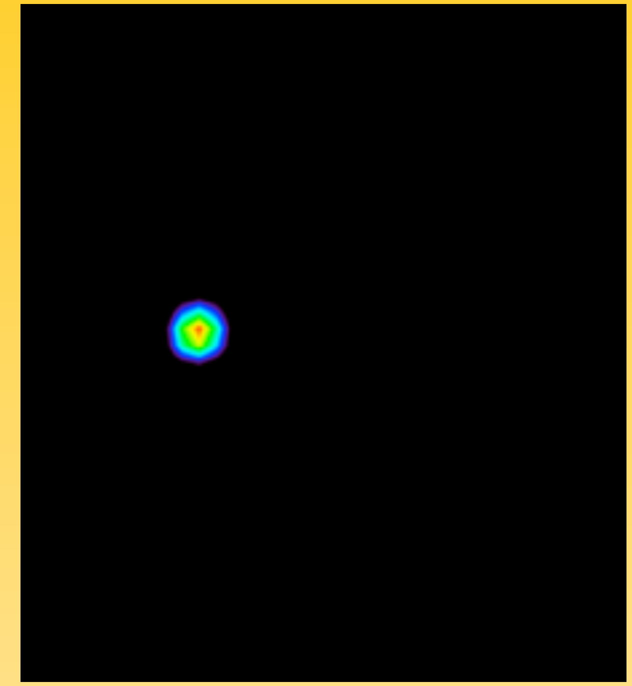

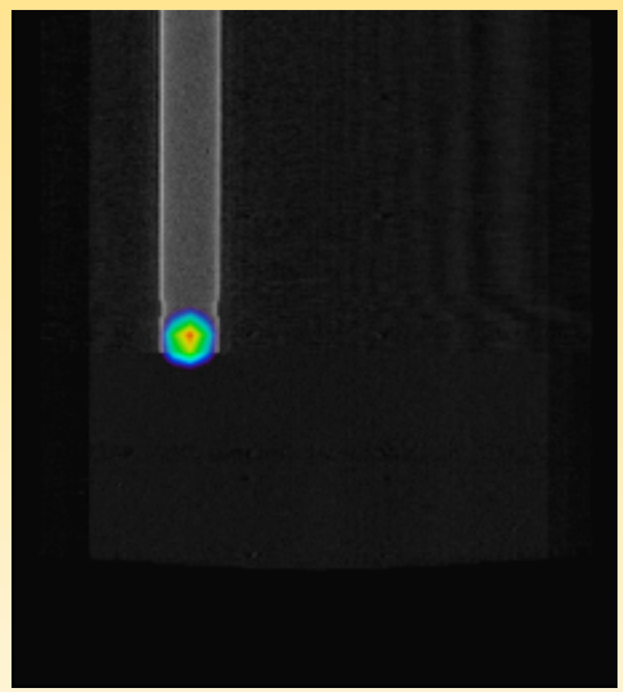

X-ray : CBCT -> anatomy

Positron : PET -> Function

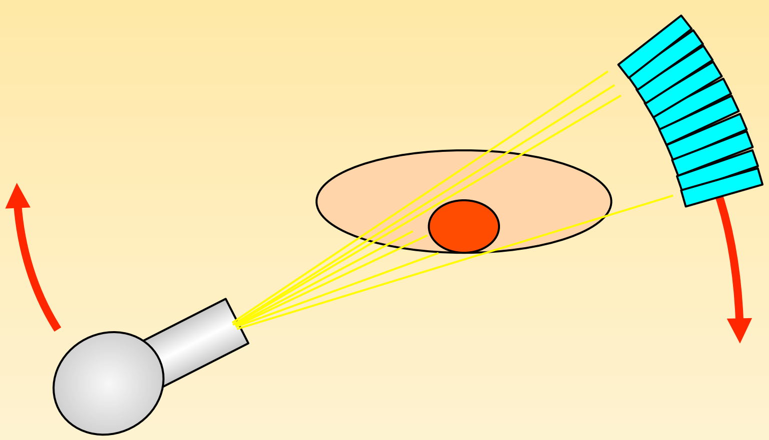

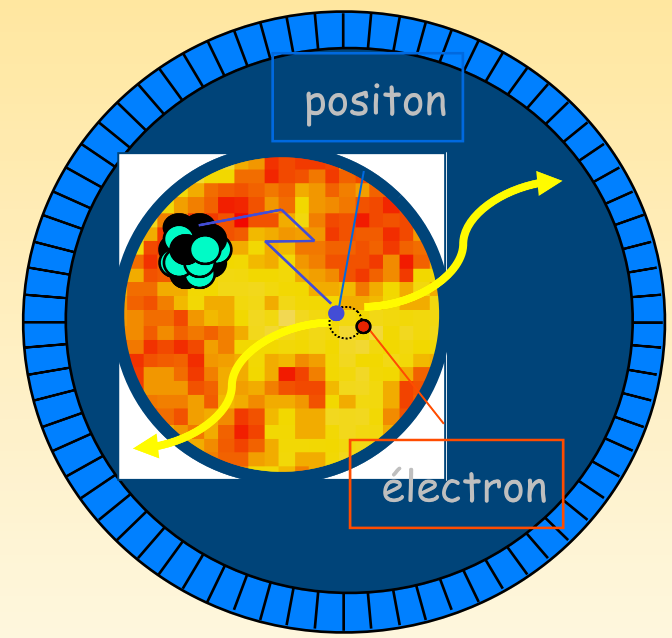

Image merging

PET/CT scan of a mouse : SIMULTANEOUS ACQUISITION

- Volume rendering
- Segmentation of lungs and kidneys
- 40 kV, 800 µA, filter Nb/Mo
- 360 projections
- 1 s/projection
- 10 000 photons/pixel

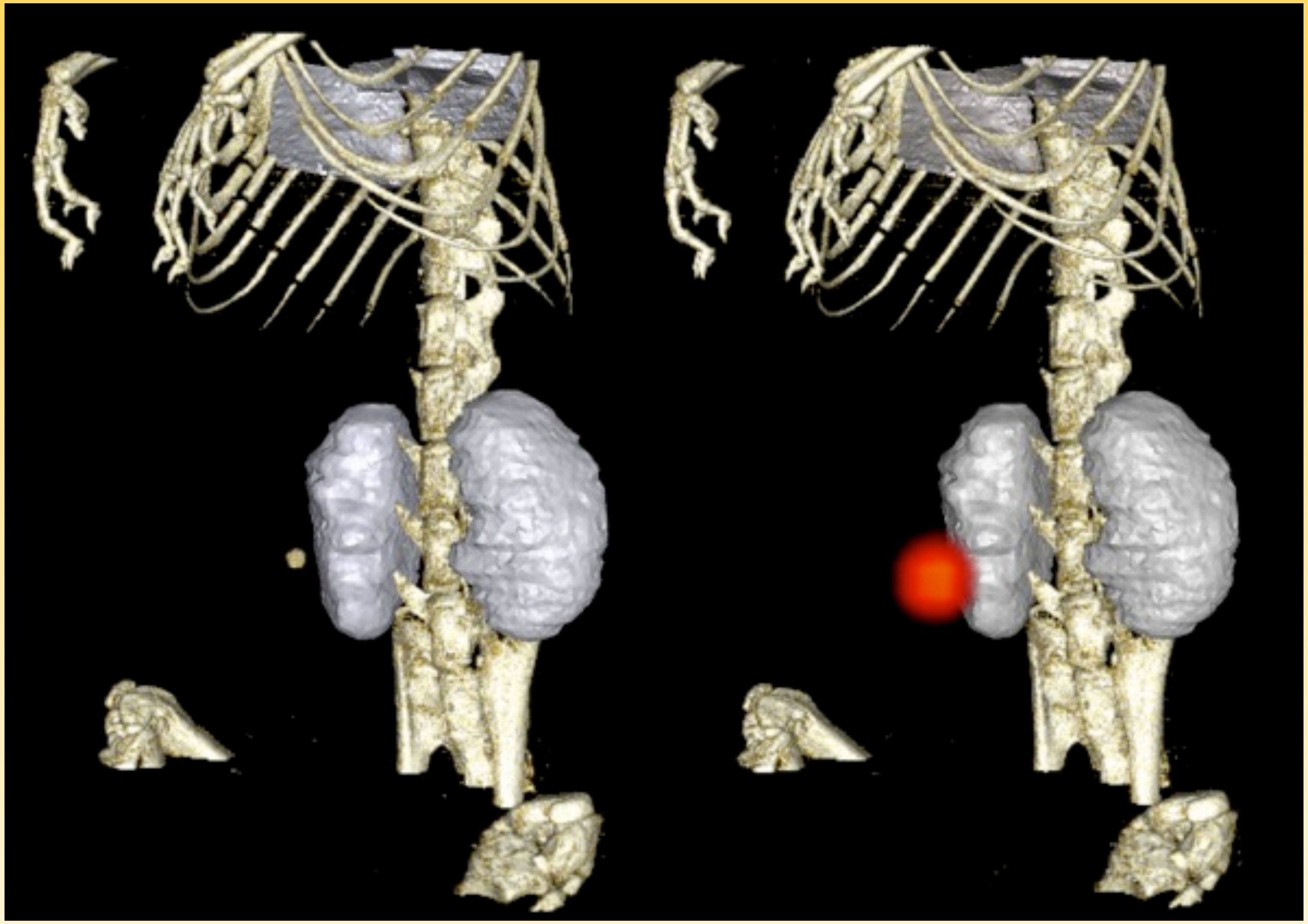

Challenges

- High quality of reconstruction while :
  - reducing the X-ray dose (CT)
  - reducing the radiotracer dose (PET)
  - reducing the exam duration (PET)

- Possible solutions :
  - Reduce the number of projections (CT)
  - Reduce the intensity of acquired signals (PET and CT)

Need to deal with pure Poisson Noise ...

III - Frameworks

Under the assumption of a monochromatic beam, a hybrid pixel measures

$$y_j = z_j \exp\left(-\left[A\mu\right]_j\right)$$

A crystal of the ClearPET measures

$$y_j = \left[Bx\right]_j$$

where the system matrices A and B incorporates geometry and corrections.

Need to deal with pure Poisson Noise ...

$$y \sim \mathcal{P}(x) \quad \longleftrightarrow \quad P(Y = y) = e^{-x}\frac{x^y}{y!}$$

Why regularization ?

Let's define $y \in \mathbb{R}^n$ the measures,

and $x \in \mathbb{R}^m, \mu \in \mathbb{R}^m$ the unknown to recover

and $A \in \mathcal{M}(\mathbb{R}^n, \mathbb{R}^m), B \in \mathcal{M}(\mathbb{R}^n, \mathbb{R}^m)$ the system matrices.

with $n << m$ in general ...

- Tomography is an (inverse) ill-posed problem !!!!
- System matrices are ill-conditioned operators..
- ... and degenerated operators, i.e. kernels non reduced to {0}.

III - CBCT Framework

Incorporating Poisson Noise

$$y_j \sim \mathcal{P}\left(z_j \exp\left(-\left[A\mu\right]_j\right)\right)$$

Log-likelihood

$$L(\mu) = -\sum_j \left\{y_j \left[A\mu\right]_j + z_j \exp\left(-\left[A\mu\right]_j\right)\right\}$$

General objective function

$$\hat{\mu} = \arg\min_x -L(\mu) + \lambda J(\mu)$$

$$\hat{\mu} = \arg\min_\mu \sum_j \left\{y_j \left[A\mu\right]_j + z_j \exp\left(-\left[A\mu\right]_j\right)\right\} + \lambda J(\mu)$$

III - PET Framework

Incorporating Poisson Noise

$$y_j \sim \mathcal{P}\left([Bx]_j\right)$$

Log-likelihood

$$L(x) = \sum_j \{y_j \log([Bx]_j + \epsilon) - [Bx]_j\}$$

General objective function

$$\hat{x} = \arg\min_x -L(x) + \lambda J(x)$$

$$\hat{x} = \arg\min_x \sum_j \{[Bx]_j - y_j \log\left([Bx]_j + \epsilon\right)\} + \lambda J(x)$$

Without regularization

10 000 photons in white, 360 projections

MLEM algorithm : no regularization

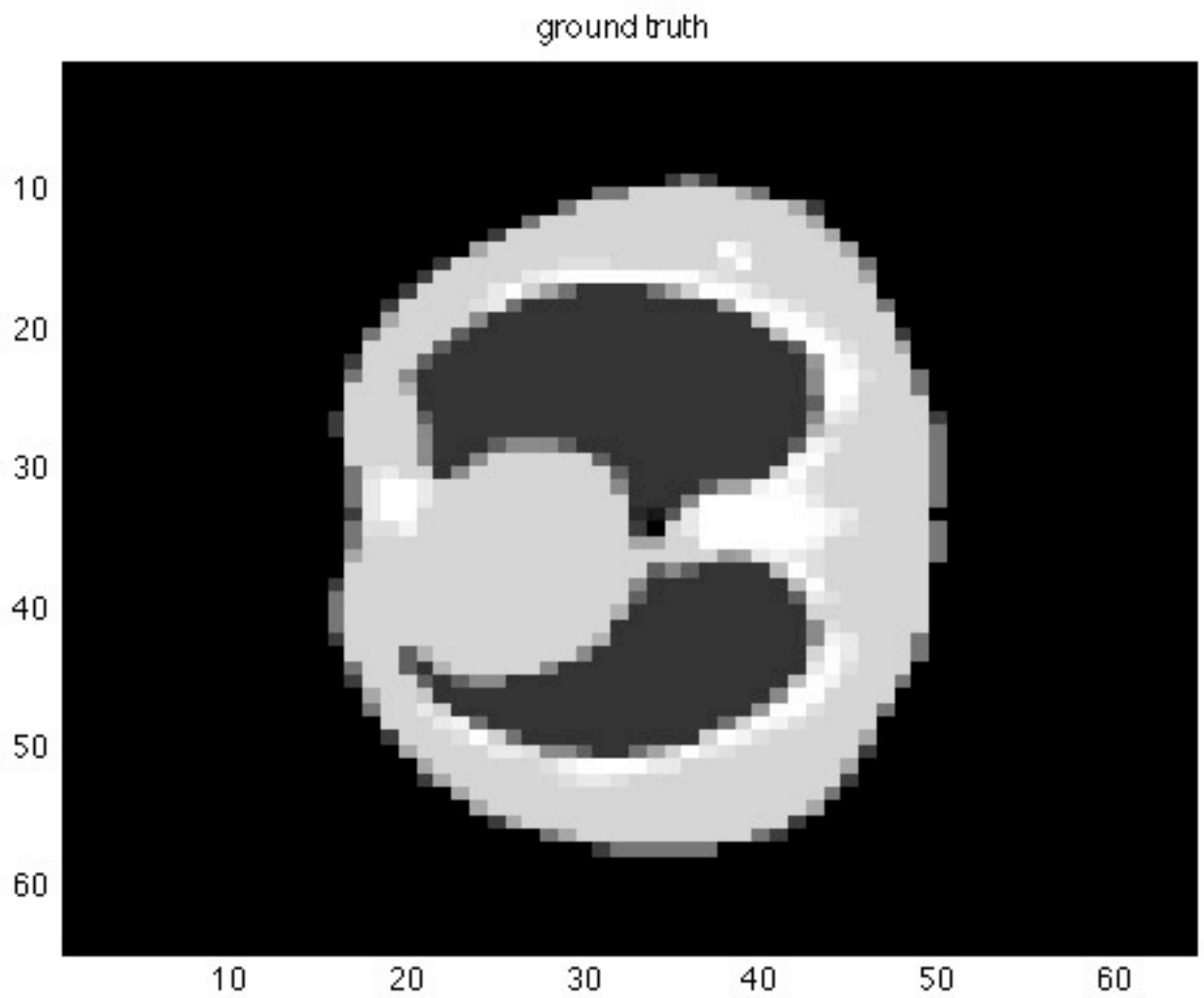

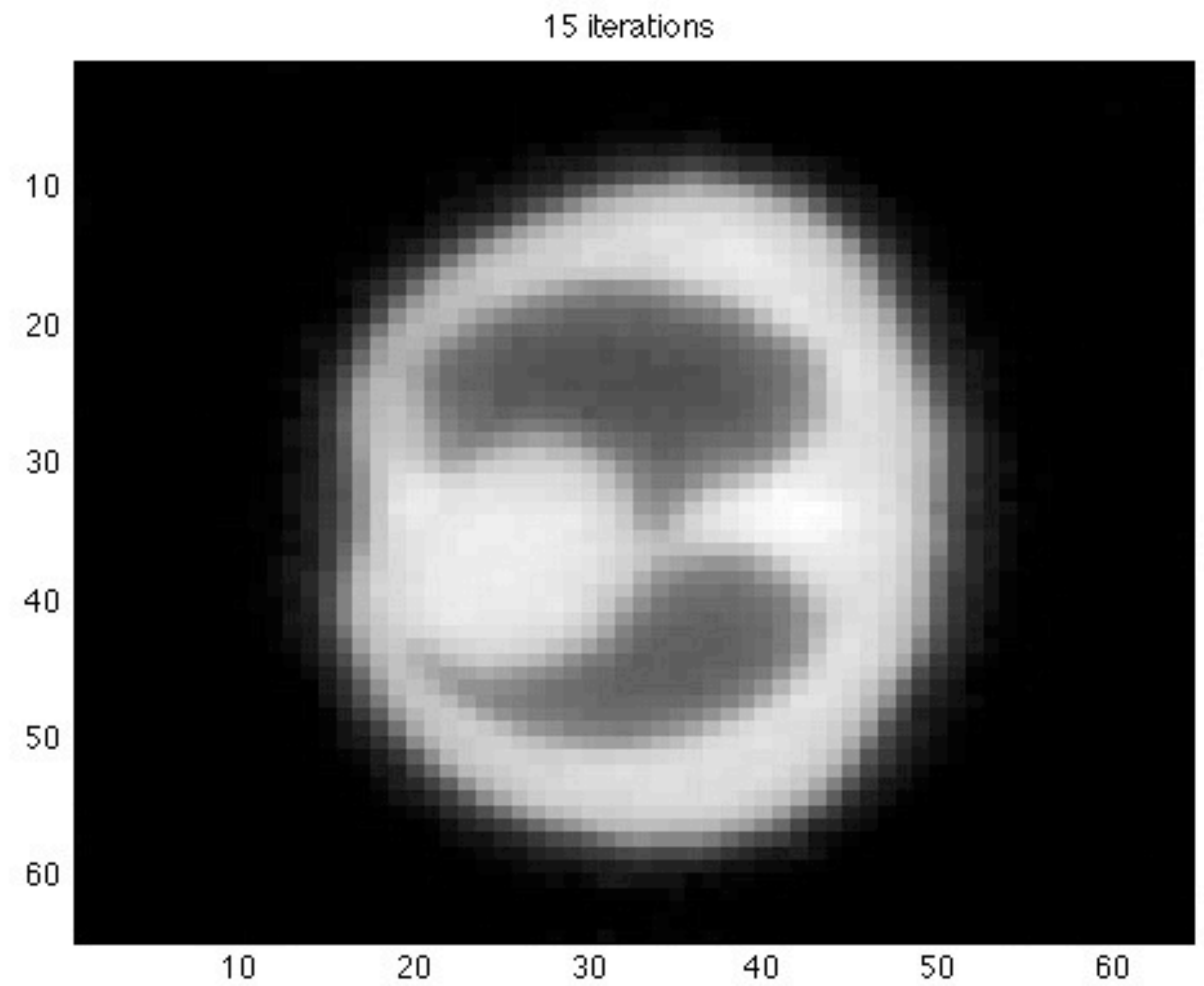

Without regularization

10 000 photons in white, 360 projections

MLEM algorithm : no regularization

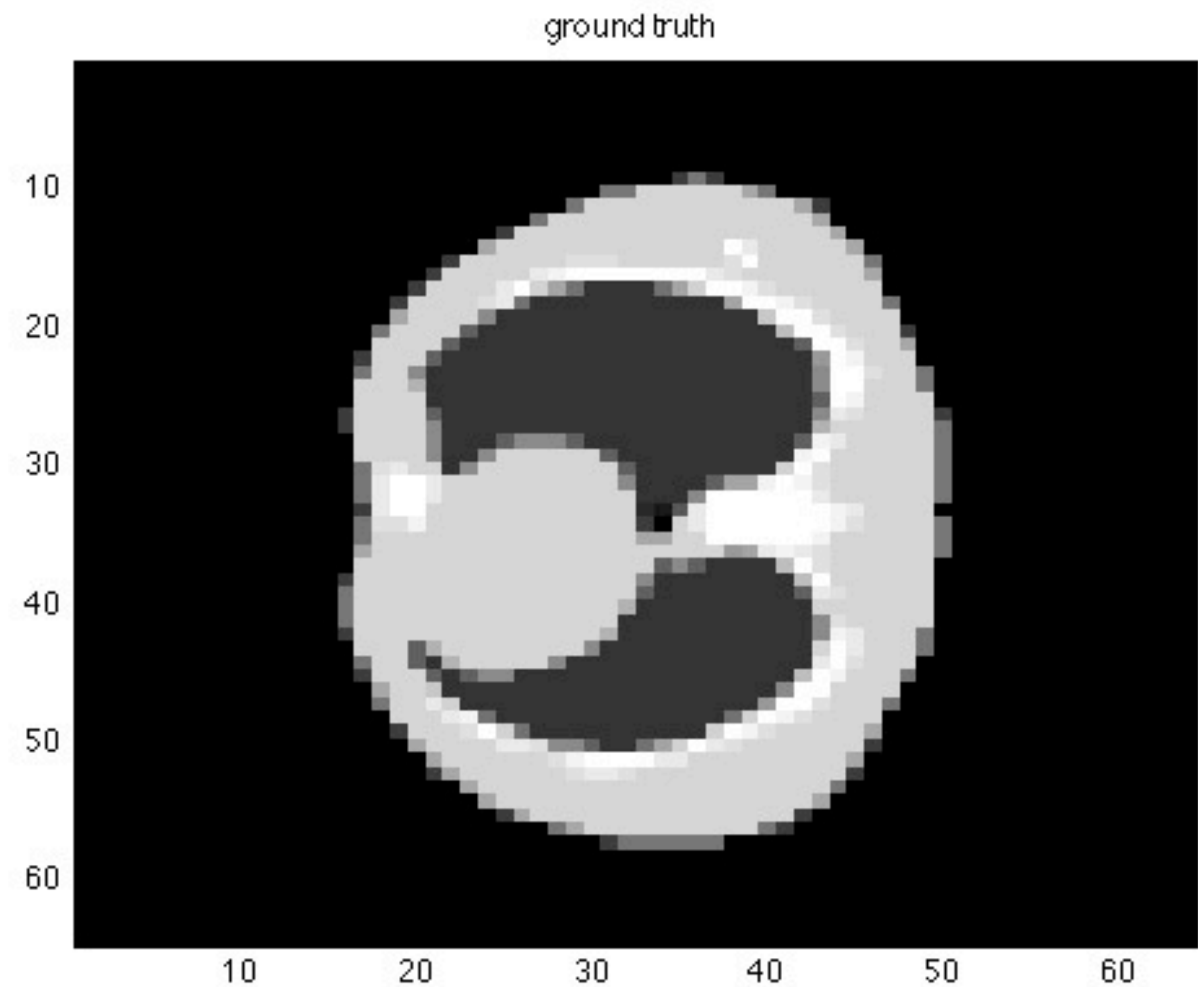

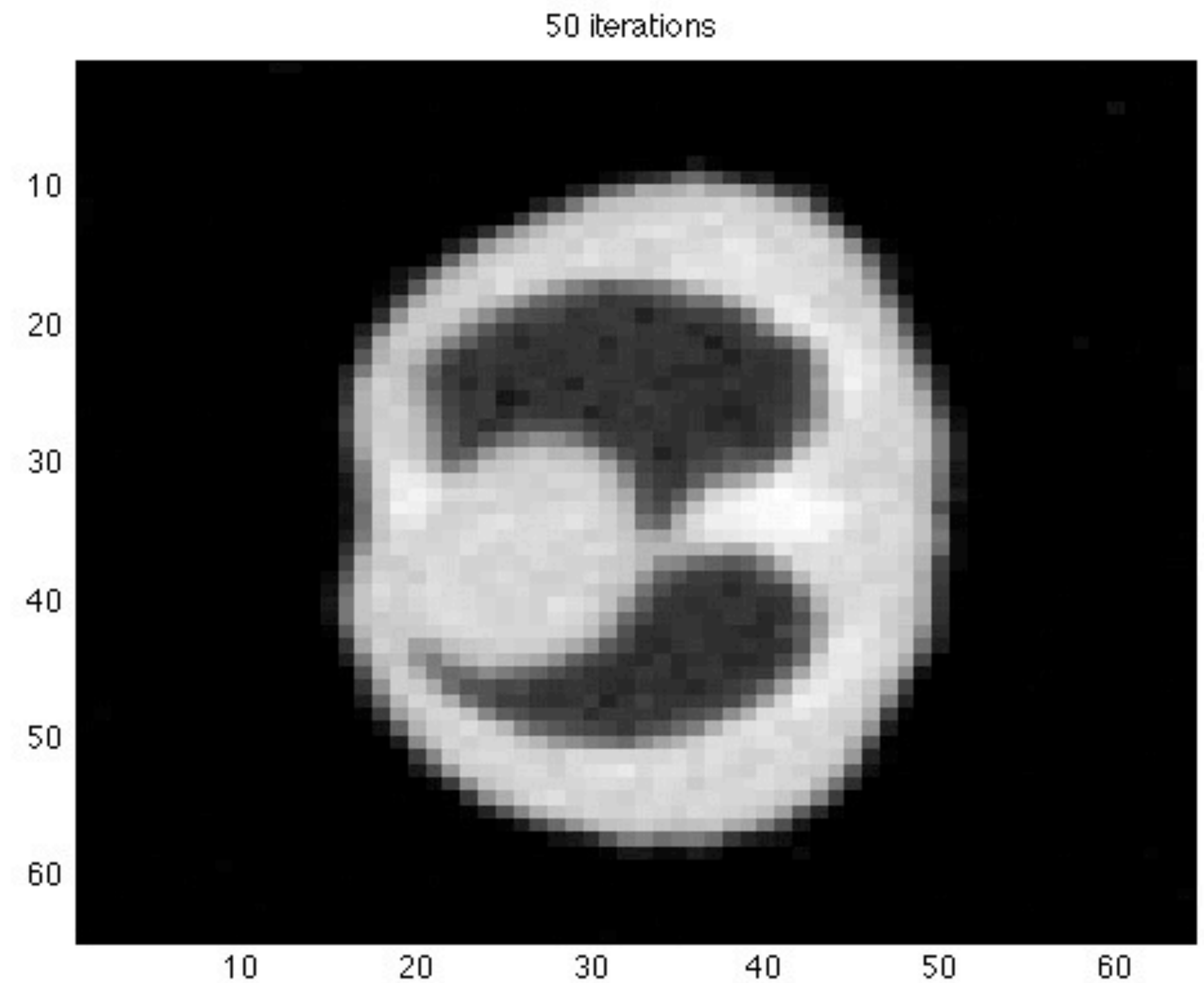

Without regularization

10 000 photons in white, 360 projections

MLEM algorithm : no regularization

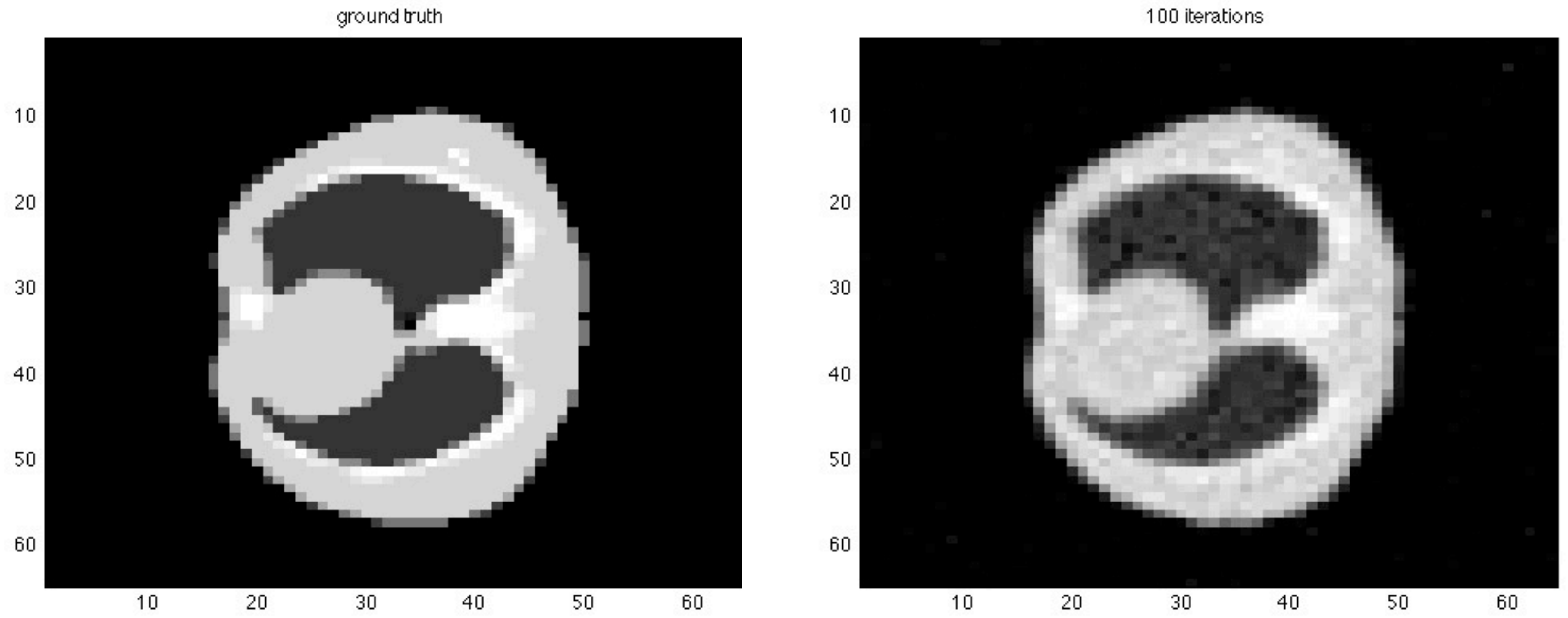

Without regularization

10 000 photons in white, 360 projections

MLEM algorithm : no regularization

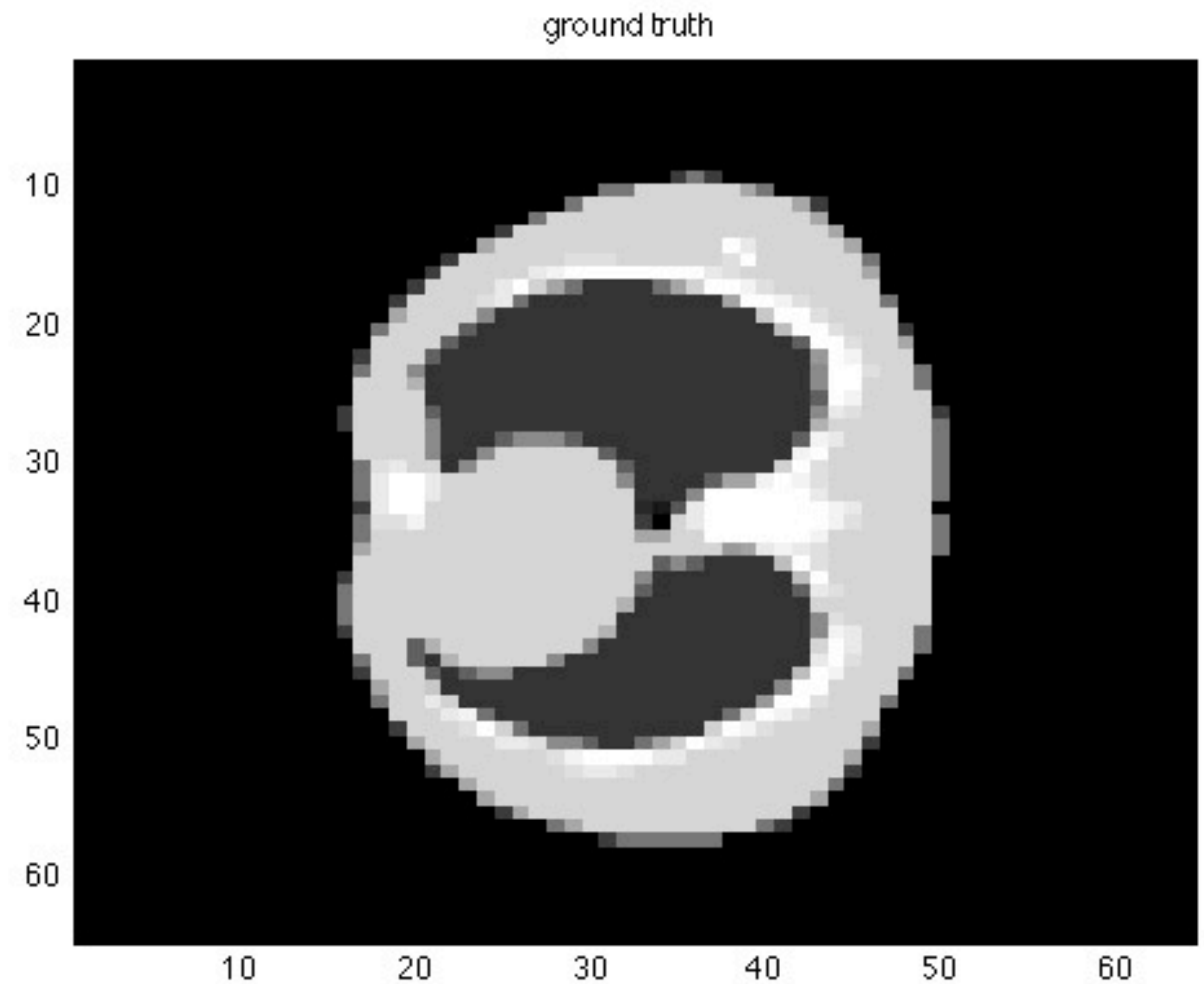

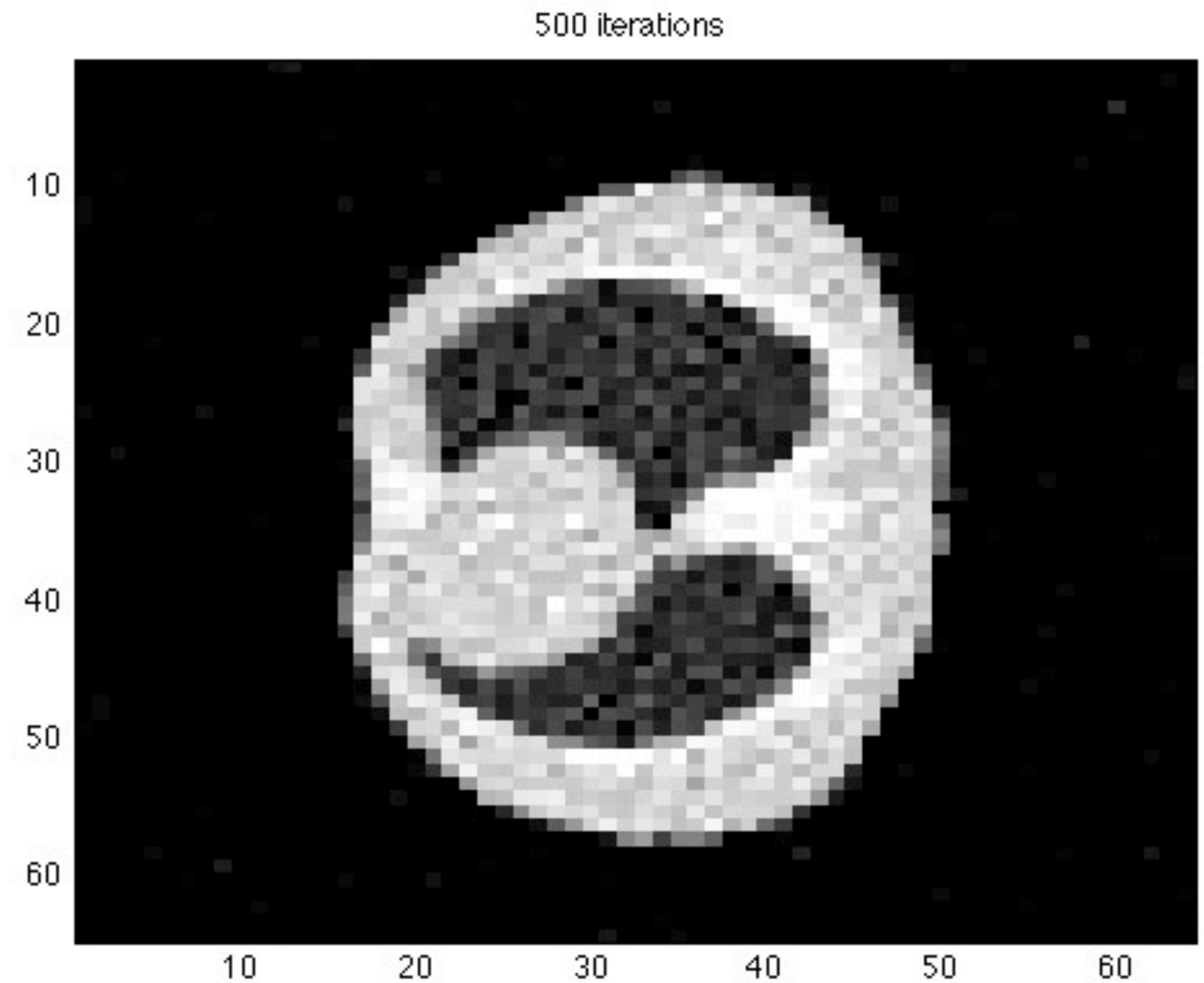

III - Tested Models of sparsity

- The discrete total variation of u is then defined by:

$$J_{TV}(u) = \sum_{1 \leq i,j \leq N} |(\nabla u)_{i,j}|$$

- A regularized version of the total variation:

$$J_{TV}^{reg}(u) = \langle \sqrt{\alpha^2 + |\nabla u|^2}, 1 \rangle = \sum_{1 \leq i,j \leq N} \sqrt{\alpha^2 + |(\nabla u)_{i,j}|^2}$$

- A sparsity-inducing norm on a frame expansion (wavelets, curvelets, ...):

$$J_{l_1,\varphi}(u) = \sum_{\lambda \in \Lambda} |\langle u, \varphi_\lambda \rangle| = \|R_\varphi(u)\|_{l_1}$$

III - Solvers

Generally speaking, how to solve :

$$\arg\min_{x \in X} F(Kx) + G(x)$$

with F and G proper, convex, lower semi-continuous functions,
K continuous linear operators.

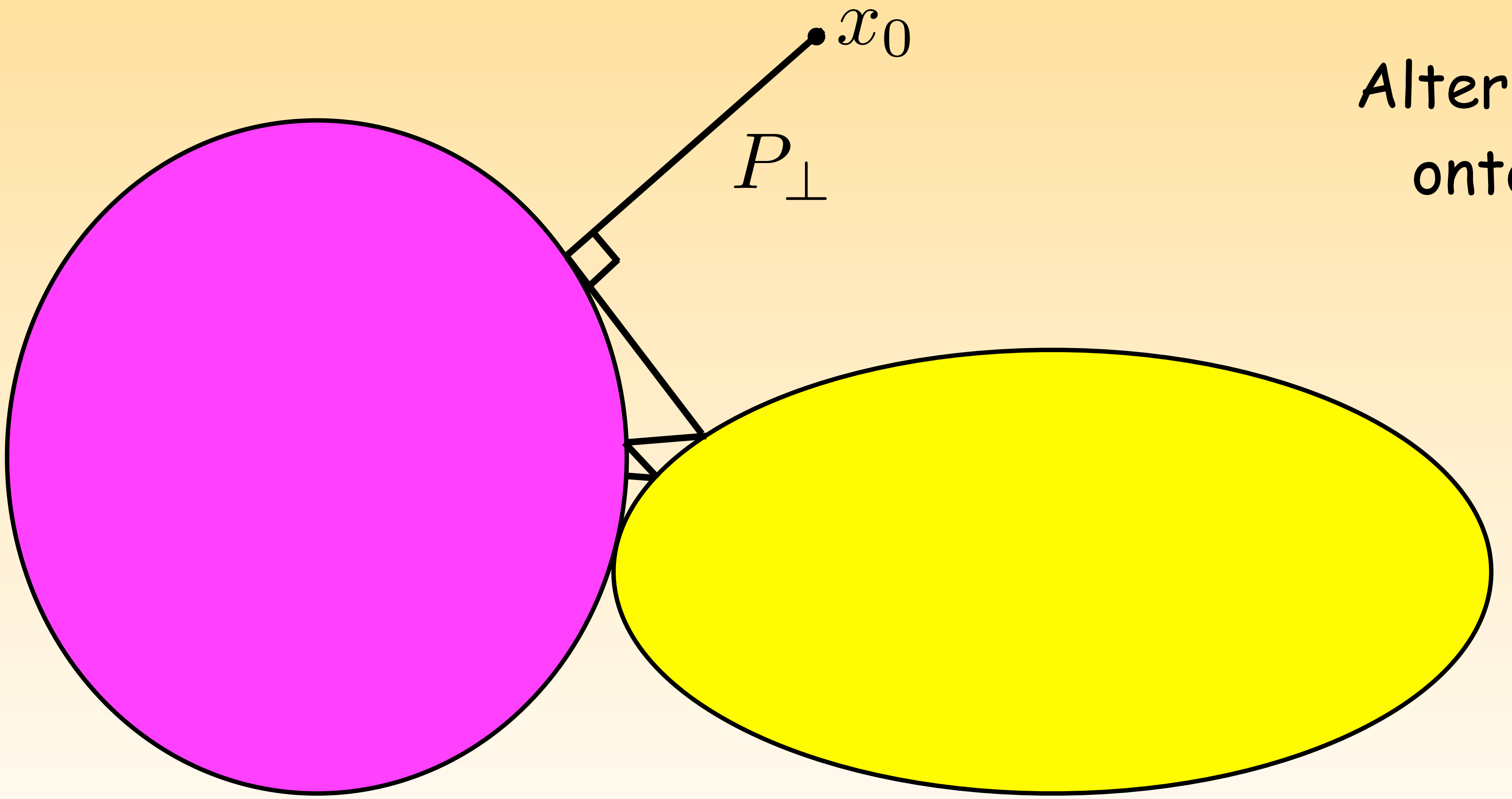

Alternate projection
onto convex sets
(APOCS)

III - Solvers

The recent Chambolle-Pock primal-dual solver is a generalization of APOCS to non-differentiable functions using the proximity operators.

Let define the Legendre-Fenchel conjugate function of F : $F^*(y) = \max_{x \in X}(\langle x, y \rangle) - F(x))$

Then the primal-dual equivalent problem is formulated as :

$$\min_{x \in X} \max_{y \in Y}(\langle Kx, y \rangle + G(x) - F^*(y))$$

General iterations of the solver :

- *Initialization:* Choose $\tau, \sigma > 0$, $(x_0, y_0) \in X \times Y)$, and set $\bar{x}_0 = x_0$.

- *Iterations* $(n \geq 0)$*:* Update $x_n, y_n, \bar{x}_n$ as follows:

$$\begin{cases} y_{n+1} = (I + \sigma \partial F^*)^{-1}(y_n + \sigma K \bar{x}_n) \\ x_{n+1} = (I + \tau \partial G)^{-1}(x_n - \tau K^* y_{n+1}) \\ \bar{x}_{n+1} = 2x_{n+1} - x_n \end{cases}$$

IV - Results on synthetic data

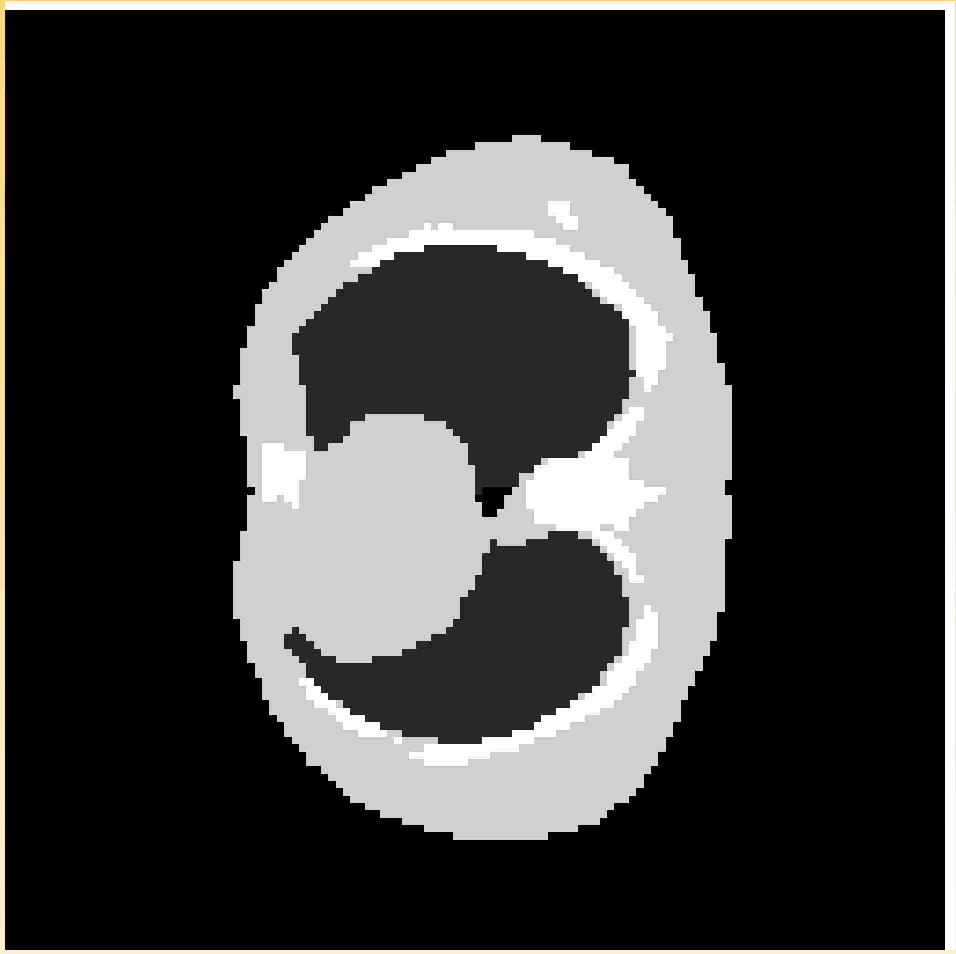

Ground Truth
CT

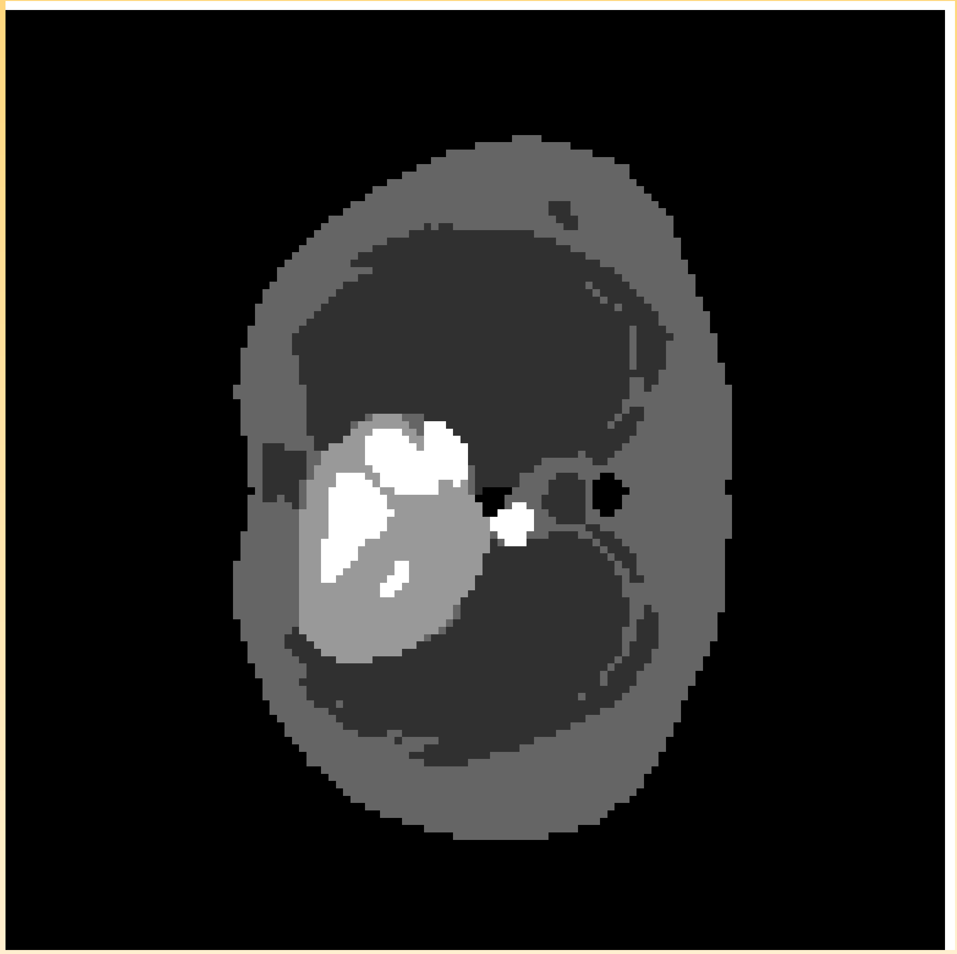

Ground Truth
TEP

CBCT , Z = 10 000 photons

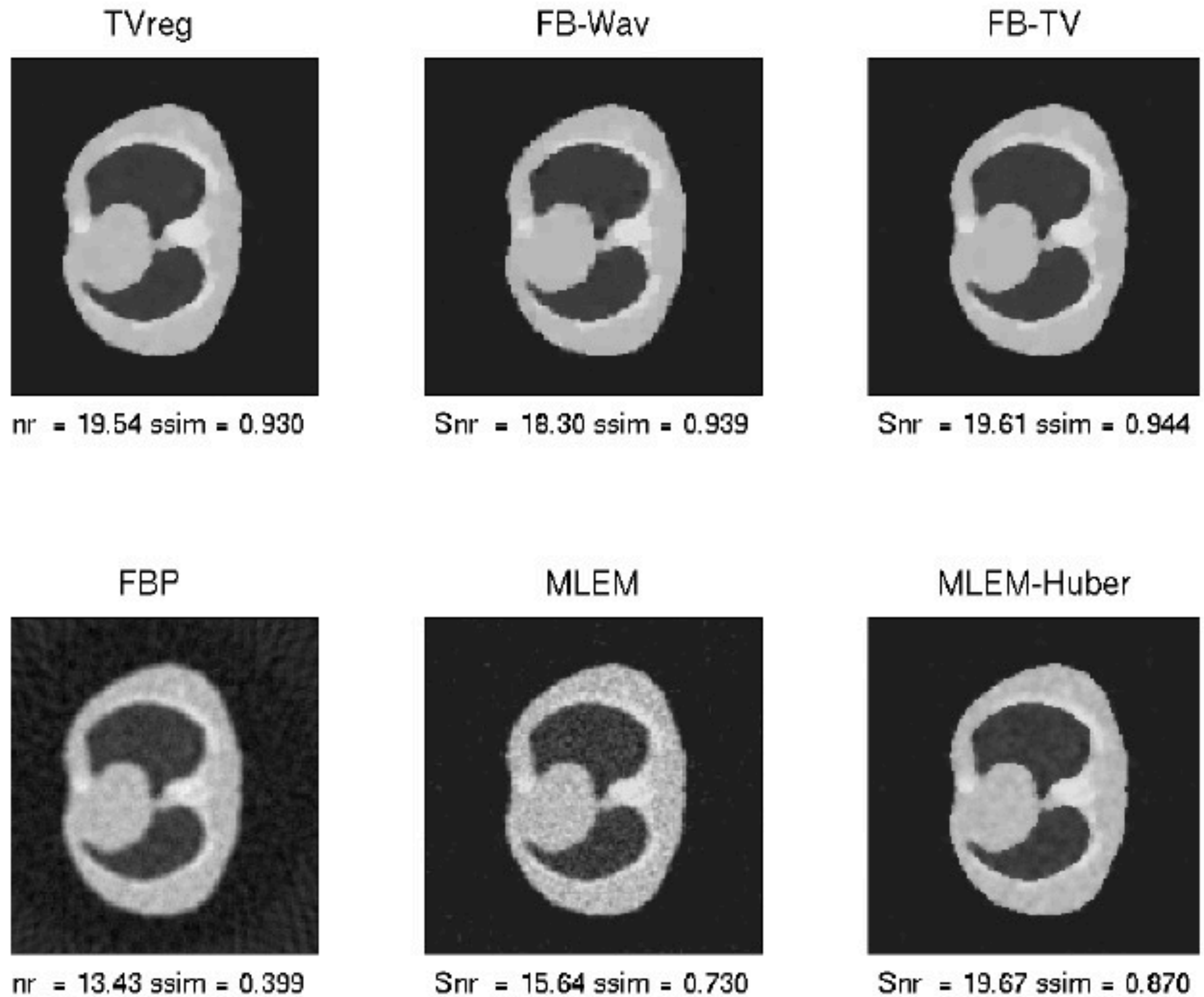

Figure 2: CT reconstruction, photon count z=10000

CBCT , Z = 1 000 photons

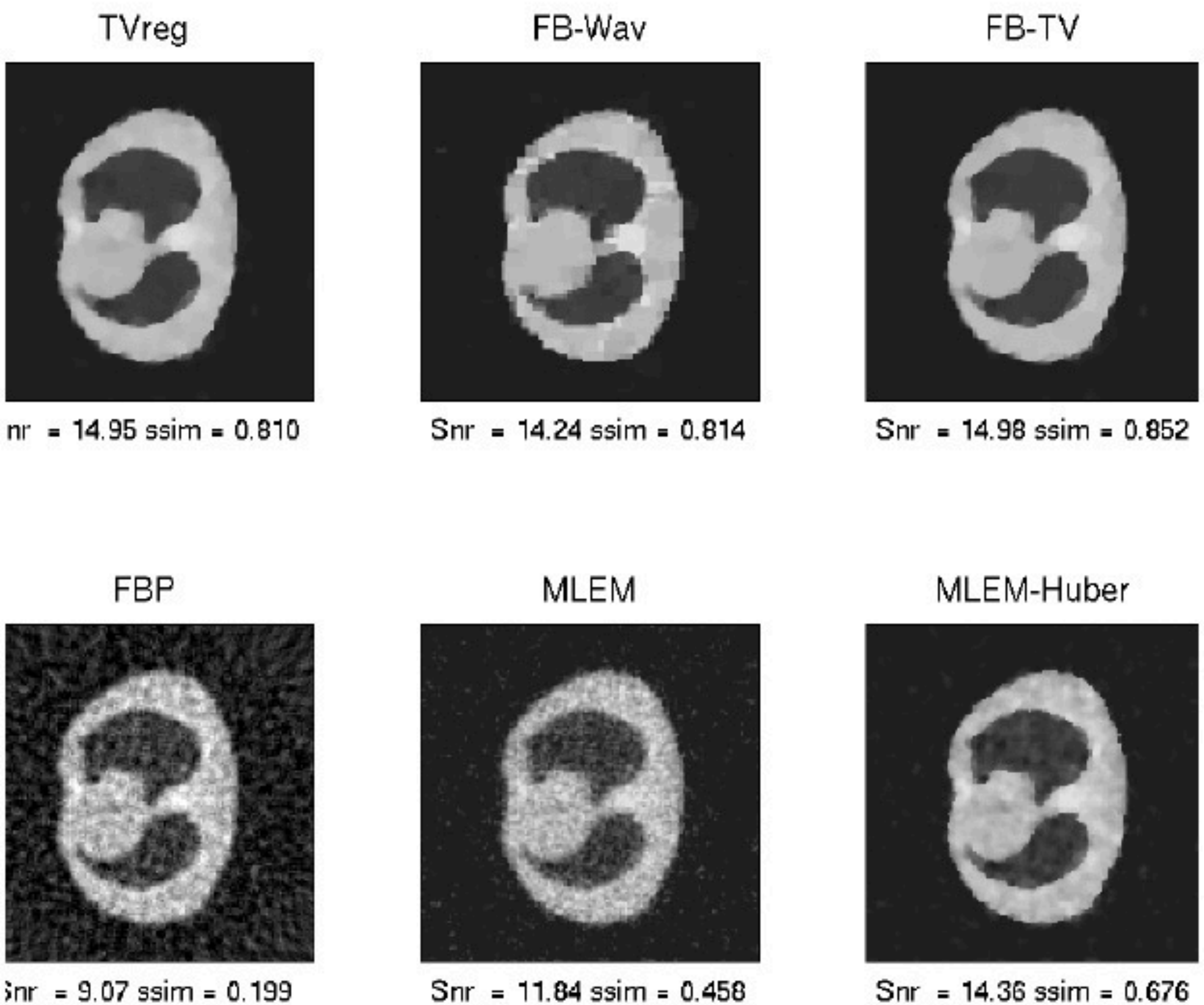

Figure 3: CT reconstruction, photon count z=1000

CBCT , Z = 100 photons

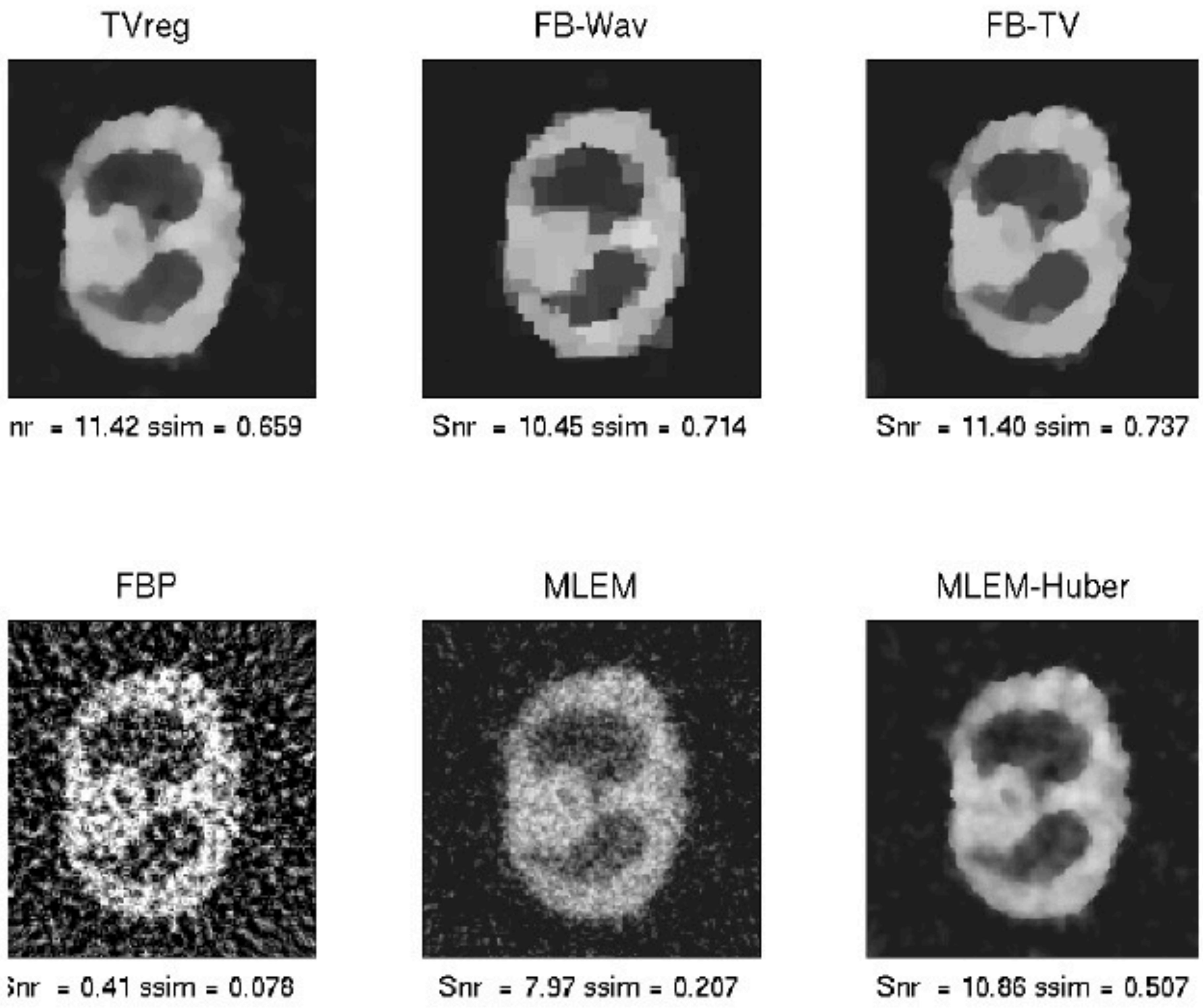

Figure 4: CT reconstruction, photon count z=100

Algorithm	snr	ssim	λ	nb. iterations	time (s)	nb. realizations
TVreg	19.57	0.900	300	300	44	100
TVreg	19.51	0.924	450	300	44	100
FB-Wav	**18.63**	**0.938**	75	300	110	100
FB-TV	**19.61**	0.916	300	300	85	100
FB-TV	19.56	**0.941**	450	300	86	100
FBP	13.40	0.395	-	-	0.12	25
MLEM	15.60	0.711	-	120	46	25
MLEM-Huber	**19.61**	0.856	2e5/9e-4	1000		25

Table 1: CT reconstruction, photon count z=10000

Algorithm	snr	ssim	λ	nb. iterations	time (s)	nb. realizations
TVreg	**15.06**	0.808	200	300	36	100
TVreg	14.93	0.811	300	300	36	100
FB-Wav	14.06	0.826	25	300	110	100
FB-TV	**15.10**	**0.845**	200	300	85	100
FB-TV	14.95	**0.853**	300	300	86	100
FBP	9.08	0.201	-	-	0.09	25
MLEM	11.86	0.462	-	43	14	25
MLEM-Huber	14.52	0.680	7e5/9e-4	752		25

Table 2: CT reconstruction, photon count z=1000

Algorithm	snr	ssim	λ	nb. iterations	time (s)	nb. realizations
TVreg	**11.34**	0.625	80	300	32	100
TVreg	11.28	0.624	100	300	32	100
FB-Wav	10.62	**0.695**	10	300	110	100
FB-TV	**11.35**	**0.690**	80	300	78	100
FB-TV	11.32	**0.690**	100	300	78	100
FBP	0.44	0.076	-	-	0.07	25
MLEM	7.90	0.200	-	17	5.67	25
MLEM-Huber	10.78	0.489	3.5e4/9e-4	605		25

PET , count = 500 000

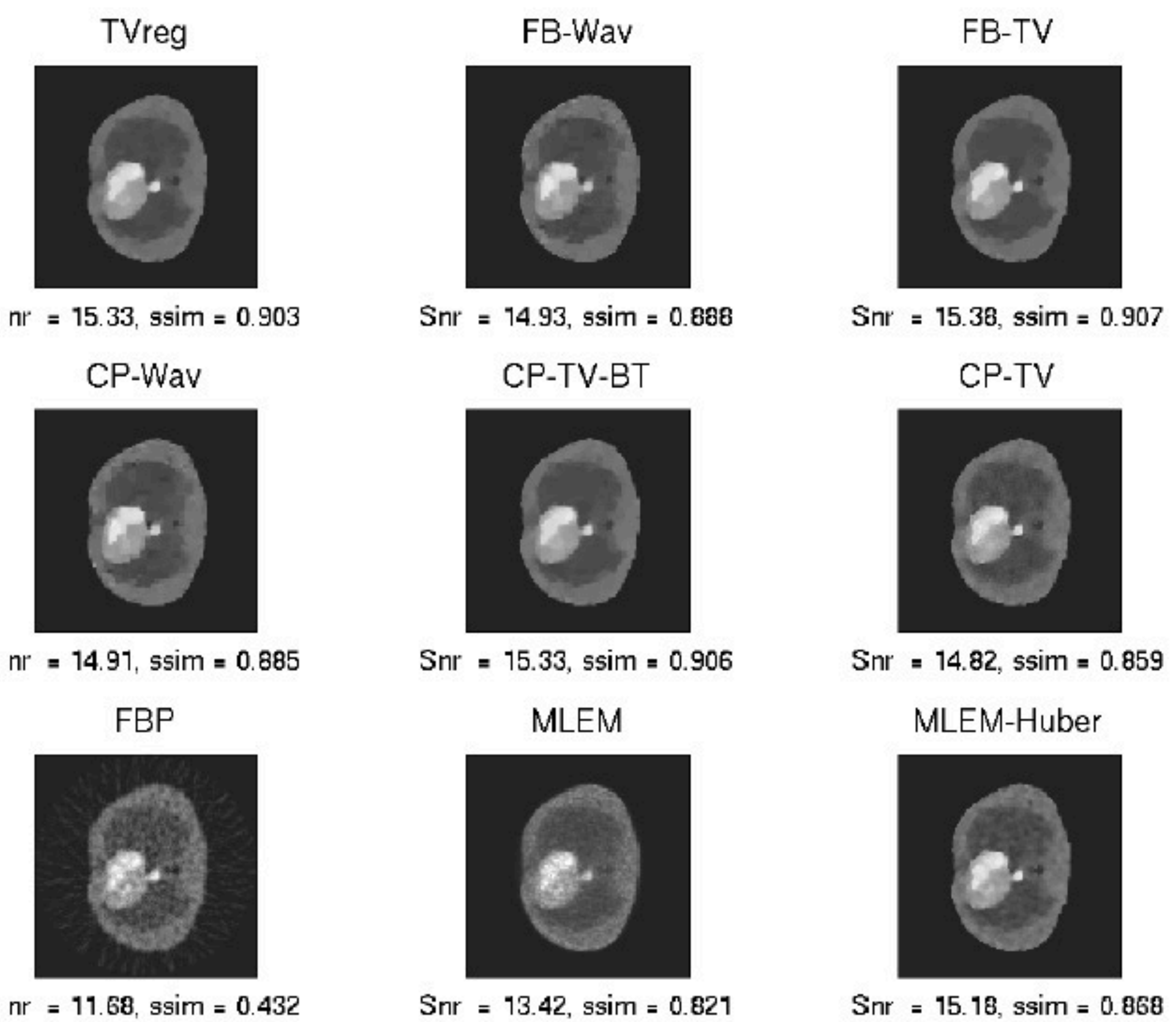

Figure 5: TEP reconstruction, detector efficiency fcount=500000

PET , count = 200 000

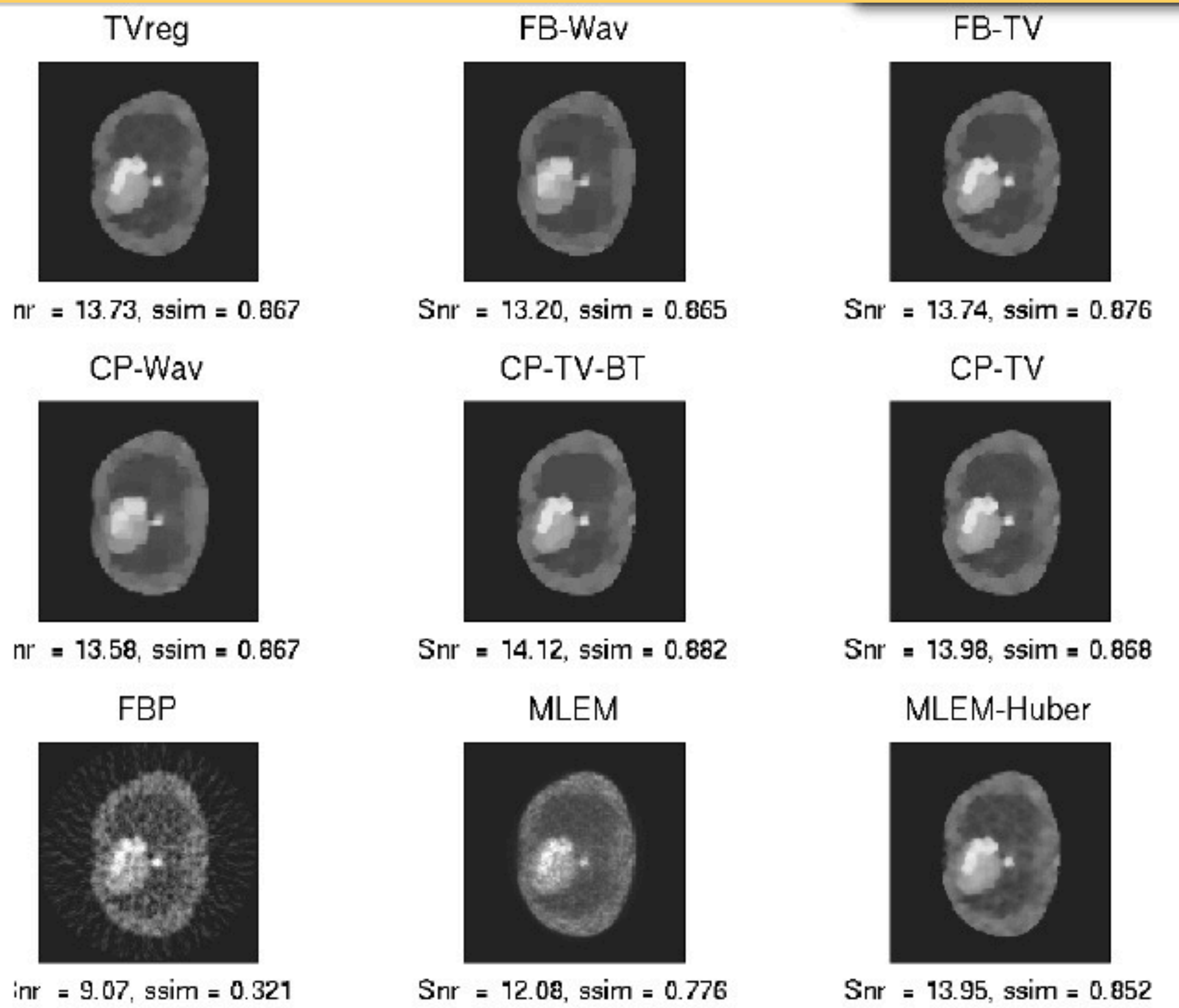

Figure 6: TEP reconstruction, detector efficiency fcount=200000

PET , count = 100 000

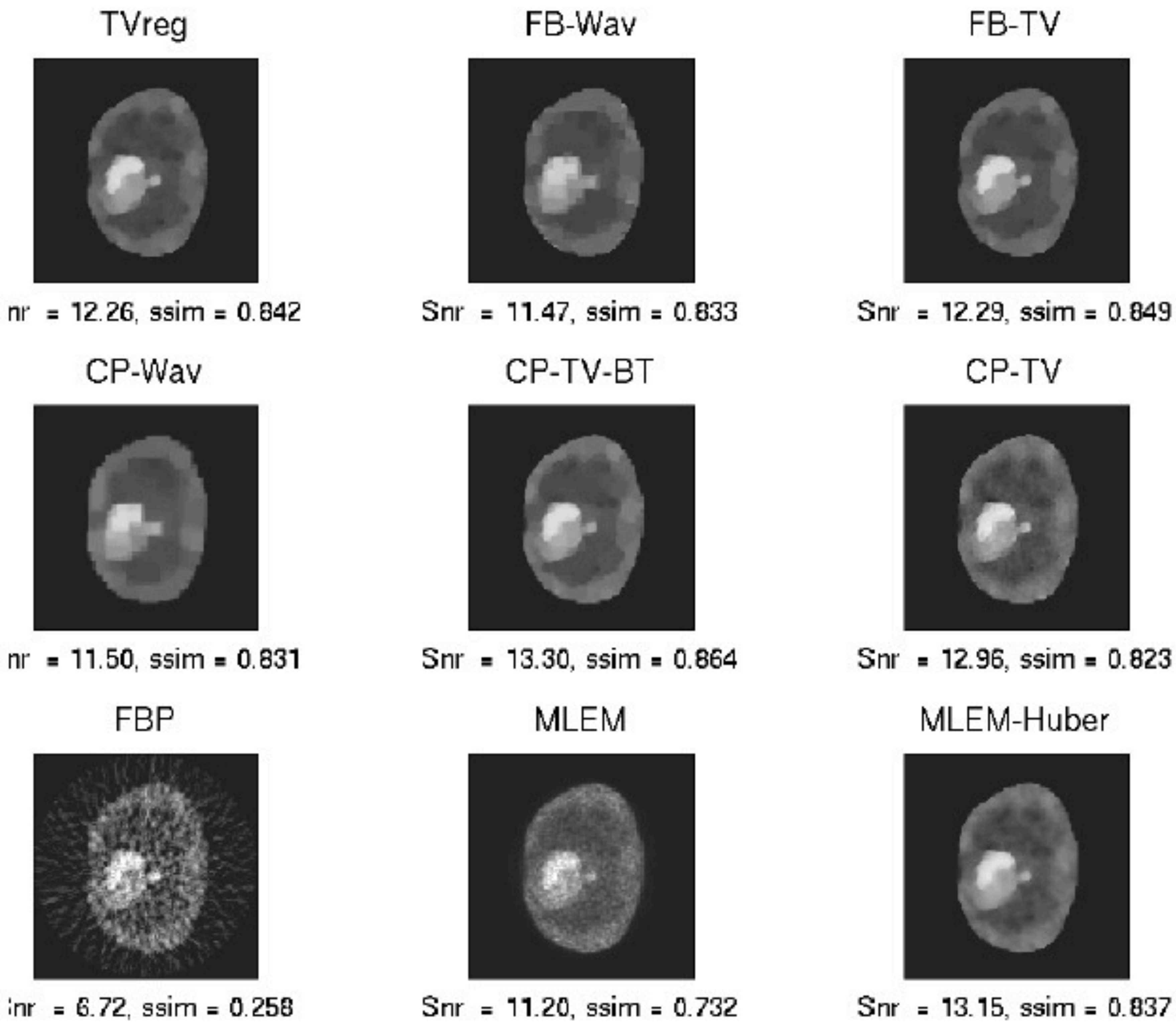

Figure 7: TEP reconstruction, detector efficiency fcount=100000

Quantitative results, PET , count = 500 000

Algorithm	snr	ssim	λ	nb. iterations	time (s)	nb. realizations
TVreg	**15.33**	0.902	0.70	200	10	15
TVreg	15.08	0.899	1.05	200	10	15
FB-Wav	14.77	0.889	0.10	150	89	25
FB-TV	**15.37**	0.905	0.70	100	62	15
FB-TV	15.19	**0.909**	1.05	100	62	15
CP-Wav	14.68	0.885	0.10	80	63	25
CP-TV-BT	15.32	0.905	0.70	80	63	15
CP-TV-BT	14.89	**0.906**	1.05	80	62	15
CP-TV	14.84	0.860	0.70	400	266	15
CP-TV	14.55	0.858	1.05	400	265	15
SPIRAL	15.17	0.905	0.70	100	76	10
SPIRAL	14.82	0.904	1.05	100	80	10
FBP	11.59	0.429	-	-	0.04	25
MLEM	13.38	0.819	-	17	2	25
MLEM-Huber	15.22	0.866	0.9/0.25	267	46	25

Table 4: TEP reconstruction, detector efficiency fcount=500000

Quantitative results, PET , count = 200 000

Algorithm	snr	ssim	λ	nb. iterations	time (s)	nb. realizations
TVreg	13.68	0.866	0.50	200	11	100
TVreg	13.40	0.856	0.75	200	11	100
FBwav	13.11	0.867	0.0875	150	89	50
FB-TV	13.71	0.875	0.50	100	65	100
FB-TV	13.56	**0.882**	0.75	100	65	100
CPwav	13.46	0.870	0.0875	100	79	50
CP-TV-BT	**14.17**	0.882	0.50	100	82	100
CP-TV-BT	14.00	**0.888**	0.75	100	83	100
CP-TV	**14.01**	0.867	0.50	150	107	100
CP-TV	13.77	0.867	0.75	150	107	100
SPIRAL	13.40	0.872	0.50	100	65	100
SPIRAL	13.13	0.874	0.75	100	67	100
FBP	9.03	0.322	-	-	0.07	25
MLEM	12.08	0.774	-	12	2	25
MLEM-Huber	13.97	0.853	0.9./0.25	274	53	25

Table 5: TEP reconstruction, detector efficiency fcount=200000

Quantitative results, PET , count = 100 000

Algorithm	snr	ssim	λ	nb. iterations	time (s)	nb. realizations
TVreg	12.12	0.841	0.40	200	13	10
TVreg	11.89	0.835	0.60	200	?	10
FBwav	11.55	0.834	0.0625	150	89	50
FB-TV	12.14	0.847	0.40	100	68	10
FB-TV	11.98	0.853	0.60	100	71	10
CPwav	11.65	0.835	0.0625	50	40	50
CP-TV-BT	**13.13**	**0.862**	0.40	50	46	10
CP-TV-BT	12.90	**0.867**	0.60	50	45	10
CP-TV	12.86	0.823	0.40	100	78	10
CP-TV	12.66	0.825	0.60	100	77	10
SPIRAL	11.77	0.841	0.40	100	86	10
SPIRAL	11.58	0.843	0.60	100	84	10
FBP	6.66	0.254	-	-	0.08	25
MLEM	11.06	0.731	-	10	2	25
MLEM-Huber	**12.92**	0.837	0.8/0.25	278	58	25

Table 6: TEP reconstruction, detector efficiency fcount=100000

V - Future challenges

1 - Reducing the dose may mean :

- Reducing the statistics
- Reducing the number of projections

→ More adapted sparsity models to biomedical images ?

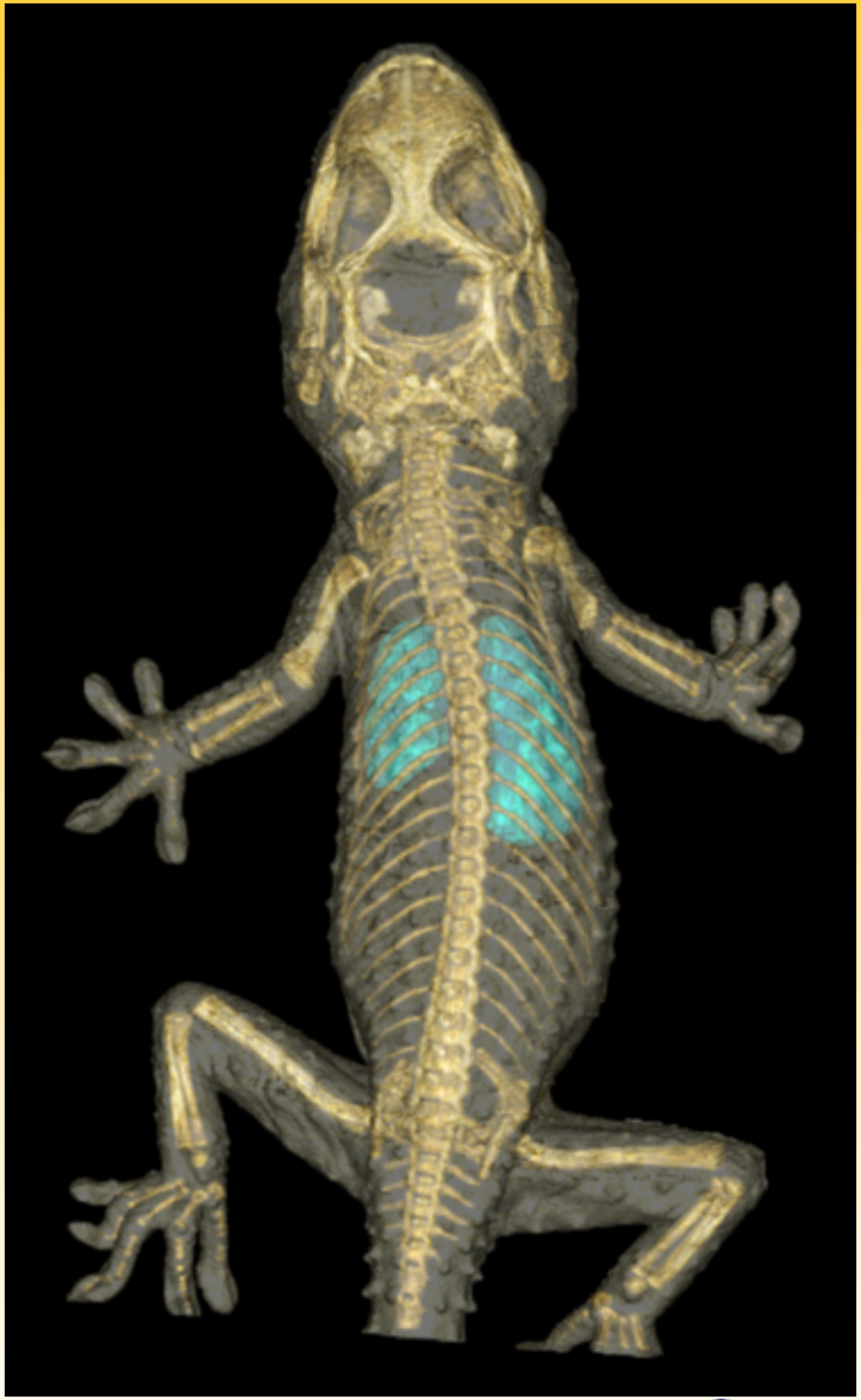

2 - Go towards color imaging !

- Energy selection ! ..
- Acquire directly color information ?

Go towards X-color imaging : concept

Contrast magnification

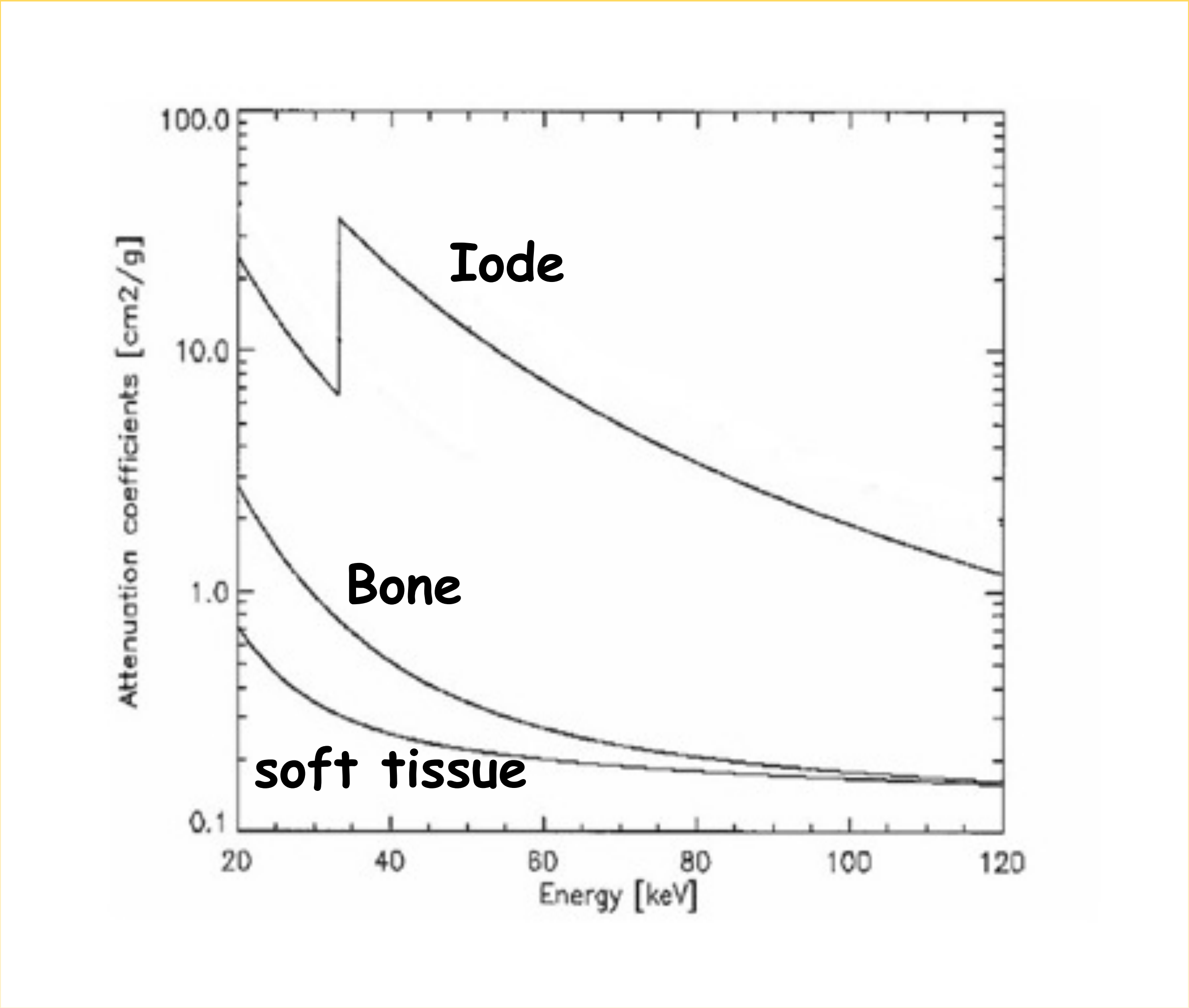

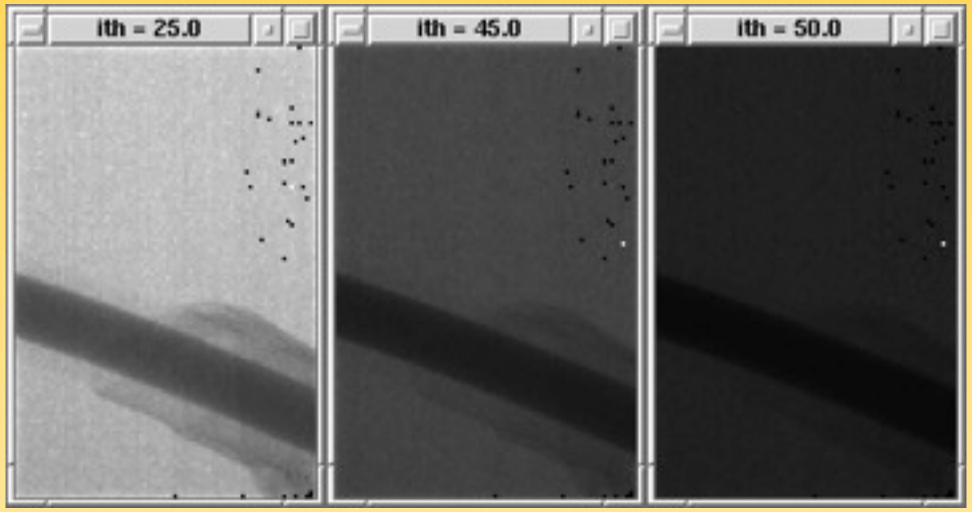

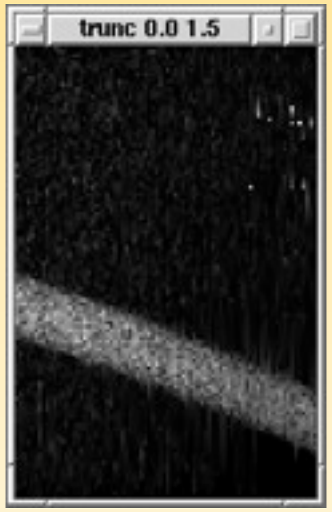

Go towards X-color imaging : concept

CdTe efficient until almost 100 keV

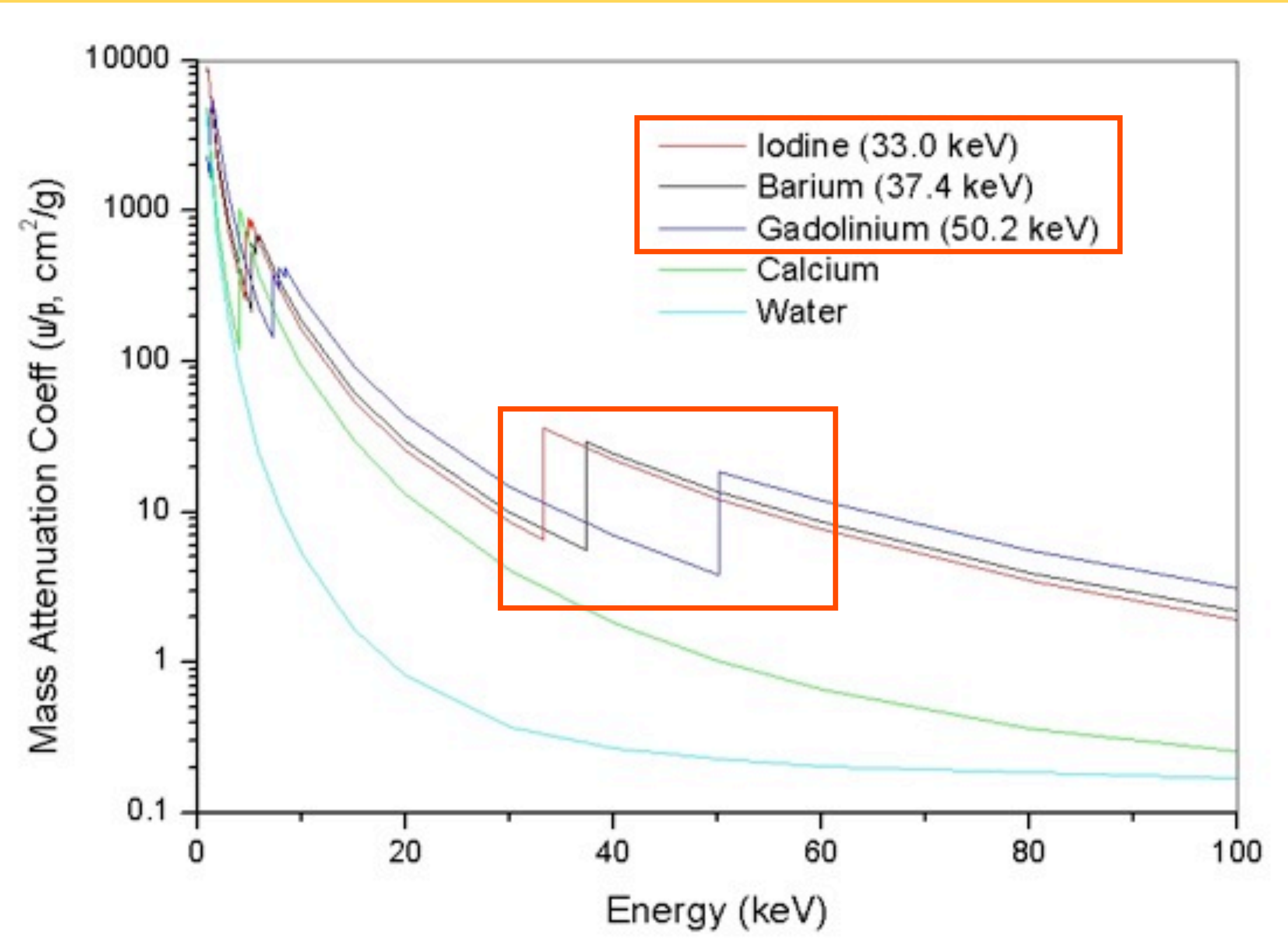

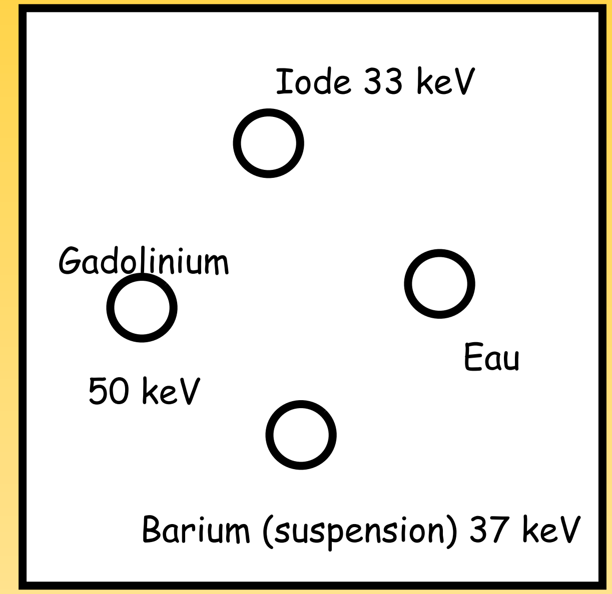

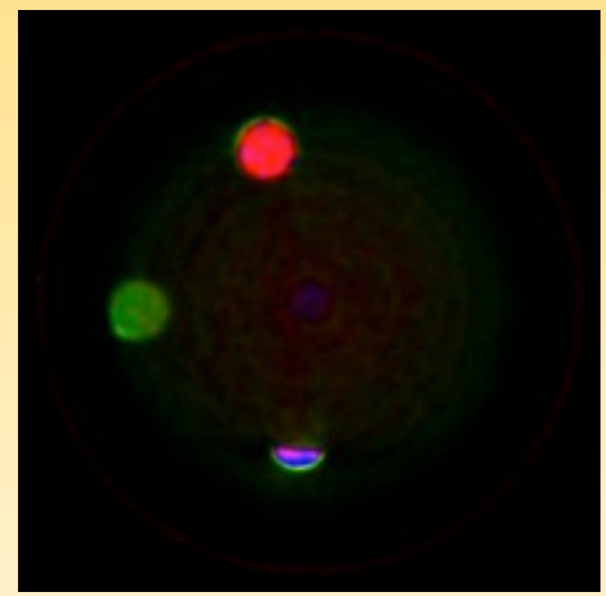

courtesy: A. Butler, MARS Biomedical Imaging Ltd.

3 pharmaceutical, perspex phantom

University Albert-Ludwigs in Freiburg
and university of Canterbury

Go towards X-color imaging : concept

Iode : circulation pulmonaire

Barium : poumons

Calcium : os normaux

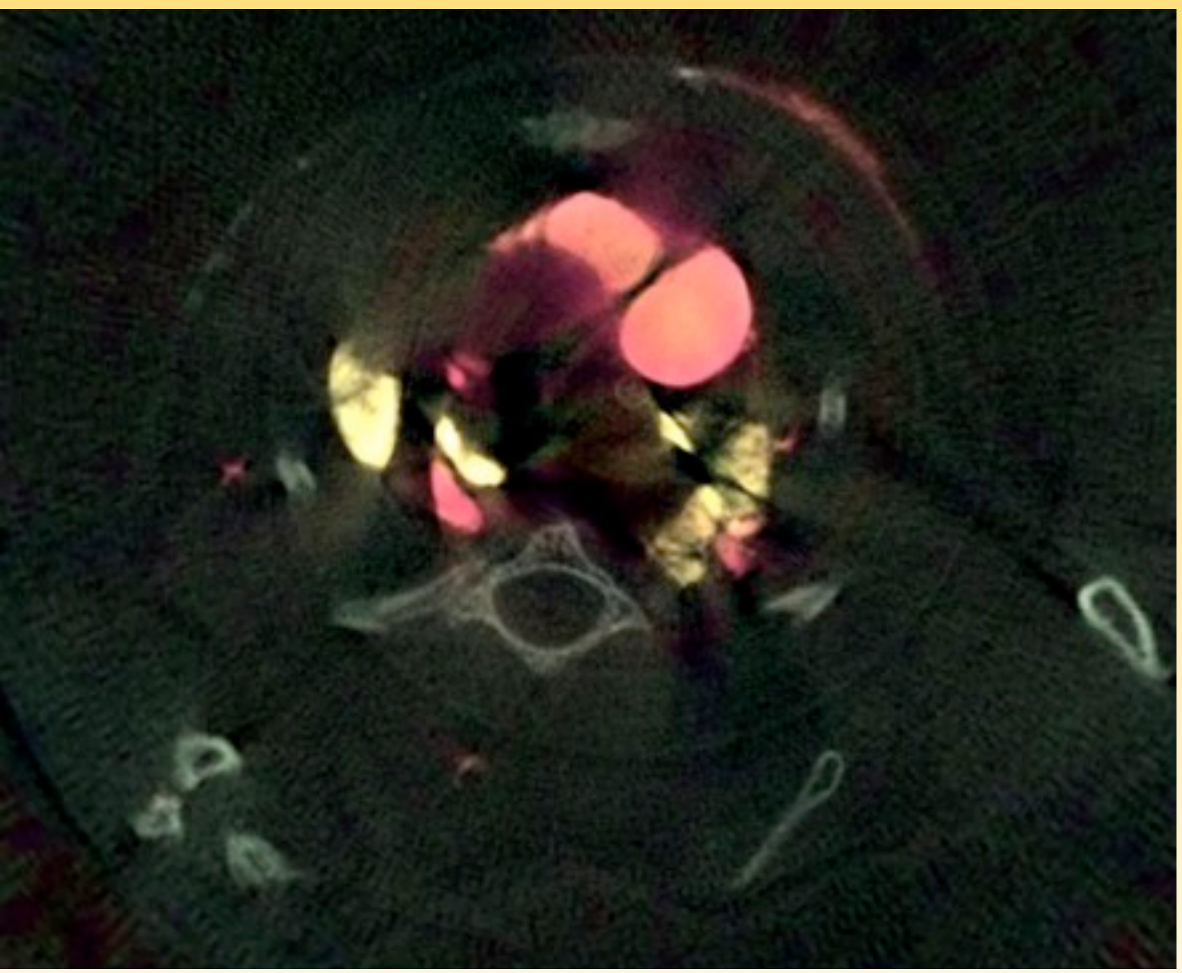

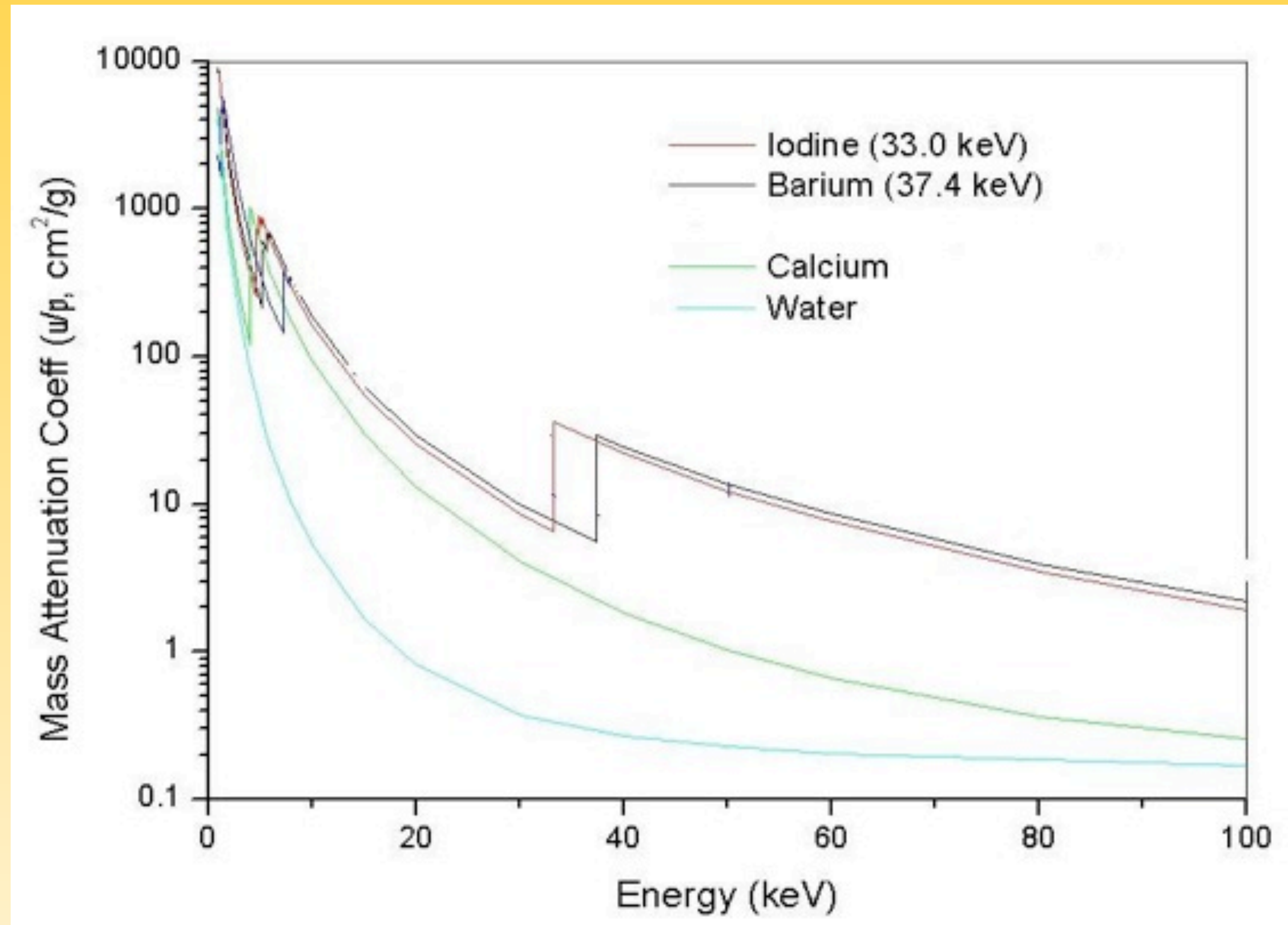

Quantitative system developed at Erlangen-Nürnberg

courtesy: A. Butler, MARS Biomedical Imaging Ltd.

Towards CBCT Color Imaging

Measurements of our W-source spectra with different filters

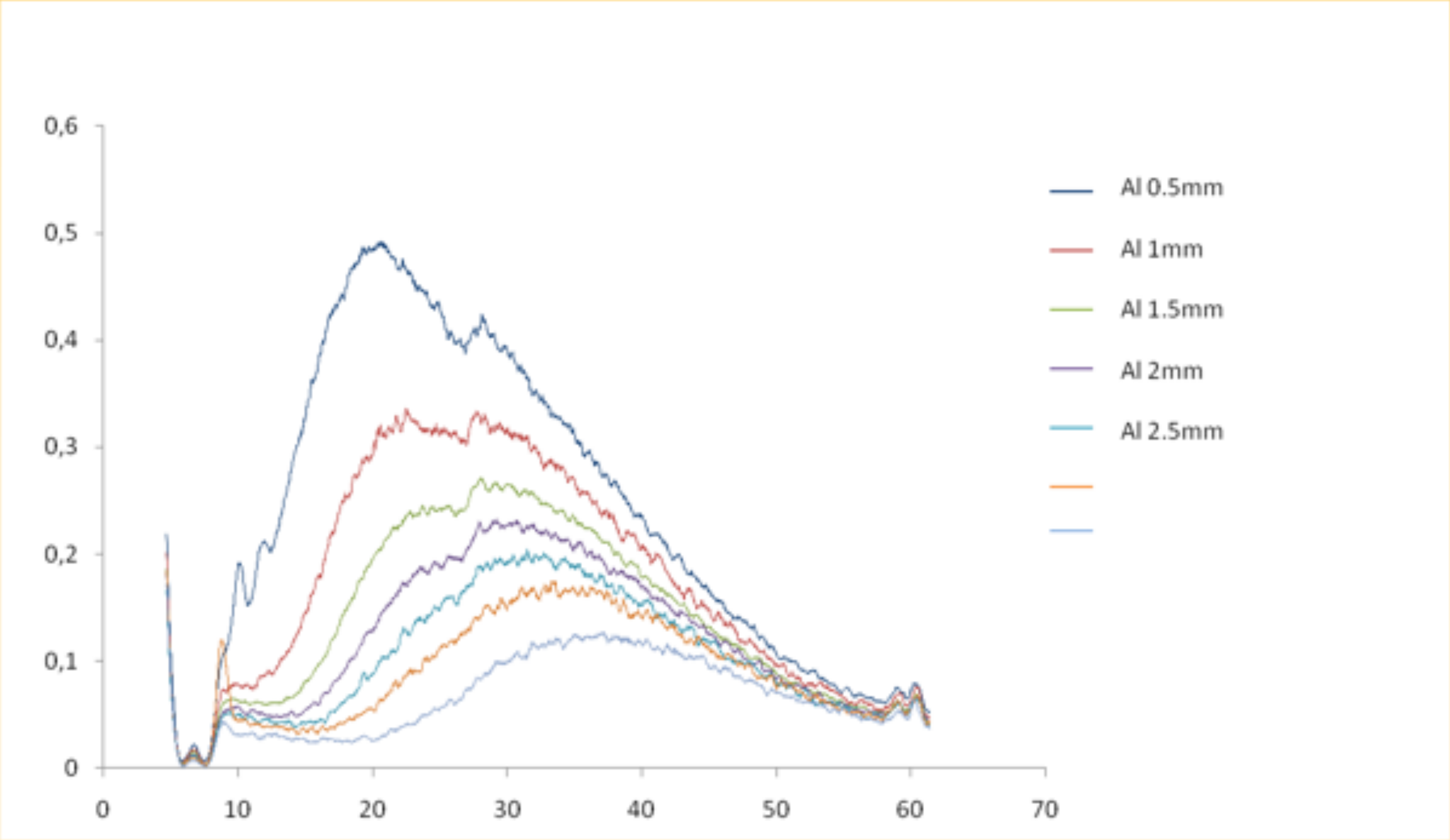

$$I_j(E) = I^0(E) e^{\left(-\int_{r_j} \mu(l,E)dl\right)} \qquad y_{j,T} = \int_T^{\infty} I_j(E) dE$$

No more (obvious) linearity ... sad news !

Conclusion

New XPAD3 hybrid pixels camera for X-ray photon counting developed at CPPM :

CT-Scanner based on hybrid pixels.

Simultaneous PET/CT scanner for bimodality images.

Simulations as well as real acquisitions have proven the reliability of hybrid pixels for micro-CT scanner and PET/CT !

Adapted algorithms :

For low dose : Poisson noise to take into account

For small number of projections : regularization needed ... sparsity basis ?

For color imaging : adapt the acquisition framework ... CS theory for help ?

Implementation on GPUs strongly speeds-up the reconstruction (between 100 and 300 times faster compared to CPUs). Being implemented for iterative methods...